UNIVERSITY OF CALIFORNIA,

IRVINE

Heterogeneous Integration of Microfluidics on Printed Circuit Boards for Lab-on-Chip Applications

DISSERTATION

submitted in partial satisfaction of the requirements
for the degree of

DOCTOR OF PHILOSOPHY

in Electrical and Computer Engineering

by

Sarkis Babikian

Dissertation Committee:
Professor Guann-Pyng Li, Chair
Professor Michael Green
Associate Professor Ahmed Eltawil

2016

DEDICATION

To Mom & Dad

To my family

To you I owe my success

TABLE OF CONTENTS

Page

LIST OF FIGURES

Page

LIST OF TABLES

Page

ACKNOWLEDGEMENTS

I would like to express my deep appreciation and gratitude to my advisors Professor G.P. Li and Professor Mark Bachman. This work would not have been possible without their guidance, vision and support. I will remain grateful for having the wonderful opportunity to be a part of the Li/Bachman group, where I grew professionally and as a person as well.

I would like to thank Professors Michael Green, Ahmed Eltawil and Abraham Lee for kindly taking a place in my qualifying exam and dissertation committees and evaluating my work.

I would like to acknowledge the institutions and foundations that generously supported this work:

-The Achievement Rewards for College Scientists (ARCS) foundation (The ARCS award)

-The Broadcom Foundation (EECS Dpt. Broadcom Fellowship)

-The EECS department

-The Center for Advanced Design and Manufacturing of Integrated Microfluidics (CADMIM)

-The National Science Foundation (NSF)

Without this generous and crucial support this work would not have been accomplished.

I would like to acknowledge my project collaborators in Stanford University: Professor Juan Santiago, Lewis Marshall and Crystal Han.

I would also like to thank the people with whom I walked this journey: My lab manager Lily Wu. The INRF clean room workers and staff, Richard Chang Renee Pham, Brittany Gray and Tina Tom. The EECS department workers Ronnie Gran and Amy Pham. My lab mates Sara Saedinia, Jason Luo, Peyton Paulick, Weseley Muranami, Michael Klopfer, Mark Merlo, Sungjun Kim, Nizan Friedman, Dogukan Yildirim and Minfeng Wang. My undergraduate research assistant students: Garine Shamirian, Brian Soriano, Nuthan Hegde, Nick Farabee, Shirin Ghafarkan, Nazaneen Pastulishe and Bao Tran. My friends, Aras Pirbadian, Pawel Starakiewicz and Davit Hovhannisyan.

And finally, a word of appreciation and gratitude to my parents, my family and my uncle Dikran and his family. I dedicate this work to my mom, to my dad, to my brothers Tro and Saro and to my significant other, Garine.

Sarkis Babikian
August 6, 2016

CURRICULUM VITAE

Sarkis Babikian, Ph.D.

6363 Adobe Circle Rd., Irvine, CA 92617, Tel: (818) 397-1194,
sbabikia@uci.edu

EDUCATION

- University of California Irvine, Irvine 2011-2016
  PhD in Electrical Engineering
- University Of California Irvine, Irvine 2009-2011
  Master of Science in Electrical Engineering
- University Of Damascus, Damascus 2003-2008
  Bachelor of Science in Electrical Engineering

EXPERIENCE

- Graduate Student Researcher; University Of California, Irvine
  June 2010 – June 2016
  Developed heterogeneous integration architecture and fabrication technology for Lab-on-Chip devices (portable microfluidic devices used for point of care diagnostics applications.)
  Accomplished tasks:
  - Designed, fabricated and characterized prototype microfluidic devices for Lab-on-Chip applications.
  - Designed and fabricated novel microfluidic components for integrated Lab-on-Chip devices.
  - Performed experiments, analyzed experimental data and wrote technical papers.
  - Accomplished collaborative projects with an industrial advisory board and a team of researchers
  - Presented in several international conferences and technical meetings.
  - Trained/supervised a team of undergraduate engineering students to accomplish short period undergraduate research projects.

- Teaching Assistant; University of California, Irvine
  January 2011-March 2014
  Supervised laboratory sessions, graded homework and exams and provided assistance to electrical engineering students for their senior design projects.
- Internship in Technical University of Ilmenau , Ilmenau
  July 2007-October 2007

Worked in a team of two students to design a solar power system and conducted experiments on photovoltaic cells.

- Internship in Muller Company, Damascus
  July 2006-September 2006
  Assembled and tested power switching and control panels for industrial use.

SKILLS

- Microfabrication and prototyping (Photolithography, replica molding, machining, electroforming)
- Laboratory instruments
- Circuit design and microcontrollers
- Simulation tools (Matlab, Simulink , Comsol)
- Computer aided design (CAD) and Microsoft Office

PUBLICATIONS AND PRESENTATIONS

- "A digital signal processing assisted microfluidic PCB for on-chip fluorescence detection"
  S. Babikian, G.P. Li and M. Bachman
  Submitted for publication, 2016
- "Fluidic Electro-Mechanical Components"
  S. Babikian, G.P. Li and M. Bachman
  Manuscript in preparation, 2016
- "Packaging Architecture for Fluidic Components in Microfluidic PCBs"
  S. Babikian, G.P. Li and M. Bachman
  IEEE 66th Electron. Components Technol. Conf. submitted for publication, 2016
- "Portable Micro-fluidic-opto-electronic Printed Circuit Board For Isotachophoresis Applications"
  S. Babikian, G.P. Li and M. Bachman
  µTAS pp. 1293–1295, 2015
- " Integrated Bioflexible Electronic Device for Electrochemical Analysis of Blood"
  S. Babikian, G.P. Li and M. Bachman
  IEEE 65th Electron. Components Technol. Conf. pp. 685 – 690, 2015
- "Ethylene-Vinyl Acetate as a low cost encapsulant for hybrid electronic and fluidic circuits,"
  S. Babikian, W. a. Cox-Muranami, E. Nelson, G. P. Li, and M. Bachman,
  IEEE 63rd Electron. Components Technol. Conf., pp. 1800–1805, May 2013.
- "Microfluidic thermal component for integrated microfluidic systems"
  S. Babikian, L. Wu, G. P. Li, and M. Bachman
  IEEE 62nd Electron. Components Technol. Conf. pp.1582–1587,May 2012

- "Integrated printed circuit board device for cell lysis and nucleic acid extraction"
  L. A Marshall, L. L. Wu, S. Babikian, M. Bachman, and J. G. Santiago
  Anal. Chem., vol. 84, no. 21, pp. 9640–5, Nov. 2012
- "Laminate Materials for Microfluidic PCBs"
  Sarkis Babikian, Brian Soriano, G.P. Li and Mark Bachman
  International Symposium on Microelectronics: 2012, Vol. 2012, No. 1, pp. 000162-000168
- "Microfluidic printed circuit boards"
  L. L. Wu, S. Babikian, G.-P. Li, and M. Bachman
  IEEE 61st Electron. Components Technol. Conf., pp. 1576–1581, May 2011

Presentations:

- IEEE 66th ECTC Conference, Las Vegas 2016
- 19th µTAS Conference, Geongju 2015
- Medical Electronics Symposium, Marylhurst Univ. Portland 2015
- IEEE 65th ECTC Conference, San Diego 2015
- IEEE 62nd ECTC Conference, San Diego 2012
- iMAPS Conference, San Diego 2012
- ASME 6th Frontiers in Biomedical Devices Conference, Irvine 2011
- Lab Automation Conference, Palm Springs 2011

AWARDS AND SCHOLARSHIPS

- 2015 and 2014 ARCS (Achievement Rewards For College Scientists) award recipient
- 2015 UCI Electrical Engineering Fellowship recipient (Broadcom Foundation Fellowship)
- 2010 Hajen Foundation scholarship recipient
- 2008, Ranked first among graduates of the Electrical Engineering Department.
- 2008, 2007 and 2006 best student award recipient from University of Damascus.
- 2008, and 2006 Calouste Gulbenkian Foundation scholarship recipient
- 2007 Scholarship recipient to attend extracurricular program in Germany.

LANGUAGES

· English, Armenian, Arabic.

ABSTRACT OF THE DISSERTATION

Heterogeneous Integration of Microfluidics on

Printed Circuit Boards for Lab-on-Chip Applications

By

Sarkis Babikian

Doctor of Philosophy in Electrical and Computer Engineering

University of California, Irvine, 2016

Professor G. P. Li, Chair

Microfluidic technology has important applications in Point-of-Care (POC) diagnostics, and in high throughput screening and sequencing through the introduction of small, automated and portable microfluidic devices commonly known as Lab-on-Chip (LOC) devices, and Micro Total Analysis System (μTAS). These devices can perform biochemical and fluidic assays in automated fashion, using smaller amounts of samples and in faster periods of time when compared to traditional methods. However, LOC devices require the integration of active fluidic components as well as a wide array of sensors and actuators on the chip, which has presented a significant challenge in the traditional methods of fabricating microfluidics. In this dissertation, the use of the Printed Circuit Board (PCB) is proposed as

a heterogeneous integration platform for microfluidic LOC devices. A novel heterogeneous integration architecture is demonstrated that enables the integration of microfluidics, electronics and optics on PCBs, and promotes standardized, scaled and cost effective fabrication of LOC devices. The fabrication and integration processes are described by demonstrating several microfluidic LOC devices built on PCBs, and integrated with key LOC functions on the chip, such as sample preparation, analyte extraction, and optical detection.

1. INTRODUCTION

1.1. Microfluidics and Lab on Chip

Microfluidic technology has the potential to enable new capabilities and applications in the fields of molecular biology, analytical chemistry and point of care medical diagnostics, through the realization of the concept: “Lab on a Chip” or “Micro Total Analysis System” [1-5]. This concept aims to produce small, portable, hand held devices that are capable of performing biological and chemical assays, which are typically performed in conventional laboratories using large scale equipment. Microfluidic technology enables the reproduction of assays on small chips, Lab-on-Chip devices, which would give rise to important applications in two main areas. The first is the high throughput molecular analysis such as screening for drug discovery and DNA sequencing. Droplet based LOC devices, as shown in figure 1c, would have significant advantages over traditional methods. Micro droplets generated on a microfluidic chip would replace the conventional physical wells of a microarray as the compartments or reaction chambers of the high throughput assay [6]. This would reduce the sample and reagent volumes by up to a million times and yield higher throughput analysis and overall lower cost of analysis.

The second significant area for LOC devices is the Point-of-Care (POC) diagnostics. LOC devices would perform diagnostic tests at the point of care

eliminating the need to visit the laboratory or a health center [2, 5]. Such devices are also crucial for diagnosing and treating patients in remote areas with limited or no access to medical infrastructure. Examples are many and diverse, such as the battle fields in war zones or the poor underdeveloped countries with pathogen outbreaks, pollution and contamination problems. Such devices should perform high quality tests in very short period of time (few minutes). They should be operated or used by non-professionals (in the form factor of the home glucose meter) and should also be in part disposable. The portability of the device is very crucial and therefore it should be powered and operated by a battery or via a portable device such as a lap top computer or a smart phone.

The key enabling technology of LOC devices is the microfluidics technology. A microfluidic chip has microchannels that are less than 1 mm, in one dimension at least, as shown in figures 1a and 1b. These channels are capable of processing very small volumes of fluids, in the order of nano liters to femto liters. The flow regime in these channels is laminar (Figure 1d), since the Reynolds number is less than 1. At this scale the inertial forces are negligible compared to the surface tension forces. These unique properties of the fluids at micro scale govern the microfluidic assays and create novel methods and techniques for sample analysis. However, the most important advantages that microfluidics may offer from the user point of view are the reduction in sample and reagent volumes and the portability of the device. To receive such benefits from microfluidic LOC devices, these

devices have to be very portable and operate with minimal dependence on other equipment. Therefore it is essential to integrate sensors, actuators and other active components in the microfluidic chip. Hence, an integration platform is needed for LOC devices [1-5].

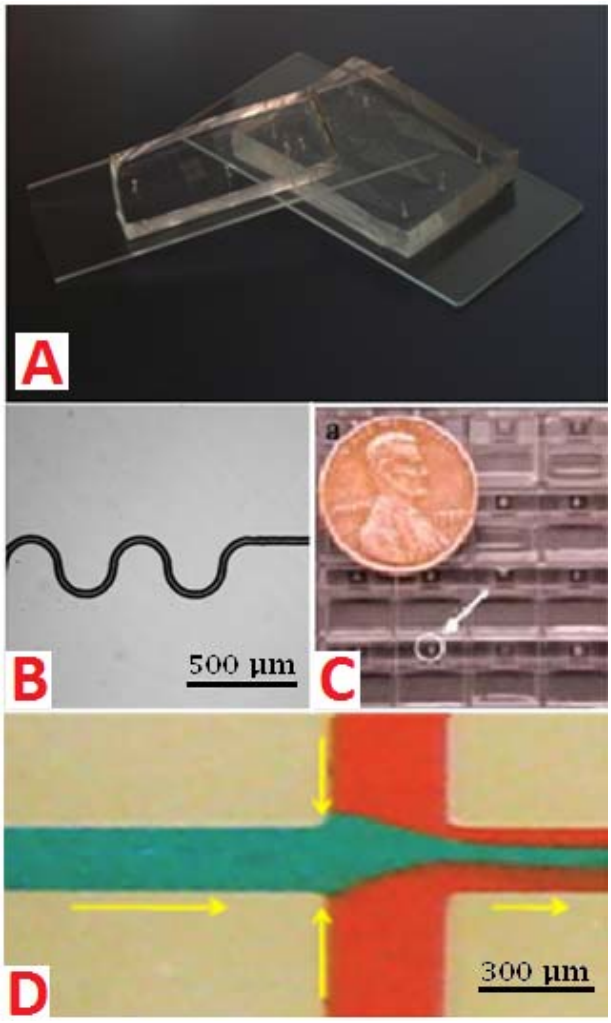

Figure 1-1 Microfluidics

A: micorfluidic device molded in PDMS and sealed with glass. B: a microchannel. C:10 nL droplet in contrast to a penny's size. D: Laminar flow in microchannels

1.2. Heterogeneous integration of Lab-on-Chip

Microfluidics is the core enabling technology for Lab-on-Chip devices. However, heterogeneous integration is essential to realize LOC devices. Passive microfluidic chips cannot perform assays without off-chip equipment. Generally speaking, there is a diverse set of functions needed to perform any given biochemical or fluidic assays [1, 5]. Figure 1-2 summarizes these functions and the required transducer technology and materials needed to integrate the functions on the chip. Fluid transport and manipulation functions include pumping fluids, mixing sample fluids with reagents, storing fluids on the chip, etc. These would require integration of pumps, mixers, valves and reservoirs on the microfluidic chip. These fluidic components are typically fabricated with polymers; however they may also need thin film layers of conductor or semiconductor material to facilitate electromechanical actuation and sensing in these components. On the other hand bio-chemical assays require several processes starting with the preparation of the raw sample for the analysis, then extraction and isolation of target analytes from the complex matrix of the sample, amplification and hybridization of these analytes with bio-sensors, and the detection of the signal through signal transduction by different means (optically, electrochemically, etc.). For sample preparation procedures special functions are needed on the chip such as temperature controlled heating and reagents mixing. Thus, integration of resistive heaters and electrodes is

needed, which are typically fabricated by thin film conductor materials. Analyte extraction and isolation may involve electrophoretic assays (such as electrophoresis and isotachophoresis) which would require high electric fields in the microchannel. Other separation techniques involve functionalized surfaces which would capture the target analytes [18], such as DNA/RNA microarrays [19] or immunoassays (such as in ELISA)[20]. Amplification of target analytes often requires temperature cycled and controlled assays, such as Polymerase Chain Reaction (PCR) [21], and Recombinase Polymerase Amplification (RPA) [22, 23] on the chip, which would require integration of heaters, coolers and thermistors on the chip. Target analyte detection involve hybridization of the target molecules with label molecules (such as DNA/RNA probes or molecular beacons for detecting nucleic acids, antibodies for detecting proteins, and other probes such as nanoparticles, etc.) which would transduce the “bio signal” to another form; optical, fluorescent, colorimetric, magnetic or electrochemical, etc. Finally compatible sensors are needed on the chip to detect the signal. This would require the integration of conductor and semiconductor material on the chip (metals, semiconductors). Thus, looking at the diversity of the functions and components in an LOC device and the diversity of the materials and processes needed to integrate these functions on the LOC, it is clear that a heterogeneous integration technology is needed on the chip to fabricate LOC devices.

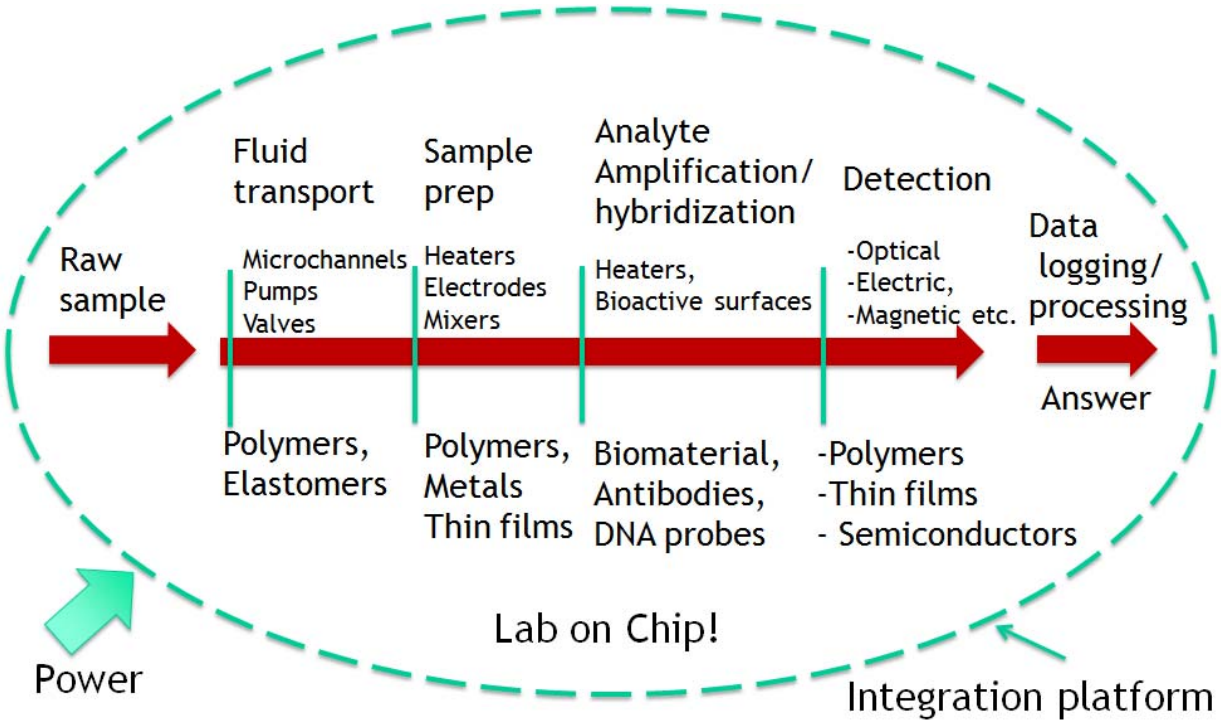

Figure 1-2 Essential functions and components of LOC device

Each component is built with different materials and processes, therefore heterogeneous integration is needed for LOC devices

1.3. State of The Art in Integrated Microfluidics

Current microfluidic chips are rather simple and passive. They consist of microfluidic channels molded in polymers or etched in glass as shown in figures 1-1a, 1-3 and 1-4, and at best they might incorporate electrodes or resistive heaters [4,7,8]. For example, fluids are often pumped with syringes or external pumps; optical detection is almost entirely performed by optical microscopes and benchtop readers as shown in figure 1-3. The technology lacks standard manufacturing methods and infrastructure to readily produce highly integrated LOC devices in high volumes and low cost. Early

LOC devices were built on silicon substrates because semiconductor industry had mature and standard processes. However, soon it was realized that semiconductors like silicon are not optimum material for building microfluidics due to their high cost and incompatibility with biochemical assays [2,4]. Today Polydimethylsiloxan (PDMS) and glass are the most common materials to rapidly prototype devices for research purposes [7] although integration of active components is not possible in these devices. Highly integrated complex devices have been built in many research laboratories using variety of materials and different fabrication techniques [7,9-11]. However, most of these devices are crafted prototypes for specific applications or research purposes. Each of these devices is fabricated using different choices of materials, design and integration strategies. They do not provide a standard solution for integrated LOC devices.

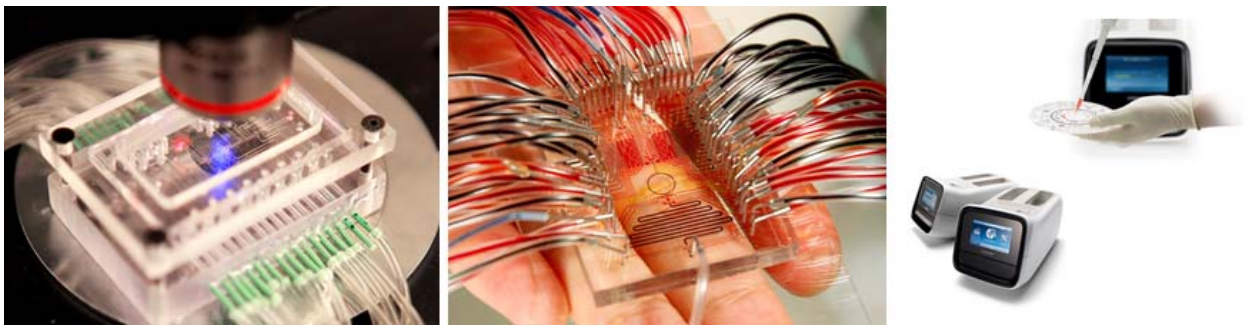

Figure 1-3 State of the art of LOC devices

Most LOC devices are passive microfluidic chips. No components/ functions integrated on chip. Need off-chip/benchtop supporting devices and tools.

The need for standardized integrated microfluidics is also evident in research laboratories where rapid prototyping of LOC devices is required. There is again a lack of standard methods to integrate functions quickly and easily into laboratory prototypes. When a researcher needs to build a microfluidic device with certain functionality, he/she has to custom design and fabricate their entire device. This means that the researcher should either be knowledgeable about the aspects of design and manufacturing of all the components of their microfluidic device, or should seek the assistance elsewhere for this matter.

The commercial sector mainly utilizes injection molding and hot embossing to produce microfluidic devices in high volume [8]. Following these methods it is possible to produce simple disposable chips in thermoplastics and polymers like Poly(methyl methacrylate) (PMMA), as shown in figure 1-4. It is even possible to monolithically integrate heaters and electrodes; however pumps, valves and other fluidic functions and electronic sensors are difficult to incorporate into the polymer chips. Integration of electrodes and resistive heaters is either part of the molding process, by inserting metallic elements into the mold before injecting the polymer (insert molding), or a post molding process that involves deposition and patterning of metal traces on molded chips [8-11].

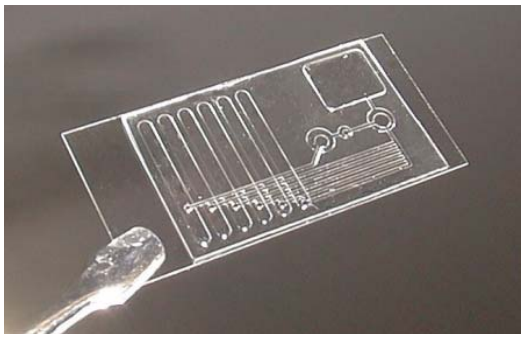

Figure 1-4 A Passive microfluidc chip

Microfluidic chips are fabricated in polymers by injection molding or hot embossing.

Table 1-1 LOC Functions and their integration on chip

Function	Elements	Integration
Fluid Manipulation and Actuation	Channels, Reservoirs	Directly replicated on chip by micro-patterning processes
	Pumps	Not integrated/ off-chip
	Mixers, Valves, droplet generation	Monolithic integration demonstrated, require off-chip pumping/pressure control
	Heaters, Electrodes	Monolithic integration demonstrated
Electrochemical Detection	Electrodes	Monolithic integration demonstrated
Optical detection	Optics	Off-chip/ monolithic integration demonstrated

1.4. PCB Based Microfluidics

The printed circuit board (PCB) is the standard platform for building most of the electronic systems today. Taking advantage of such a standardized platform which also has standard and mature fabrication processes is an attractive idea. Indeed, attempts have been reported to utilize the manufacturing tools and processes of PCBs to either build microfluidic components, such as micro-channels, pumps and valves or to integrate components into the printed circuit board itself [12-17]. Lian *et al.* [14] used the PCB as a platform for building a DNA sensing system. As part of the design, they monolithically integrated resistive heaters into the layers of the printed circuit boards to reach hybridization/detection temperatures of 35–40◦C enabling on-chip hybridization and electrochemical detection. Kontakis *et al.* [15] presented a PCB based microfluidic system, which was again monolithically integrated with an array of thermal sensors to monitor flow rates in a microchannel fabricated on top of the PCB using SU-8 photoresist and PMMA, as shown in figure 1-5. The sensors were built by sputtering a thin layer of platinum on a layer of SU-8, prior to the channel fabrication. Wu *et al.* [16] presented a modular integration approach to combine microfluidics with standard electronic components using PCB. Electronic chips were flipped and mounted on the bottom side of the PCB, whereas previously drilled access holes on the PCB maintained an interface between the microfluidic channel on the topside of

the PCB and the active area of the sensor underneath. The microfluidic part was built in glass and temporarily bonded to PCB using a layer of PDMS. In droplet based microfluidics, Gong *et al.* [17] demonstrated that multi-layer PCBs are very suitable for device fabrication. The device consisted of two boards aligned against each other and each had an array of electrodes (copper pads in this case) covered with dielectric material. Droplets of fluid were sandwiched between the two boards and manipulated using the electro-wetting phenomenon.

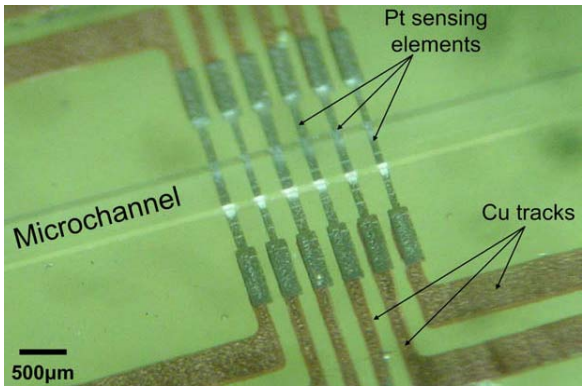

Figure 1-5 Monolithically integrated electrodes in PCB based microfluidics (example from literature) [15]

1.5. Summery

As of today, standard micro-molding and mass production techniques of polymer microfluidic chips are not capable of producing highly functional, integrated microfluidic LOC devices. However, they allow for monolithic integration of some simple functionality on the chip. On the

other hand, most of the integrated microfluidic devices are laboratory prototypes built for research purposes and designed for one specific application or experiment. Single functions are usually integrated on the chip with monolithic processes which may not be suitable to integrate other functions on the same chip. Therefore, they do not provide a standard solution for scaled fabrication of integrated LOC devices. Standardized fabrication and integration methods for microfluidics are much needed and are very essential for the wide and successful application of LOC technology.

Post semiconductor manufacturing processes (PSM) [24] such as the PCB and the packaging of electronic components represent very attractive technologies to fabricate standard integrated LOC devices. These processes are mature and standardized and feature high resolutions that allow manufacturing at micro scale. They provide the designer with a wide range of materials that can be incorporated on the same substrate allowing the making of optimized and standardized devices for LOC applications. In this work it will be demonstrated that PSM processes are very compatible and feasible to produce highly functional and cost effective standardized microfluidic LOC devices, and therefore the PCB can be a heterogeneous integration platform for fabricating integrated microfluidics.

1.6. References:

1. A. van den Berg , T.S.J. Lammerink "*Micro Total Analysis Systems: Microfluidic Aspects, Integration Concept and* Applications" Topics in Current Chemistry, (1998)Vol. 194
2. G. M. Whitesides, *"The Origins and the Future of Microfluidics"* Nature 2006, 442, 368–373
3. H. Becker "*Microfluidics: a technology coming of age"* Med Device Technol (2008) 19:21–24
4. M. Biehl, T. Velten "*Gaps and Challenges of Point-of-Care Technology*" IEEE Sensors Journal, Vol. 8, No. 5, May 2008
5. C. D. Chin, V. Linder, and S. K. Sia, *"Commercialization of microfluidic point-of-care diagnostic devices.,"* Lab Chip, vol. 12, no. 12, pp. 2118–34, Jun. 2012.
6. S. The, R. Lin, L. Hung and A. P. Lee "*Droplet microfluidics"* Lab Chip, 2008, 8, 198–220
7. J. C. Mcdonald, G. M. Whitesides "*Poly(dimethylsiloxane) as a material for fabricating microfluidic devices"* Acc. Chem. Res. 35, 491 (2002).
8. U. M. Attia, J. R. Alcock "*Integration of functionality into polymer-based microfluidic devices produced by high-volume micro-moulding techniques"* Int J Adv Manuf Technol (2010) 48:973–991
9. P. D.,G. George, S. Tiwari, J. Goettert "*Monolithic fabrication of electro-fluidic polymer microchips"* Microsyst Technol (2009) 15:463–469
10. Shize Qi *et al.* "*Microfluidic devices fabricated in poly(methyl methacrylate) using hot-embossing with integrated sampling capillary and fiber optics for fluorescence detection"* Lab Chip, 2002, 2, 88–95
11. L. Hartley, K. Kaler, O. Yadid-Pecht "*Hybrid Integration of an Active Pixel Sensor and Microfluidics for Cytometry on a Chip"* IEEE Transactions on Circuits and Systems-I:Regular papers, Vol. 54, No.1, January 2007
12. Ansgar Wego, Stefan Richter, Lienhard Pagel *Fluidic microsystems based on printed circuit board technology J. Micromech. Microeng. 11 (2001) 528–531*
13. A. Wego, L. Pagel "*A self-filling micropump based on PCB technology* " Sensors and Actuators A 88 (2001) 220-226
14. K. Lian *et al. "Integrated microfluidic components on a printed wiring board platform"* Sensors and Actuators B 138 (2009) 21–27
15. K. Kontakis *et al. "A novel microfluidic integration technology for PCB-based devices: Application to microflow sensing"* Microelectronic Engineering 86 (2009) 1382–1384
16. A. Wu, L. Wang, E. Jensen, R. Mathies, B. Boser "*Modular integration of electronics and microfluidic systems using flexible printed circuit boards"* Lab Chip, 2010, 10, 519–521

17. J. Gong *et al.* "*Two-Dimensional digital microfluidic system by multi-layer printed circuit board"* Micro Electro Mechanical Systems, 2005 726 – 729
18. A. M. Foudeh, T. F. Didar, T. Veres, and M. Tabrizian, "*Microfluidic designs and techniques using lab-on-a-chip devices for pathogen detection for point-of-care diagnostics.,*" Lab Chip, vol. 12, no. 18, pp. 3249–66, 2012.
19. V. Afanassiev, V. Hanemann, and S. Wölfl, "*Preparation of DNA and protein micro arrays on glass slides coated with an agarose film"* Nucleic Acids Res., vol. 28, no. 12, p. E66, 2000
20. E. Eteshola and D. Leckband, *"Development and characterization of an ELISA assay in PDMS microfluidic channels,"* Sensors Actuators, B Chem., vol. 72, no. 2, pp. 129–133, 2001.
21. Y. S. Shin, K. Cho, S. H. Lim, S. Chung, S.-J. Park, C. Chung, D.-C. Han, and J. K. Chang, *"PDMS-based micro PCR chip with Parylene coating,"* J. Micromechanics Microengineering, vol. 13, no. 5, pp. 768–774, 2003.
22. S. Lutz, P. Weber, M. Focke, B. Faltin, J. Hoffmann, C. Müller, D. Mark, G. Roth, P. Munday, N. Armes, O. Piepenburg, R. Zengerle, and F. von Stetten, *"Microfluidic lab-on-a-foil for nucleic acid analysis based on isothermal recombinase polymerase amplification (RPA),"* Lab Chip, vol. 10, no. 7, p. 887, 2010.
23. D. M. Tourlousse, F. Ahmad, R. D. Stedtfeld, G. Seyrig, J. M. Tiedje, and S. a Hashsham, *"A polymer microfluidic chip for quantitative detection of multiple water- and foodborne pathogens using real-time fluorogenic loop-mediated isothermal amplification.,"* Biomed. Microdevices, vol. 14, no. 4, pp. 769–78, 2012.
24. Mark Bachman and G.-P. Li *"MEMS in Laminates"* Electronic Components and Technology Conference (ECTC), 2011 IEEE 61st

2. THE PRINTED CIRCUIT BOARD INTEGRATION PLATFORM

In this work, the Printed Circuit Board (PCB) is proposed as a heterogeneous integration platform for LOC devices. The PCB supports modular integration of components and functions. Following the model of electronic systems, a modular integration could be adopted for LOC devices by introducing a new set of fluidic, electrical, mechanical and optical components that are in the form factor of surface mount electronic components and also could be mounted on the PCB in a similar "pick and place" fashion. This approach would promote standardized, scalable, customizable and cost effective fabrication of LOC devices. These components could be designed, optimized and made available off-the-shelf, to be readily integrated in an LOC device. Another important feature of the PCB is its laminate architecture which supports the heterogeneous integration of different materials and functions on the board. An example of such highly integrated PCB is demonstrated by Hwang et al in [1], and shown in figure 2-1a. The cross section of the PCB shows a variety of laminate materials; copper for electric interconnects, dielectric laminates such as glass-reinforced epoxy laminate sheets (FR4) for insulation and polymer films for optical communication between components on the board. On the other hand, the heterogeneous 3D integration of functions and system components are also found today inside the packages of surface mount electronic components, as demonstrated by Lau in [2], and shown in

figure 2-1b. The fabrication tools and processes of the PCB and microelectronics packaging are already well developed and adapted to support heterogeneous and 3D integration on the board and inside the surface mount package. Examples of such processes are molding, lamination, photolithography, embossing, machining, electroforming etc.

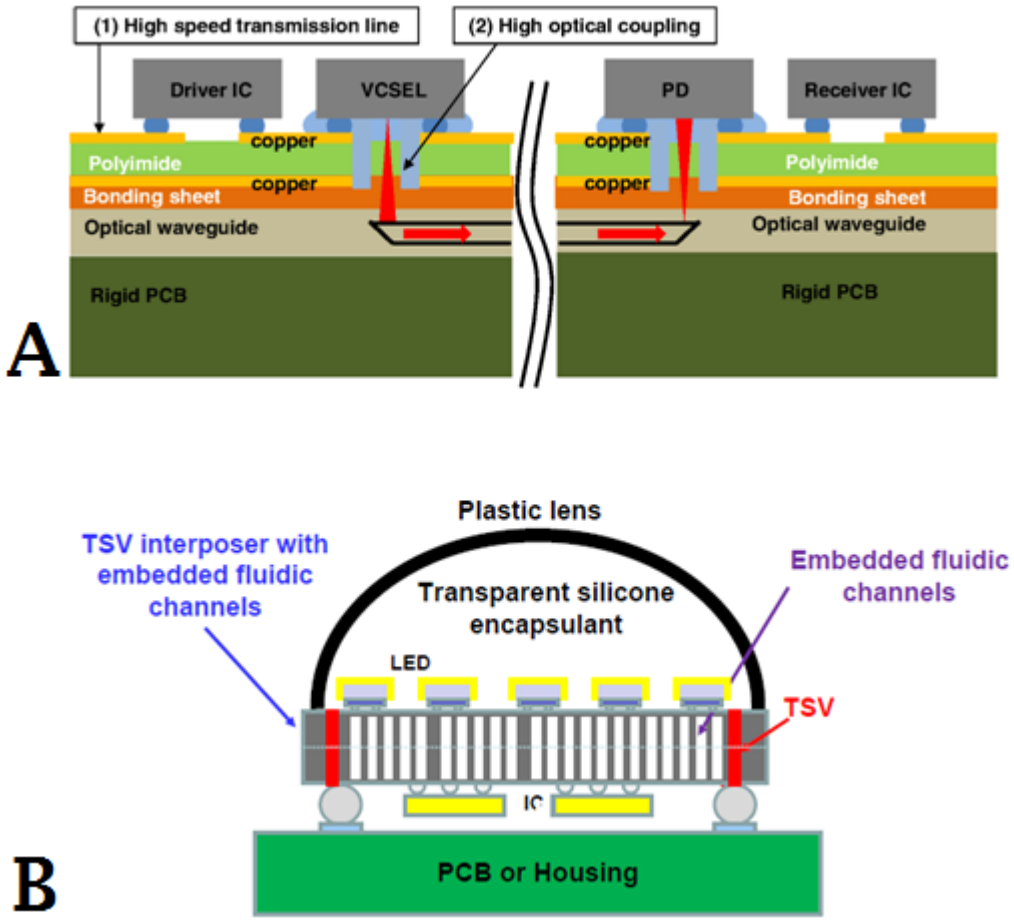

Figure 2-1 Heterogeneous integration in PCBs and in micro electronic component packsging

Examples from the literature. A: by Hwang *et al.* [1]. B, by Lau [2]

Nonetheless, specific adaptations are required to the architecture of the PCB in order to accommodate the fluidic, electro-mechanical and optical components and layers of an LOC device. This proposed architecture is shown in figure 2-2 and shall be called the “microfluidic PCB” hereafter [3]. The microfluidic PCB is a multi-layer device, demonstrated in an exploded form in figure 2-2 and by a sectional view in figure 2-3. The first layer is the electronic layer, and consists of conventional PCB and the surface mount active components of the device (fluidic, electric, optical, etc.) The second layer is an encapsulation polymer layer that encapsulates the electronic layer and forms a smooth, planarized surface for the microfluidic layer. The third layer is the microfluidic layer which is also a polymer layer and houses the microchannels of the device. An optional PCB layer could also be added on top of the microfluidic layer as required by the design of a specific device. Figure 2-3 shows a cross-sectional view of the microfluidic PCB and demonstrates the fluidic and electrical interconnections between the different layers and components of the device. In order to realize this architecture, compatible polymer lamination and patterning processes are needed to be explored and developed to demonstrate a feasible fabrication process. In general polymers are the ideal materials for laminating the encapsulation and fluidic layers on the PCB due to their properties which satisfy the process requirements and the physical requirements of these layers. Polymers can be readily laminated, cast or molded to form rigid or flexible layers on the PCB. Also, polymers can be optically clear and are

generally inert and can be made compatible with bio-chemical assays. However, there are significant challenges in the fabrication processes of microfluidic PCBs which will be discussed in the following chapter.

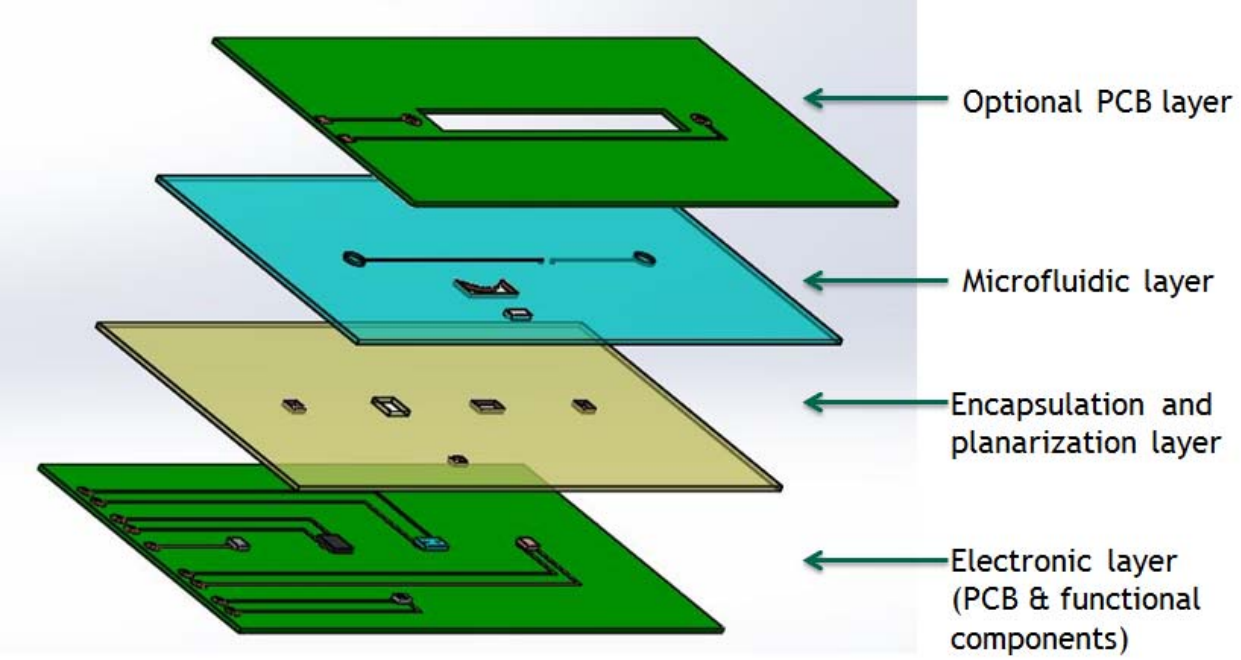

Figure 2-2 The Microfluidic PCB architecture

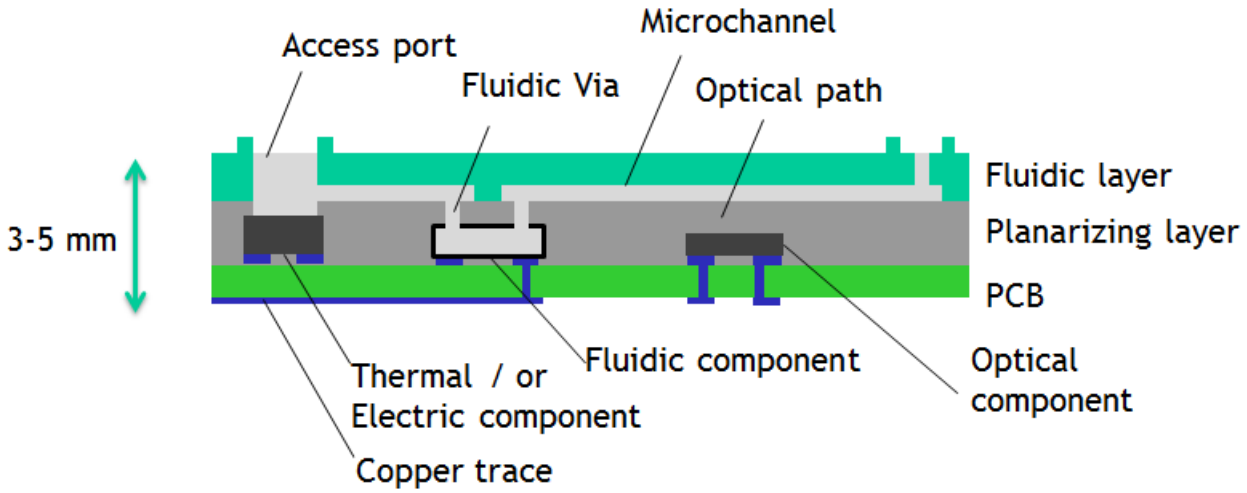

Figure 2-3 Section view of the microfluidic PCB

2.1.Refernces

1. S.H. Hwang *et al. "Vertical waveguide structure optical printed circuit board based on a low-dielectric and transparent PCB materials"* Optical Engineering 54(2), 025112
2. Lau, *"TSV for 3D integration,"* McGraw-Hill, 2012
3. Liang Li Wu, Sarkis Babikian, Guann-Pyng Li, and Mark Bachman *"Microfluidic Printed Circuit Boards"* Electronic Components and Technology Conference (ECTC), 2011 IEEE 61st 1576 - 1581

3. LAMINATE MATERIALS FOR MICROFLUIDIC PCBS

In order to fabricate the microfluidic layers on the PCB, several polymers were investigated and compatible fabrication processes for each polymer type was developed. These processes involve series of casting/lamination, planarization and patterning steps, which are scalable and cost effective. Eventually they produce rigid or flexible layers on the PCB that are perfectly clear, perfectly sealed and form adequate bonding to the PCB substrate. Figure 3-1 shows a number of microfluidic PCB prototypes fabricated on rigid (FR4) PCB substrates. These prototypes also feature standard electronic components that were mounted on the PCB and encapsulated in the polymer layers to add functionality to the device. Figure 3-2 shows flexible microfluidic devices for smart bandage applications. They are fabricated on flexible (polyester) PCB substrates using soft, rubbery polymer laminates which are conformable and can be worn on the body.

Polymers could be broadly categorized to thermosets and thermoplastics. From the group of thermosets polyurethane PU202 (Crystal Clear 202 from Smooth on Inc.) and epoxy based photoresist polymer (1002F in-house made) were investigated in this work to fabricate rigid microfluidics on the PCB [1]. From the group of thermoplastics Ethylin Vinyl Acetate (EVA) was identified as a suitable laminate film for rigid or flexible microfluidics [2]. In addition to these materials, it was demonstrated that the PDMS (Sylgard 184 Silicon Elastomer from Dow Corning Inc.), which is

the most popular and standard elastomer for prototyping microfluidics, is also feasible for fabricating microfluidic PCBs [3, 5].

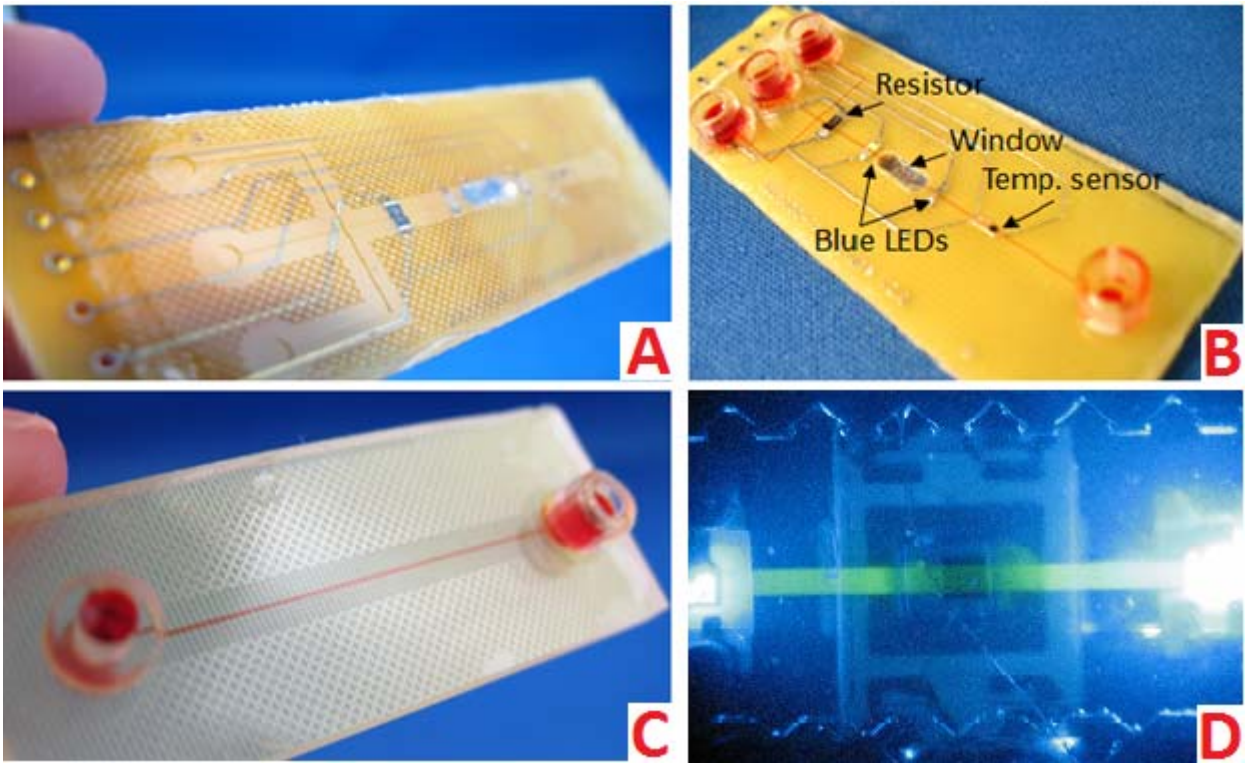

Figure 3-1 Microfluidic PCBs on rigid FR4 substrate

A&B: 1002F laminated on PCB. C: polyurethane laminated on PCB. D: EVA laminated on PCB

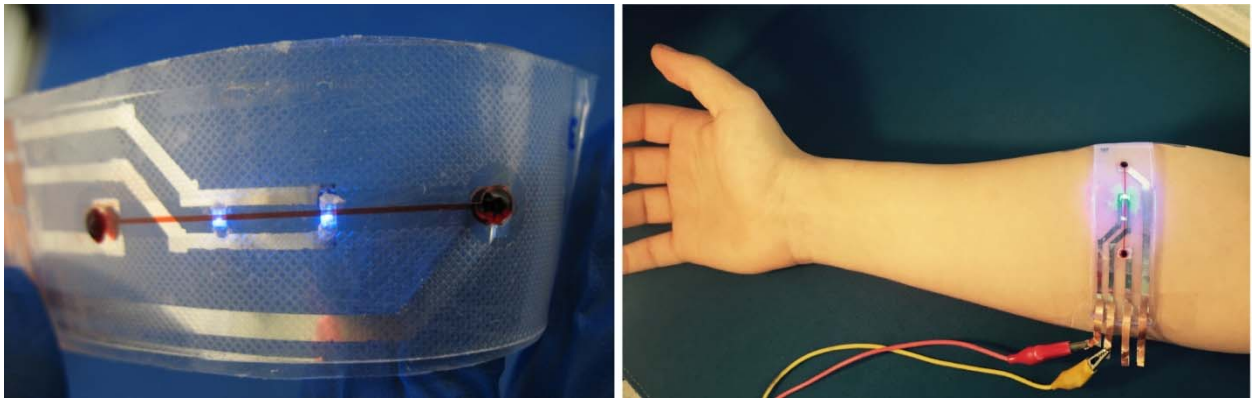

Figure 3-2 Microfluidic flexible PCBs on flexible polyester substrate and laminated EVA or PDMS [2,3]

3.1. Fabrication processes

The general process diagram of fabricating microfluidic PCBs is shown in Figure 3-1. The electronic and microfluidic layers are fabricated separately and stacked and bonded together in the final step. The electronic layer is fabricated by first fabricating the PCB with conventional PCB process, then mounting the surface mount active components on the board and finally encapsulating and planarizing the layer with polymer laminate. The microfluidic layer is molded or laminated and patterned in a parallel process and preferably using the same polymer used for encapsulating the electronic layer, in order to produce microchannels with identical channel walls.

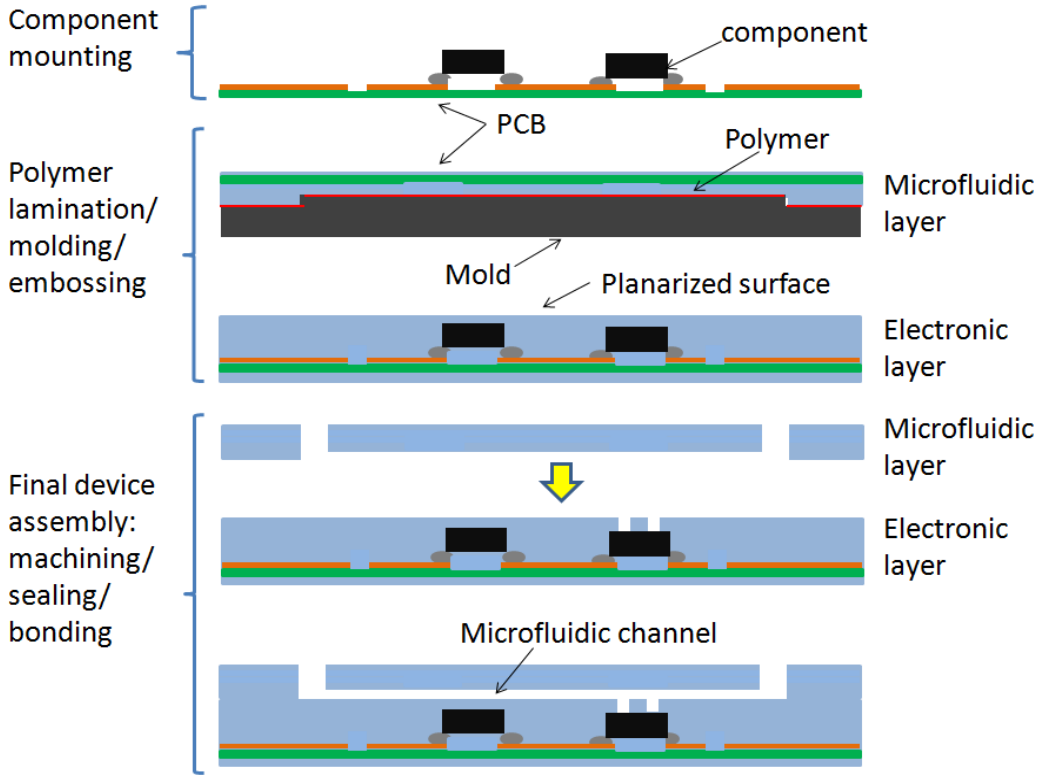

Figure 3-3 General fabrication process diagram for microfluidic PCBs

Each polymer material has its unique fabrication process and parameters and each material produces unique surface properties. Figure 3-4 highlights the differences in lamination and patterning methods of each material. EVA and 1002F are initially in solid phase. Their lamination is performed by heating the materials to their melting points (where they turn into a viscous phase) on the substrate and pressing against a Saline coated hydrophobic planar surface. In contrast the PU202 is liquid in its initial phase. The lamination is performed by casting liquid polyurethane on the substrate and letting to polymerize at controlled temperature until it reaches a soft phase where it would be pressed against Saline coated planar surface. The thicknesses of the laminated layers were controlled by spherical glass spacers embedded in the layers during the process. PDMS and polyurethane may also be casted in an open mold and cured at controlled temperature. The methods for transferring microfluidic patterns to the polymer layers also defer by the polymer type. Microfluidic patterns are transferred to 1002F either by a photolithographic process or by hot embossing. EVA and PU202 on the other hand are patterned by hot embossing and room temperature embossing (at the soft phase), respectively. In all processes sealing of microchannels is readily achieved by the flip-bonding of the microfluidic layer to the planarized layer. However, the bonding method may range between thermal bonding for EVA and 1002F, semi cured surface bonding for the polyurethane and plasma bonding for PDMS. Access ports/ fluidic vias are formed by

photolithography in the 1002F which would produce very clean cuts without debris. In EVA and PU202 and PDMS processes fluidic vias are more challenging to form and require precision machining or laser cutting, which would also produce debris that may clog the microfluidic channels if not thoroughly cleaned. Table 3-1 summarizes this discussion. The following is a detailed description of each polymer process.

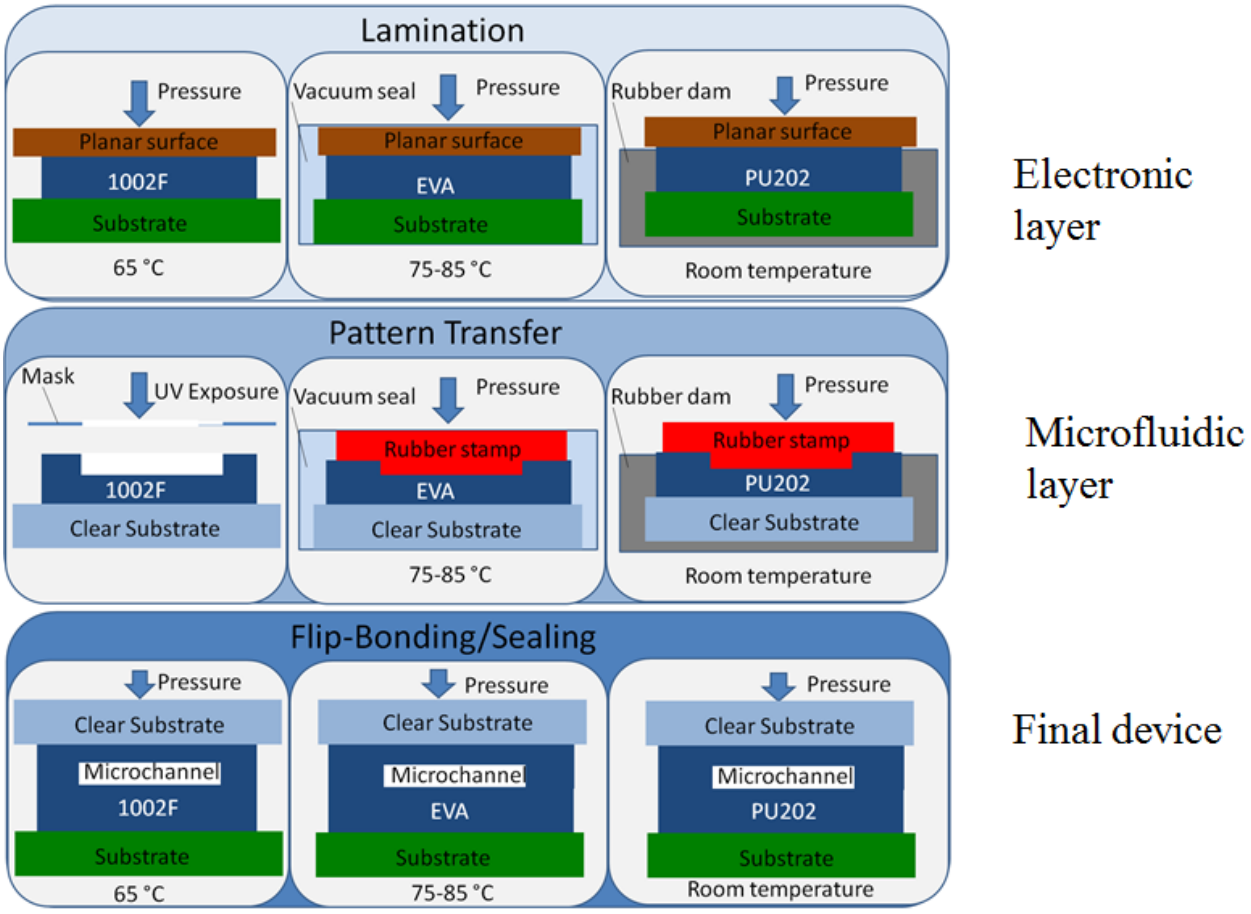

Figure 3-4 Lamination and patterning of 1002f, EVA and PU202 polymers

Table 3-1: Process parameters for EVA, 1002f, polyurethane and PDMS.

	EVA	1002F	Polyurethane	PDMS
Polymer type	Thermoplastic elastomer	Photoresist	Thermoset	Elastomer
Uncured phase	Dry film	Dry pellet	Liquid (2 part reaction polymer)	Liquid (2 part reaction polymer)
Pattern transfer	Hot embossing	Lithography /hot embossing	Embossing/ casting	Casting
Process temperature	75-95 °C	65-110 °C	Room temp. /or ~70 °C	~70 °C
Process time	~30 min	~60 min	~3 hours / or 60 min	~60 min
Bonding process	Heat & press	Heat & press	Semi cured surface & press	Plasma treatment
Holes	Machining	Lithography	Machining	Puncture

3.1.1.Polyurethane:

Polyurethanes are classified as thermoset reaction polymers [6]. Polyurethane is produced through a step growth polymerization process. Industrial polyurethanes are produced by the reaction of two liquid parts that form a system: isocyanate (Part A) and a blend of polyalcohols, catalyst and other additives (Part B). The two parts would be mixed together in specific ratios by weight or by volume and would be cured at room temperature or at elevated temperature (60-70 ºC) for accelerated polymerization. The PU202 polyurethane system had a 10:9 by weight mixing ratio of parts A and B according to the manufacturer. Two lamination and patterning processes were developed: soft embossing and casting, as shown in figure 3-5. The embossing is performed by first placing the PCB in a special container. Then liquid polyurethane PU202 is poured on the PCB with mounted electronics, in order to encapsulate the PCB board. The polyurethane is left to polymerize for 45 minutes at room temperature until it reaches a soft phase. At the soft phase the PU202 has a dough-like structure which could be embossed easily by a soft rubber stamp, such as negatively patterned PDMS stamp. Or it could be pressed and planarized with Saline coated planar surface. For the mold casting method, a double-casting process was used where the patterns were transferred onto PDMS initially and polyurethane subsequently. PDMS was chosen as an intermediate casting mold due to its flexible, rubbery nature, good precision of reproduced patterns and anti-adhesion to most surfaces. In the first stage,

a negative pattern would be transferred from a positively patterned silicon wafer to the PDMS by casting the PDMS against the wafer, degassing and curing at 65º C. In the second stage, a positive pattern would be transferred to the polyurethane by casting the polyurethane against the PDMS mold. Casting the liquid polyurethane against the PDMS mold resulted formation of undesired air bubbles at the interface between the polyurethane and the mold. In order to eliminate the bubbles the mold with cast liquid polyurethane was placed in a vacuum chamber and subjected to a vacuum pressure of 76 cmHg (degassing) for 10 minutes. The degassing eliminated all the air bubbles. The polyurethane was then cured in the oven at 65 ºC. The casting process yielded good results and demonstrated that the polyurethane is capable of reproducing the microfluidic patterns as shown in Figure 3-1 C. Bonding a polyurethane microfluidic layer to a polyurethane planarized layer can be achieved when the planarized layer is not fully cured and exhibits a semi cured tacky surface, at which point a bond can be formed between the two surfaces by gentle press.

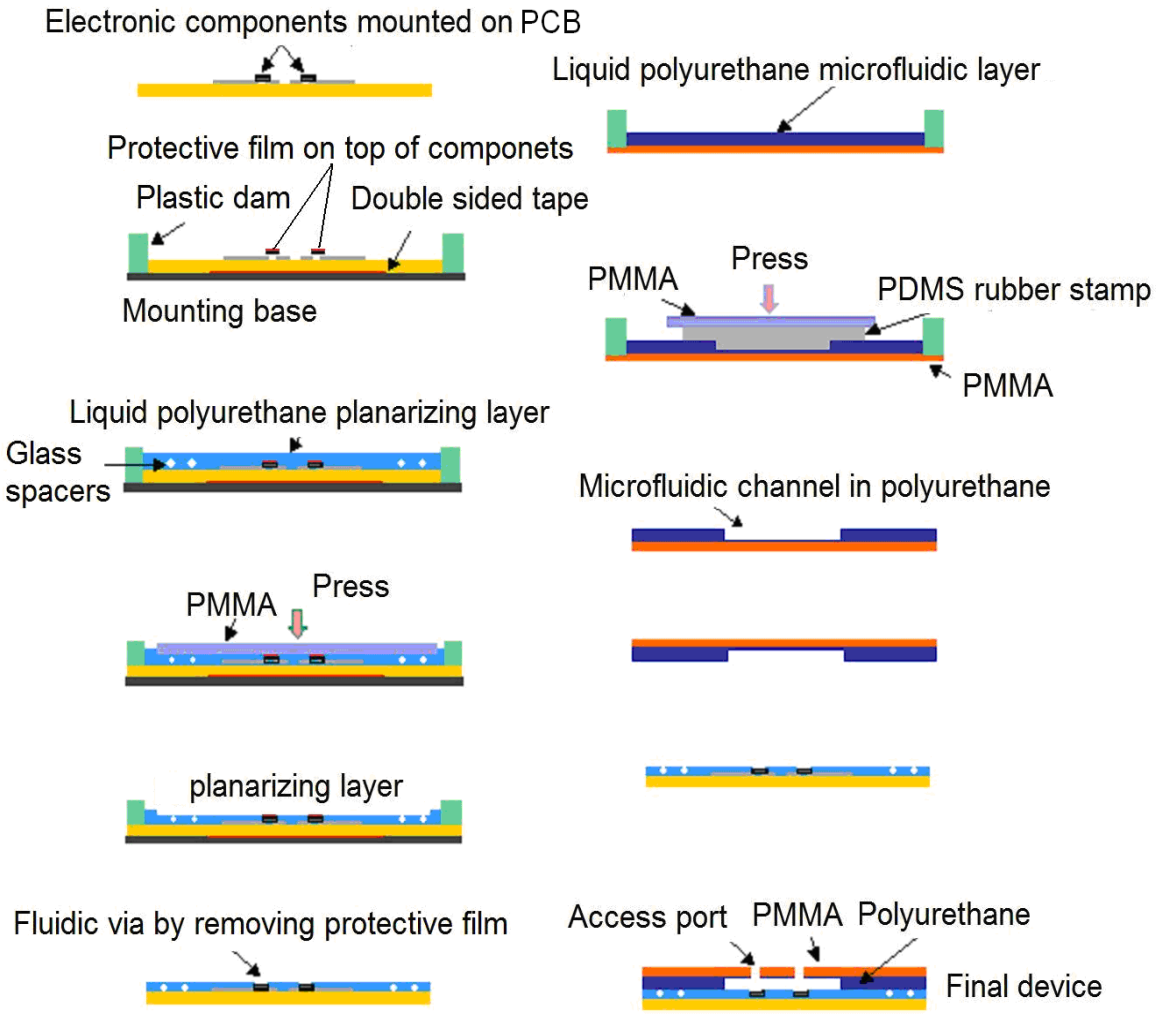

Figure 3-5 Polyurethane lamination and patterning on PCB

3.1.2. 1002F photoresist:

The dry film photosensitive material, 1002F was developed as a lithographically definable, low fluorescence polymer [7]. The negative dry resist was prepared by dissolving EPON resin 1002F (phenol,4,40-(1-methylethylidene)bis-, polymer with 2,20- ((1-

methylethylidene)bis(cyclohexane-4,1-diyloxymethylene)) bisoxirane) (Miller-Stephenson, Sylmar, CA) and UVI-6976 photoinitiator (triarylsulfonium hexafluoroantimonate salts in propylene carbonate (Dow Chemical, Torrance, CA) in acetone at a ratio of 63.2% 1002F resin to 6.3% photoinitiator to 30.5% solvent by weight. The photosensitive resist was then degassed and dried in vacuum oven at 110 ºC and 40 cm Hg until the resist had solidified indicating the complete solvent evaporation.

A lamination, planarization and embossing process was developed for microfluidic PCB fabrication using 1002F [1]. Multiple layers of 1002F can be applied to PCB at different stages in manufacturing, allowing sealed microfluidics to be integrated within multi-layer printed circuit boards. The 1002F-PCB fabrication consists of multi-layer processes using hot pressing and lithography. The fabrication process using the 1002F dry resist is shown in Figure 3-6. A dry 1002F pellet is placed on the PCB substrate with mounted components to be reflowed at 65 ºC, and then hot pressed against a PDMS coated glass slide also at 65 ºC for one minute. PDMS thin layer was used as a mold release by spin-coating and curing on the glass pressing surface. Two spacers with known thickness were incorporated during the hot pressing process to obtain the desired depth of the compressed resist. After release, the PCB surface is planarized and any embedded electronic components would be encapsulated in the 1002F layer. If the electronic component is required to be in contact with the fluidic layer such as temperature sensor, interconnects in planarizing layer could be made by

photolithography using a mask with appropriate openings for UV exposure. The substrate is then developed in SU-8 developer (1-methoxy- 2-propyl acetate, MicroChem Corp.), and followed by hard bake. The fluidic layer can be fabricated in a similar fashion including hot pressing 1002F on planarization layer with spacers to achieve required thickness, UV exposure and developing for desired microchannel pattern. Finally, the device can be sealed with tape or another thin layer of cured 1002F by lamination at 110ºC. Access ports can be prepared using disposable biopsy punches

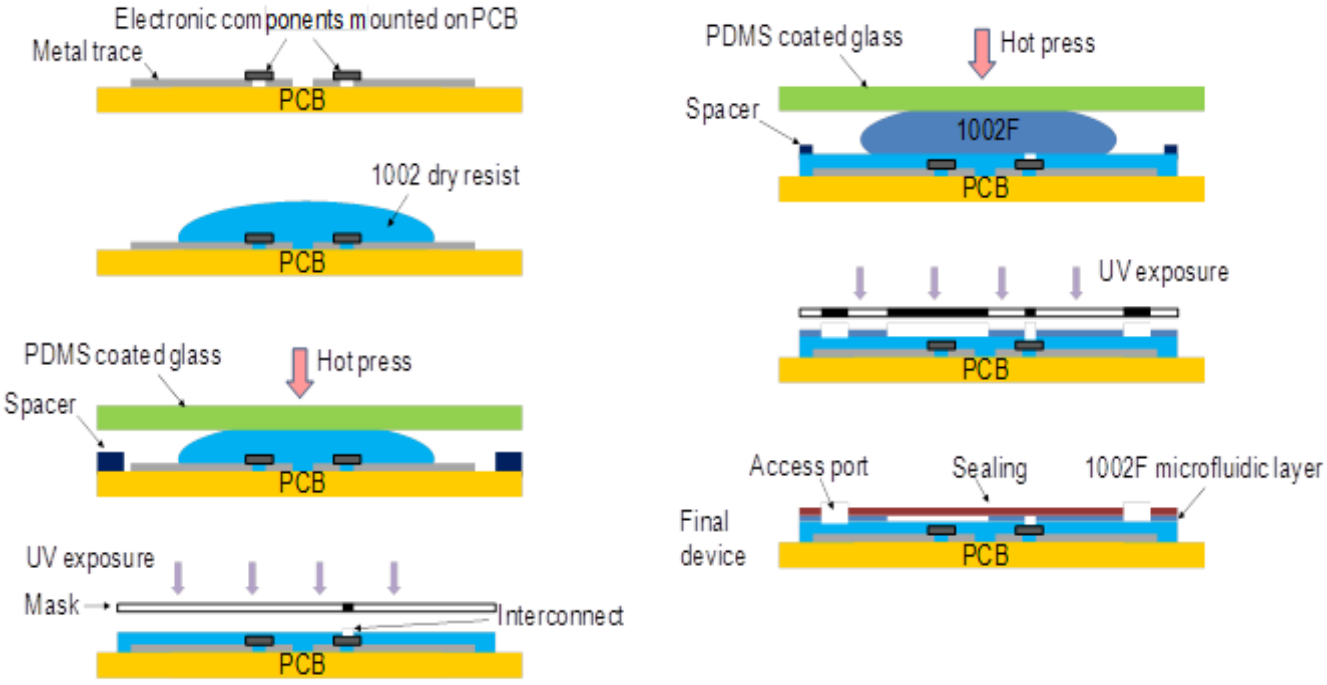

Figure 3-6 1002F photoresist lamination and patterning on PCB

3.1.3.Ethylin Venyl Acetate film:

Ethylene vinyl acetate is elastomer-like thermoplastic traditionally used as encapsulation for solar panels, also as thermal adhesive and as foam rubber for many applications. It is also incorporated in drug delivery devices that would be implanted in the body [8, 9]. The material has attractive properties for microfluidic applications. It is chemically inert, very clear, resistant to UV light, easily moldable by heating and embossing and easily forms adequate bonding to other surfaces. Lamination and patterning of EVA layers on the PCB is achieved by hot lamination and hot embossing procedures. Figure 3-7 illustrates the fabrication step by step. Layers of EVA encapsulation film are placed atop the PCB with mounted components. The assembly is placed within a vacuum press and pressed at 75-85 °C for ten minutes to encapsulate the components on the PCB and planarize the layer. The hot press in vacuum condition is important to avoid introducing air pockets in the EVA layer. Following this the microfluidic layer is fabricated in a similar fashion. Transferring micro patterns to the EVA film is realized by hot embossing the EVA by a rubber stamp which contains negative features. The rubber stamp is made by casting PDMS against a silicon wafer with positive features. The microfluidic layer is fabricated separately on a clear PMMA substrate which gives mechanical support and enhances the rigidity of the layer. Finally the microfluidic layer is bonded to the planarized layer by heating the bond and applying gentle pressure.

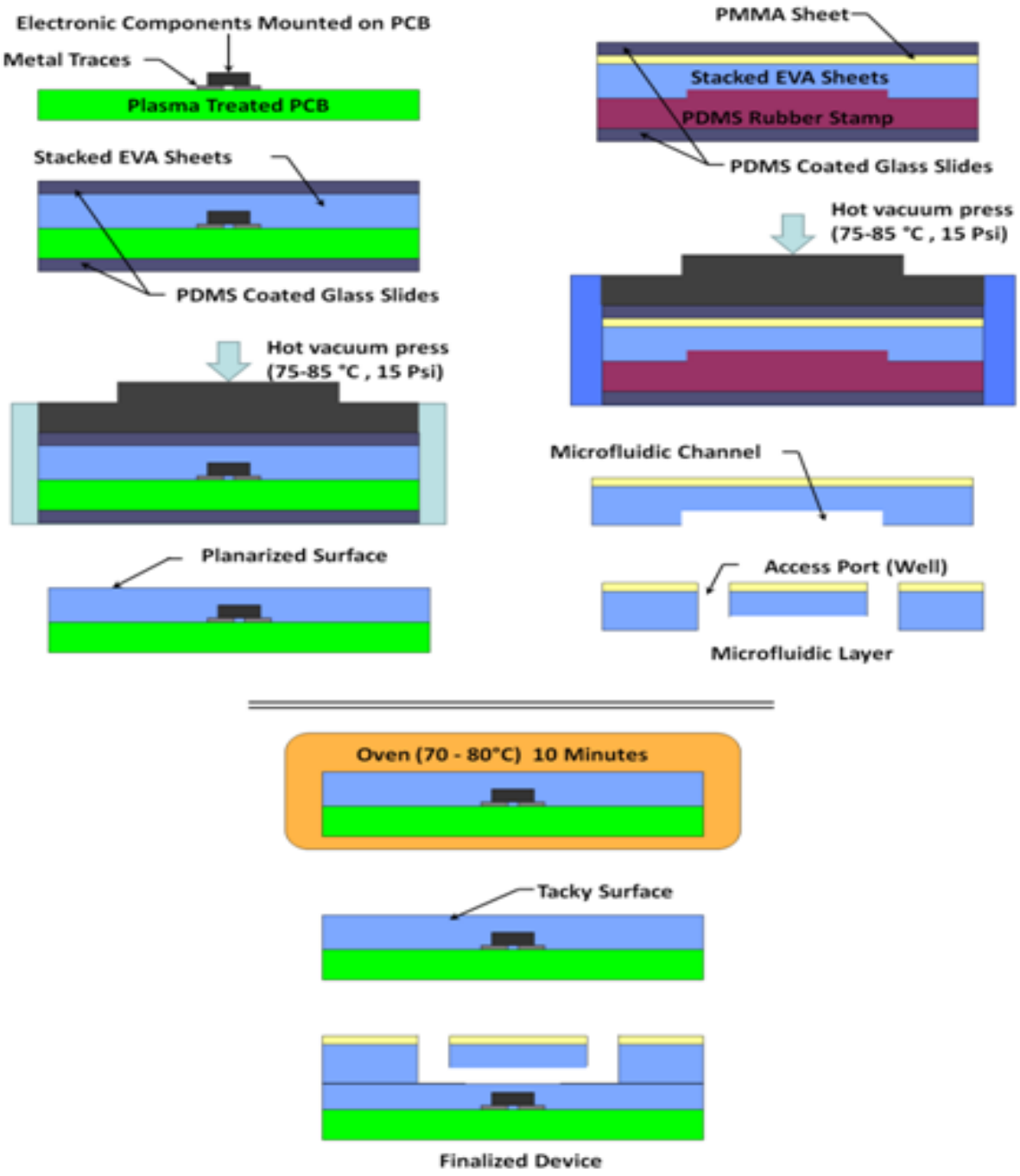

Figure 3-7 EVA lamination and patterning on PCB

3.2. Physical and Surface Properties:

The physical and surface properties of the different layers of the LOC device may have great impact on the performance of the bio-chemical assay implemented on it. Therefore it is important to characterize the materials that are used to fabricate the LOC device and study their compatibility with the bioassays. Some of the important material properties which should be considered in the design of an LOC device include: the surface properties of these materials, such as the wettability of the polymer surfaces and the zeta potential of these surfaces when immersed in liquids, which would affect the flow dynamics (both hydraulic and electrokinetic) in the microchannels of the device. Another important surface property is the adsorption of analytes (such as nucleic acids and proteins) on the material surface, which is usually undesirable inside the microchannels. Other physical properties include the optical clarity of the polymers and the autofluorescence of the materials which may interfere with the fluorescence detection function on the chip if the materials' excitation and emission spectra matches or is very close to that of the fluorescent labels used in the assay. For example, it was noticed that the PCB used in this work exhibited a green autofluorescence, as shown in figure 3-8. This would interfere with the fluorescence imaging on the chip for certain types of beads and fluorophores (such as Fluorescein and Alexa fluor 488).

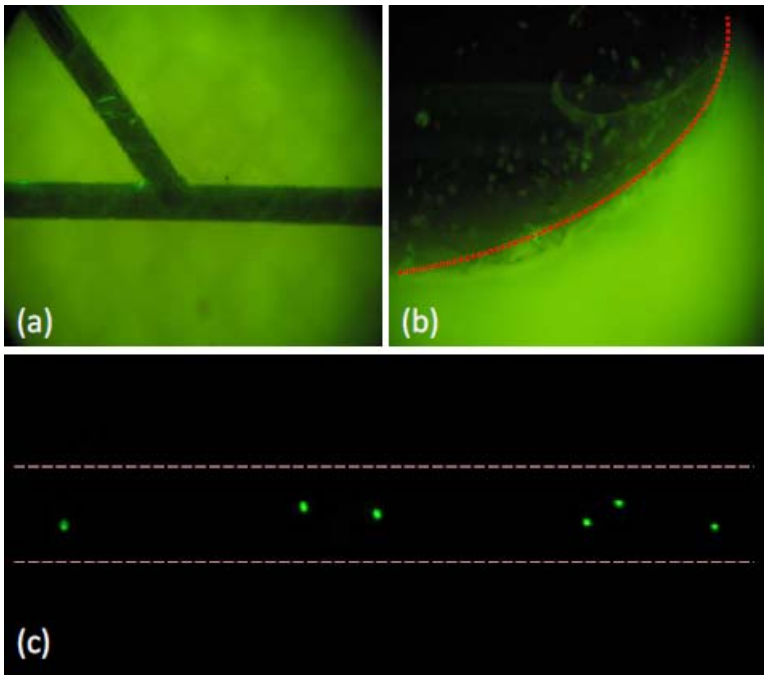

Figure 3-8 The autofluorescence of the PCB interferes with the fluorescence imaging of green beads (a&b). This should be considered in the design of the LOC device. By making "slit cuts" in the PCB this background noise could be eliminated (b&c).

To characterize polymer materials under investigation for microfluidic applications a number of surface properties were examined and measured experimentally in this work. The pattern replication quality, the surface wettability and the electroosmotic flow characteristics were investigated. First the replication quality of the micro features on the polymer surfaces were examined by Scanning Electron Microscopy (SEM). The SEM images of the patterned polymers are shown in figure 3-9. They exhibit very smooth surfaces and straight side walls, indicating the capability of these materials to reproduce quality microfluidic structures.

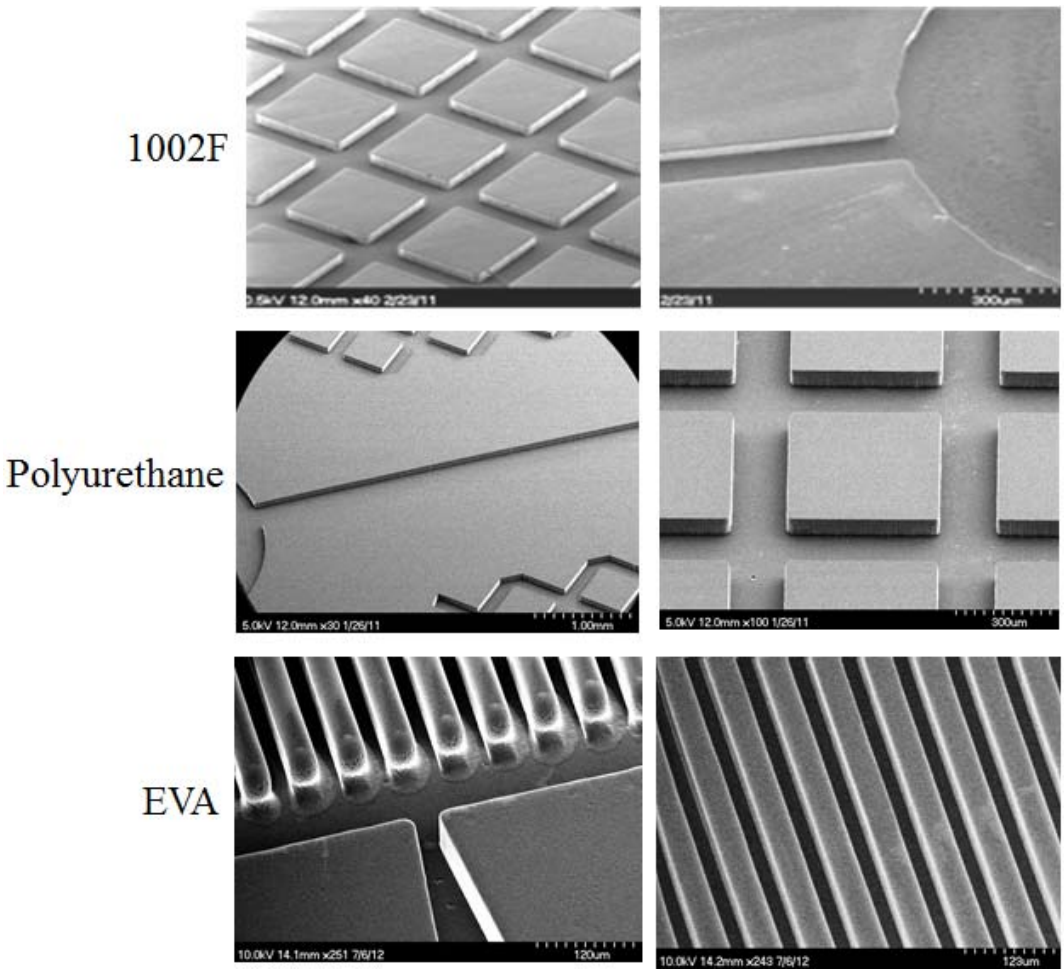

Figure 3-9 Scaning Electron Microscope (SEM) images of patternd 1002f, polyurethane and EVA laminates

3.2.1.Surface wettability:

The wettability of the walls of the microchannels may have great impact on the flow mechanics in these channels and in turn may affect the performance of the LOC device based on the given assay requirements [10,11]. For example, microchannels with hydrophobic walls would resist the flow of the fluid when is loaded to the microchannel. This might be

troublesome for LOC devices intended to perform tests in the field with small droplets of sample. In these devices it is desired to have hydrophilic walls which would facilitate self wicking of the fluids into the microchannels by the capillary forces. In case the microchannel walls are hydrophobic, the channel walls would require an additional surface chemistry to condition the surface properties. For other applications on the other hand, such as droplet based microfluidic devices, it would be desirable to have microchannels with hydrophobic walls. For example, the generation of droplets may require hydrophobic channel walls when water in oil droplets is desired to generate.

The wettability of the polymers' surfaces was measured by measuring the contact angle for each polymer. The contact angle θ at the interface between a liquid and a solid surface is shown in figure 3-10. It is a very useful parameter for characterizing solid surfaces in microfluidic applications. It determines the wettability of a surface. If the contact angle is less than 90 degrees the surface would be more hydrophilic and more wettable. If the θ is greater than 90 degrees the surface would be more hydrophobic and would have poor wettability.

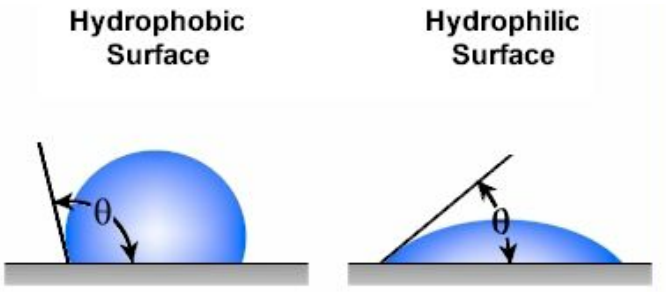

Figure 3-10 Contact angle and surface hydrophobicity

The contact angle can be measured by capturing the profile of a water droplet resting on the solid surface, and measuring the angle between the liquid-solid interface and the liquid-gas interface. Figure 3-11 shows the captured image of 100 µL droplet of pure deionized water on PDMS surface. The images of droplets on PU202, 1002F, EVA and PDMS were taken right after depositing the droplets on the surface, in order to avoid loss of droplet volume over time due to evaporation, and the contact angle was measured from the droplet profile.. The polymers exhibited different wettability as summarized in table 3-2.

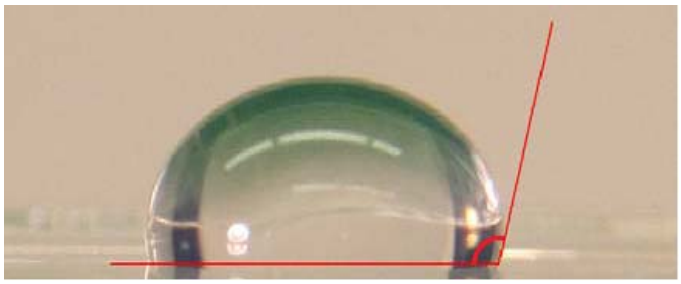

Figure 3-11 Contact angle of water droplet on PDMS

Droplet size is 100 µL

3.2.2.Electroosmotic Mobility:

Electroosmotic flow is the induced flow of liquids under the influence of direct electric field. It is most significant in capillaries and microchannels where inertial forces are negligible [12-14]. It is the result of Coulomb's force acting on the mobile charges in the electric Debye layer resulting in the movement of the entire fluid body in the direction of Coulomb force.

The Debye layer is found at the surface of any object when placed in a liquid. It consists of two layers of electric charges, as shown in figure 3-12. The first layer is a result of chemical interactions between the surface and the liquid and it is anchored to the surface. While the second layer consists of mobile ions from the liquid that get attracted to the anchored charges, however they remain loose and move under the influence of external electric field which causes the motion of the bulk of the liquid.

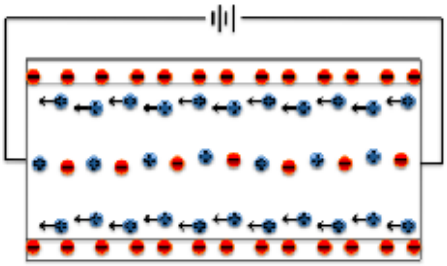

Figure 3-12 Debye layer and electroosmotic flow

The EO flow is characterized by the EO mobility of a given liquid in a well-defined microchannel. The mobility is defined by the change in linear velocity of the fluid with respect to the change in the strength of applied electric field. This ratio is depended on many factors including the material of the microchannel walls, and the pH of the electrolyte. EO flow is often an affecting factor in microfluidic devices e.g., EO pumps are commonly used to drive fluids electro-kinetically through the microchannels. In such devices it is desired to maximize the EO mobility in order to maximize the pumping efficiency. However, in other types of devices, such as capillary electrophoresis devices, the EO flow may negatively affect the

electrophoretic separation [12,14]. Therefore the EO flow is usually suppressed in these devices. Thus, it is important to understand the effect of the channel walls on the electroosmotic mobility of flowing fluids through the channels, especially when strong electric fields are present inside the microchannels.

To estimate the electroosmotic flow (EOF) mobility in microchannels built with the polymers under investigation, straight microchannels were fabricated in PU202, 1002F, EVA and PDMS with dimensions of 300 μm in width x 4 cm in length x 70 μm in depth. The channels were loaded with SDS (Sodium Dodecyl Sulfate) electrolyte (pH=8.3) mixed with 15 μm polystyrene microspheres (Polyscience, Inc.). The concentration of the microspheres was 0.2% by volume. A range of voltages between 200 V and 800 V was applied between the ends of the channels to induce EO flow. The motion of the fluid inside the channel was captured -by monitoring the microspheres- with an inverted microscope and a CCD camera for each applied voltage. The linear velocity of the fluid was calculated at each voltage by analyzing the videos. The linear velocity was plotted versus the electric field strength inside the channel. The electric field was assumed to be uniform. The slope of the obtained line represented the EOF mobility. Figure 3-13 illustrates the experimental setup. Figure 3-14 shows the flow velocity as a function to the electric field inside the microchannel.

The fluid velocity was calculated by measuring the distance (x) that beads traveled in a specific period of time ($T = t_2 - t_1$). This was done by

measuring the distance that a given bead moved between frame 1 at instance t_1, and frame 2 at instance t_2. The velocity was calculated by the following formula:

$$v = \frac{x}{(t_2 - t_1)} \times A \qquad 3\text{-}1$$

$$A = \frac{300\mu m}{d}$$

where A is a scaling factor calculated by dividing the actual width of the channel (300 μm in this case), by the apparent width (d) in the recorded video. After obtaining the EO flow characteristics the EO mobility was calculated according to the following formula:

$$\mu_{EO} = \frac{v_2 - v_1}{E_2 - E_1} \qquad 3\text{-}2$$

where v_2 and v_1 are the fluid linear velocities at electric field strength E_2 and E_1 respectively. The experimental results presented a qualitative evaluation of the four microchannels. The results indicated that each microchannel exhibited a different amount of EO flow, which clearly demonstrates the effect of the microchannel material on the electro kinetic flow inside the channel. The EO flow in PU202 and 1002F channels was higher than the flow in PDMS microchannel, whereas it was lowest in the EVA microchannel.

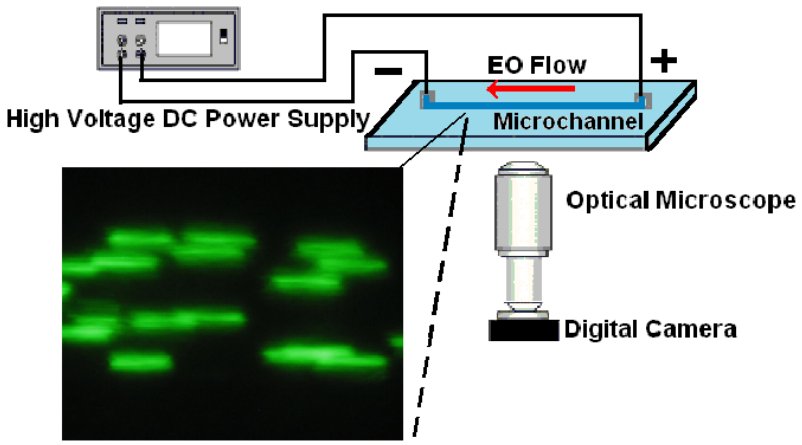

Figure 3-13 Electroosmotic flow experimental setup

Flourecent beads visualizing the EO flow in the microchannel

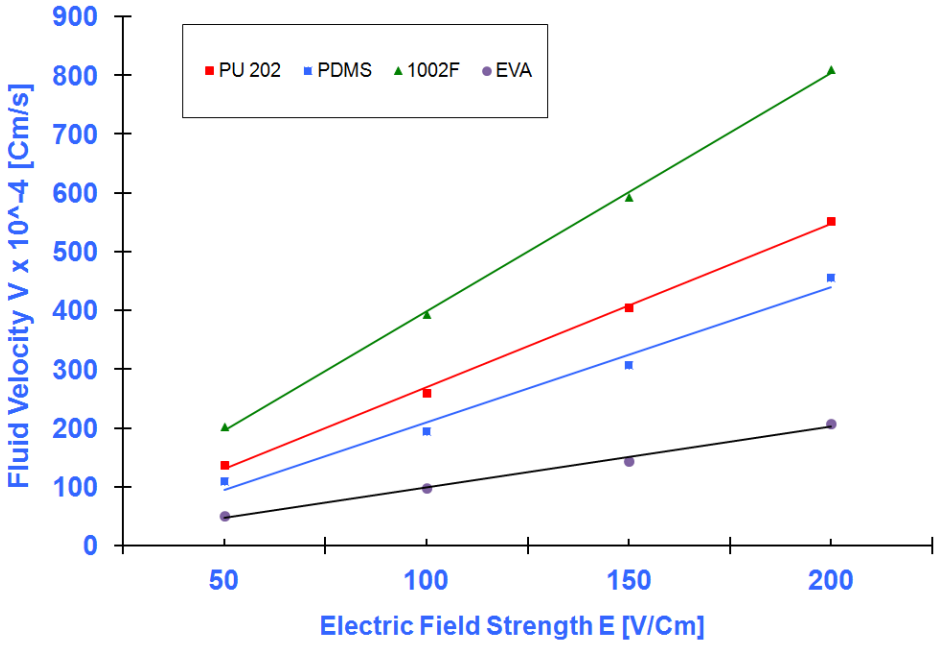

Figure 3-14 EO Flow linear velocity vs. electric field strength inside microchannels made of EVA, 1002F, Polyurethane and PDMS

Table 3-2 Physical and surface properties of EVA, 1002F, polyurethane and PDMS

	EVA	1002F	Polyurethane	PDMS
Surface contact angle θ	83 °	70 °	77 °	99 °
EOF mobility x10^{-4} [cm^2/V.sec]	1.1	3.9	2.9	2.3
Shore hardness	~40A	~80D	~80D	~40A
Index of refraction (n)	1.4~1.6			

3.3. References:

1. Liang Li Wu, Sarkis Babikian, Guann-Pyng Li, and Mark Bachman *"Microfluidic Printed Circuit Boards"* Electronic Components and Technology Conference (ECTC), 2011 IEEE 61st
2. S. Babikian, W. a. Cox-Muranami, E. Nelson, G. P. Li, and M. Bachman, *"Ethylene-Vinyl Acetate as a low cost encapsulant for hybrid electronic and fluidic circuits,"* 2013 IEEE 63rd Electron. Components Technol. Conf., pp. 1800–1805, May 2013.
3. S. Babikian, G. P. Li, and M. Bachman, *"Integrated bioflexible electronic device for electrochemical analysis of blood"* 2015 IEEE 65th Electron. Components Technol. Conf., pp. 685–690, May 2015.
4. S. Babikian, L. Wu, G. P. Li, and M. Bachman, *"Microfluidic thermal component for integrated microfluidic systems,"* 2012 IEEE 62nd Electron. Components Technol. Conf., pp. 1582–1587, May 2012.
5. S. Babikian, G. P. Li, and M. Bachman, *"Portable Micro-Fluidic-Opto-Electronic Printed Circuit Board for Isotachophoresis Applications,"* pp. 1293–1295, 2015.

6. Gum, Wilson; Riese, Wolfram; Ulrich, Henri. *"Reaction Polymers"* New York: Oxford University Press1992
7. Jeng-Hao Pai et al. *"Photoresist with Low Fluorescence for Bioanalytical Applications"* Anal. Chem. 2007, 79, 8774-8780
8. Gilby, *"Ethylene vinyl acetate copolymers, in developments in rubber technologies—3"* Applied Science, London 1982
9. Kalachandra et al. *"Stability and release of antiviral drugs from ethylene vinyl acetate (EVA) copolymer"*, J Mater Sci: Mater Med (2006) 17:1227–1236
10. Zhao, B.; Moore, J. S.; Beebe, D. J. *"Surface-Directed Liquid Flow Inside Microchannels"*. Science 2001, 291, 1023?1026.
11. Tsougeni, K.; Papageorgiou, D.; Tserepi, A.; Gogolides, E. *"'Smart" Polymeric Microfluidics Fabricated by Plasma Processing: Controlled Wetting, Capillary Filling and Hydrophobic Valving."* Lab Chip 2010, 10, 462?469
12. Shadpour, H., Musyimi, H., Chen, J. F. and Soper, S. A., *"Physiochemical properties of various polymer substrates and their effects on microchip electrophoresis performance",* Journal of Chromatography A, vol. 1111 (2006), pp. 238-251
13. K. D. Lukacs and J. W. Jorgenson *"Capillary Zone Electrophoresis: Effect of Physical Parameters on Separation Efficiency and Quantitation"* Journal of High Resolution Chromatography Vol 8, Issue 8
14. James W. Jorgenson, Krynn DeArman Lukacs *"High-resolution separations based on electrophoresis and electroosmosis"* Journal of Chromtography, 218 (1981) 209-216

4. FLUIDIC ELECTRO MECHANICAL SURFACE MOUNT COMPONENTS (FLEMS)

In previous chapters, the methods and materials for fabricating and integrating the microfluidic device on PCB with surface mount components have been discussed. By adopting these methods, it would be possible to utilize many standard off-the-shelf electronic components such as LEDs and optical sensors, etc. on the chip, as shown earlier. However, other components or functions of importance to LOC devices are not readily available. Therefore it is proposed to design and package such components in standard, surface mount form factor. This approach would resolve several of the heterogeneous integration challenges that were discussed in chapter 1. Packaging each component (sensor, actuator, etc.) in standard surface mount form factor:

- Resolves the problem of material diversity and compatibility in the integrated device
- Enables optimization and scaled production of each component (Standard microfluidics)
- Minimizes waste of valuable material (as opposed to monolithic fabrication methods)

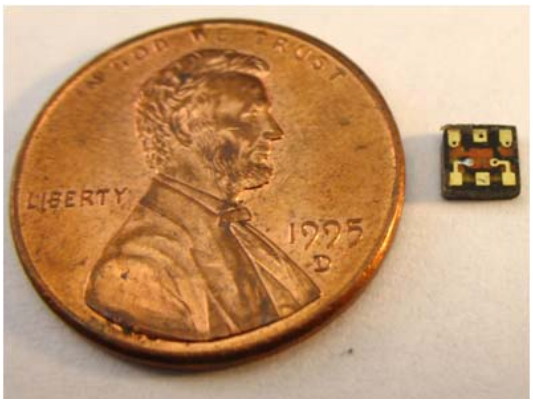

Figure 4-1 FLEMS component next to a penny

This chapter will describe the process of designing, building, and testing specialized microfluidic electro-mechanical surface mount (FLEMS) components. Figure 4.2 shows a set of FLEMS components that were designed for integration in microfluidic PCBs and characterized for LOC applications. Some of these components, such as light emitting diodes (LEDs) and CMOS imaging arrays are standard off-the-shelf devices. Whereas others, for example the electrode, the thermal component, the droplet generator, the coulter counter and the light reflector, were designed and fabricated in this work for the purpose of integrating specific functions in microfluidic PCBs that were designed for specific LOC applications as will be demonstrated in chapter 5.

FLEMS components can be generally categorized to three types:

- Components with direct contact with fluids; such as electrodes and heaters.

- Components with fluid passing through; such as pumps, valves, droplet generators, mixers, etc.
- Components that are isolated from fluids; such as optical components

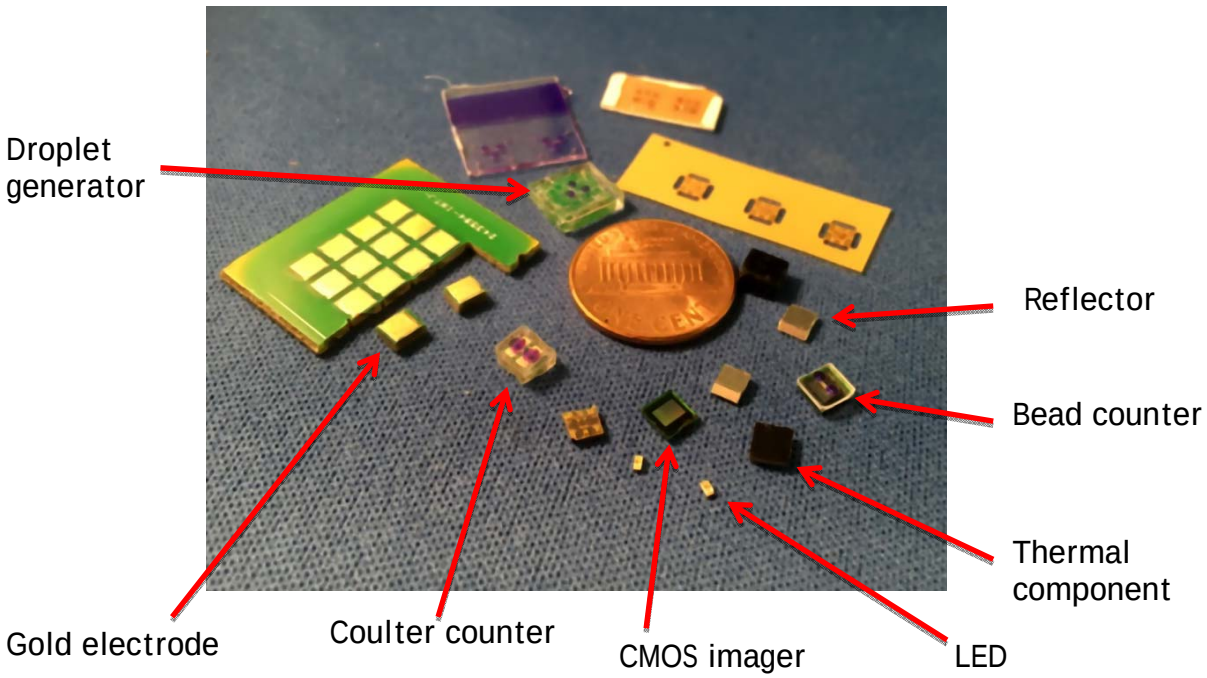

Figure 4-2 FLEMS components

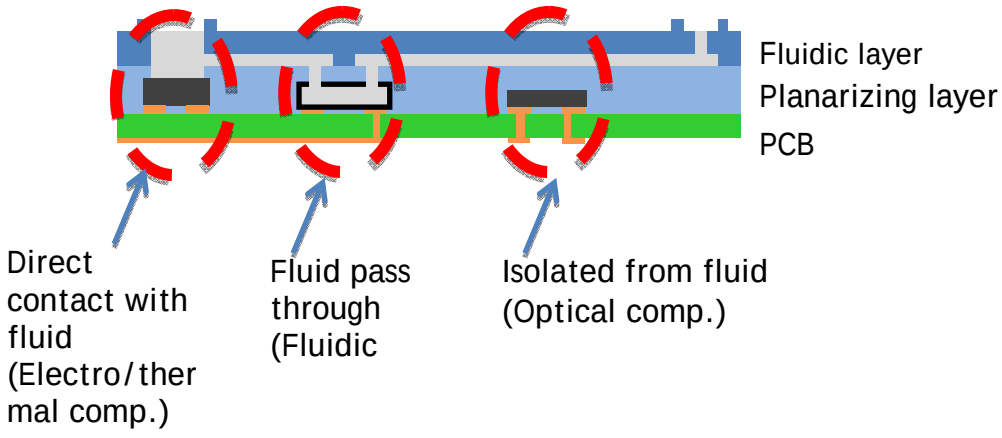

Figure 4-3 Types of FLEMS components

The surface mount packaging greatly standardizes the component and function integration on the board. However, the class of fluidic components would require a special surface mount packaging architecture which should facilitate the fluidic interconnects of the components, since fluids should pass through these components. The fluidic component packaging architecture will be discussed in the following section. All types of components can be scaled for batch fabrication in a panel array form factor as shown in figure 4-4. In such approach it is also feasible to follow laminate based multilayer component fabrication, where the component arrays would be fabricated by stacking and bonding multiple layers, whereas each layer could be fabricated in different materials and processes. These fabrication processes are also known as the post semiconductor manufacturing processes (PSM) [1].

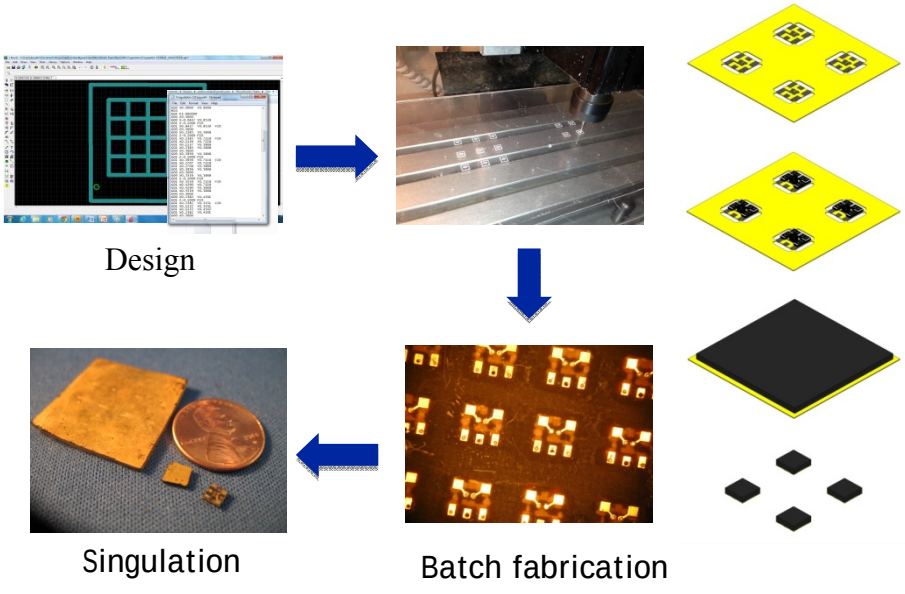

Figure 4-4 Scaled fabrication of FLEMS

4.1. Packaging of fluidic components:

The packaging and integration of fluidic components in microfluidic PCBs is not trivial because conventional surface mount packaging processes are not compatible with fluidics [2]. The microfluidic components often require microchannels and cavities inside the components. For example, pumps and valves typically require a fluidic cavity with moving membrane. Therefore, such components need fluidic interconnects in addition to electric interconnects to the main microfluidic board. Moreover, these interconnects and cavities have to be sealed and protected during the integration process on the microfluidic PCBs as the process involves lamination of polymer material in liquid or viscous phase, which would find its way into the component if the fluid access openings are not properly sealed. After lamination and planarization, the removal of the sealing layers must be facilitated to release the embedded component for its proper functioning.

In general fluidic components can be categorized in two groups: actuators that control the flow of the fluid in a microfluidic system (pumps, valves, droplet generators, etc.) and sensors that process or analyze the fluid (imagers, electrochemical sensors, etc.). However, from packaging perspective all components in either group have the same requirements: fluid inlets/outlets and electric interconnects. Thus a universal package design for fluidic components is proposed that has a surface mount form

factor with electric pads at the bottom of the component and fluid inlets/outlets on top of the component as shown in figure 4-5. These are intended to be mounted on a PCB using standard SMT soldering techniques, then encapsulated in a planarizing layer, with a microfluidic layer laminated on top. This design also features protective sacrificial plugs patterned on the package during the packaging process in order to seal the fluid inlets/outlets of the component, thus protecting them during encapsulation as shown in figure 4-5. Figure 4-5 also shows the cross section of the fluidic component when embedded in the laminated layers of the microfluidic PCB.

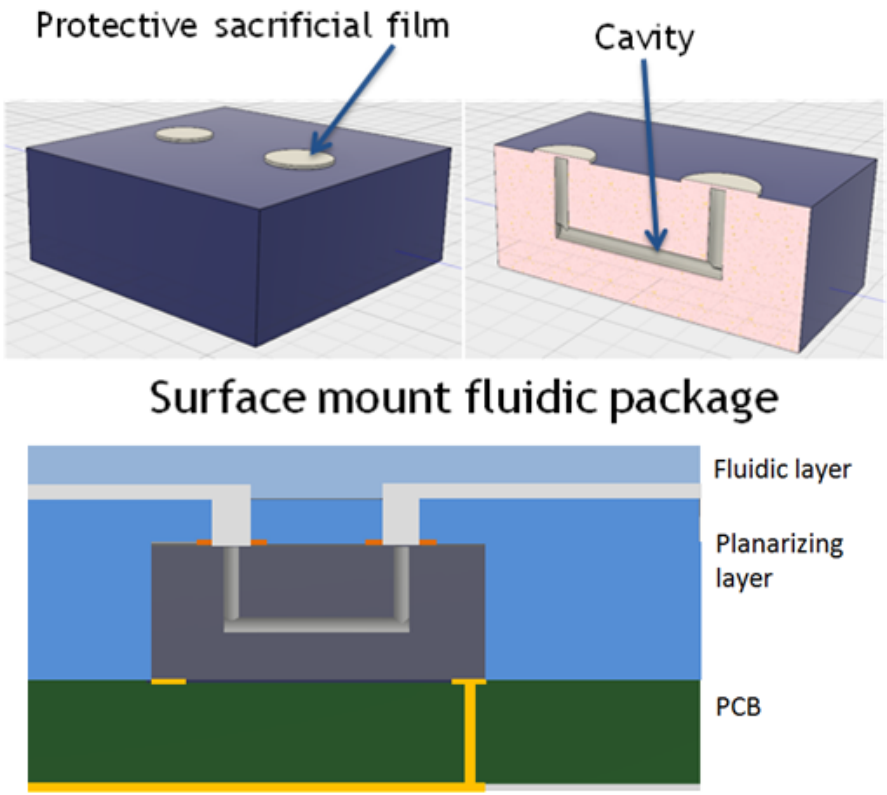

Figure 4-5 Fluidic component packaging architecture

Figure 4-6 illustrates the process of embedding the fluidic components in microfluidic PCBs. After encapsulation and planarization, the protective sacrificial plugs are etched or dissolved with compatible solvent to allow fluid flow from the main microfluidics layer through the component.

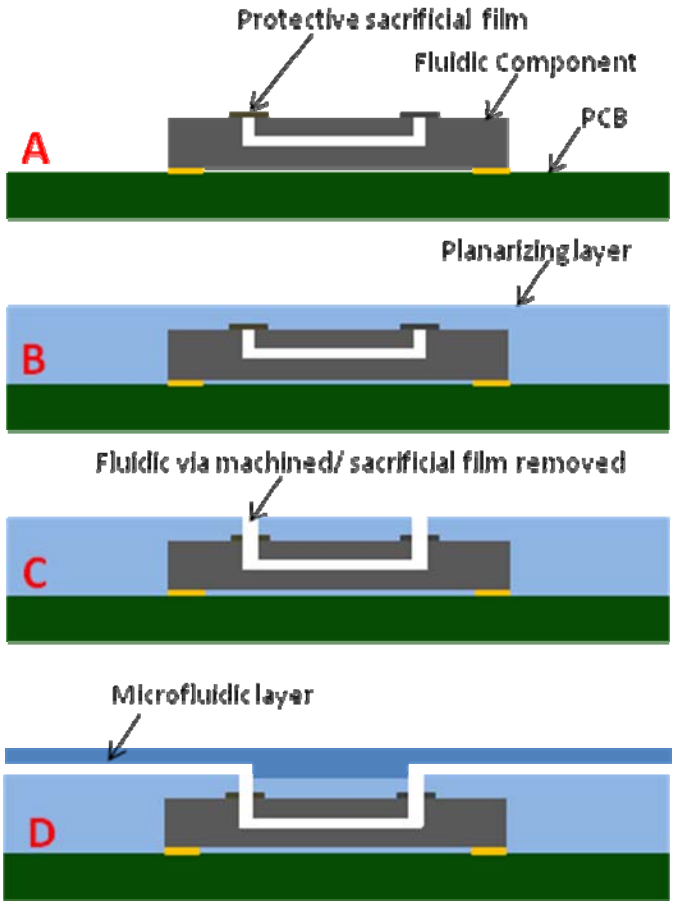

Figure 4-6 Fluidic component integration process on microfluidic PCBs

4.2. References:

1. Mark Bachman and G.-P. Li *"MEMS in Laminates"* Electronic Components and Technology Conference (ECTC), 2011 IEEE 61st
2. S. Babikian, G.P. Li and M. Bachman *"Packaging Architecture for Fluidic Components in Microfluidic PCBs"* IEEE 66th ECTC Conf. submitted for publication, 2016

5. MICROFLUIDIC PCB DEVICES AND APPLICATIONS

In this chapter several microfluidic PCB LOC devices are demonstrated with applications ranging from droplet based microfluidics, to point of care diagnostics. All of these devices were fabricated following the processes and technologies described in the previous chapters. Several FLEMS components were also designed, fabricated and embedded in these microfluidic PCB devices to integrate several functions on the chip.

5.1. Droplets generation device:

Droplet based microfluidics can offer great advantages for high throughput molecular analysis, such as screening (drug discovery) and sequencing (DNA sequencing) [1]. Droplet based microfluidic device can generate thousands of droplets in small devices. Each droplet is used as a reaction chamber to perform thousands of molecular reactions in parallel. Thus, nano liter size droplets would replace the conventional microarrays which would yield the following improvements in high throughput assays:

- Reduction in volume size for sample and reagents (~ 10^6 times)
- Faster analysis, higher throughput
- Lower analysis cost

Figure 5-1 shows a droplet based LOC device built in microfluidic PCB technology. The device features two surface mount fluidic components: a droplet generator component (shown in figure 5-2) and a Coulter counter

component (shown in figure 5-3) connected in series.

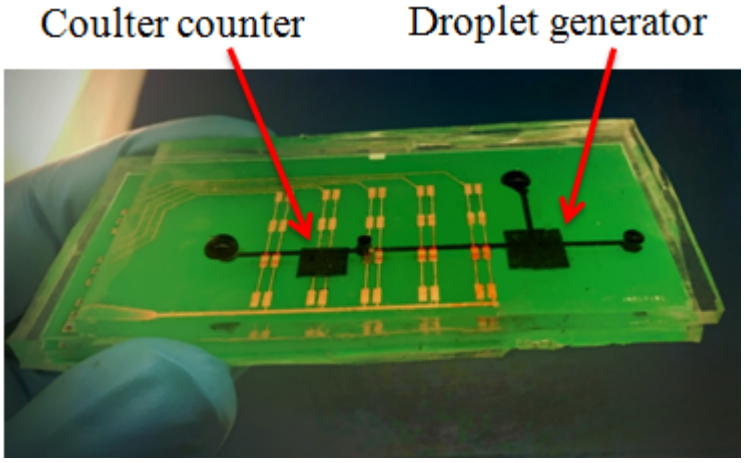

Figure 5-1 Droplet generation device

The droplet generator is a 4 mm x 4 mm x 2 mm component with 3 fluidic inlets/outlets. The cavity design of the component is a simple T junction [2] as shown in figure 5-2. Droplets are formed as two immiscible fluids meet at the junction. The size of the droplets is governed by equation 5-1.

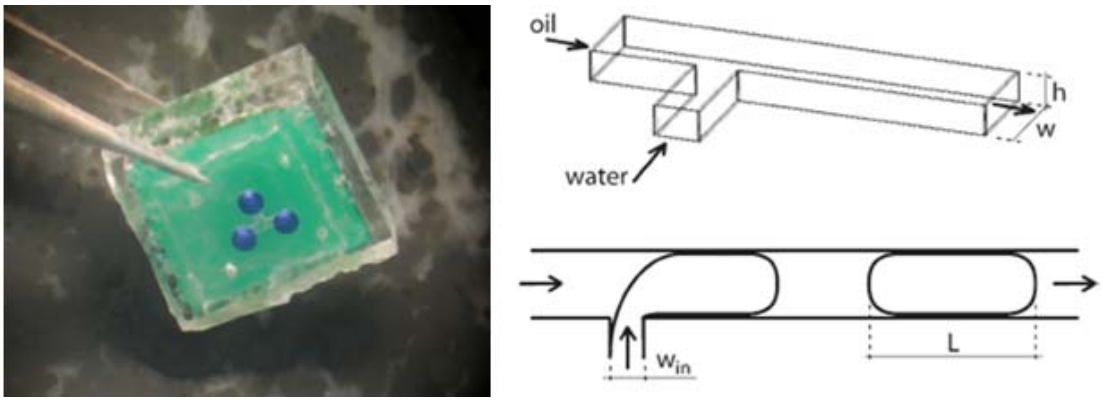

Figure 5-2 Droplet generator fluidic component in surfae mount package

$$\frac{L}{w} = 1 + \alpha \frac{Q_{in}}{Q_{out}} \qquad 5\text{-}1$$

Where L is the length of the droplet, w is the width of the microchannel, α is

a constant and Q_{in} and Q_{out} are the water and oil/droplet flow rates respectively.

The Coulter counter, on the other hand, is a 3 mm x 3 mm x 2 mm component. It was integrated in order to count the generated droplets. The Coulter counter is a particle counting and sizing device [3] based on measuring the particle electric impedance, as shown in figure 5-3. It consists of two electrodes separated with a microchannel. As a particle (or a droplet in this case) flows through the microchannel the electrical impedance of the channel would change. This change is recorded as a proportionate change in the DC current through the electrodes of the device.

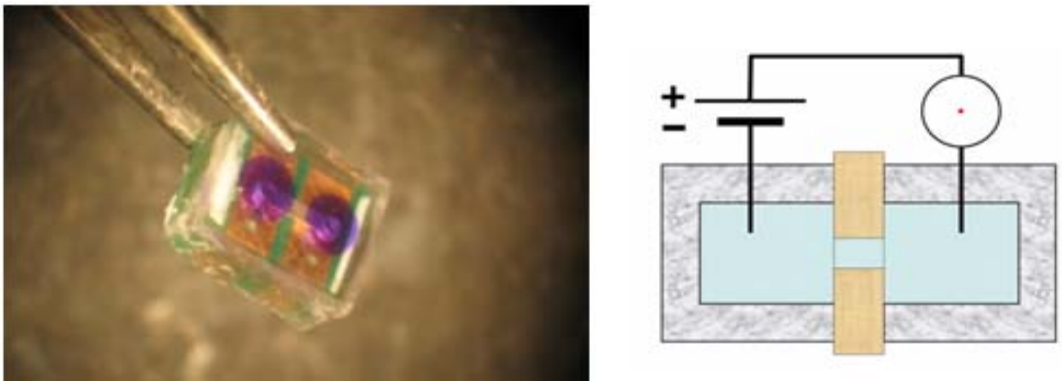

Figure 5-3 Coulter counter fluidic component in surface mount package

The fluidic components were fabricated in arrays and by stacking and bonding of two layers: A fluidic layer which hosts the component cavity and fluidic inlets; and the substrate (a PCB layer) which hosts the electric pads and interconnects of the component. The fluidic layers of the components were machined in thin sheets of PMMA using CNC tool. Following, a dry film

photoresist (from DuPont) was heat laminated on the machined PMMA layer and lithographically patterned in order to create the sacrificial sealing caps on the fluidic inlets of the component, as shown in figure 5-4. Then, the fluidic layers were bonded to the substrate layers of each component using adhesive. In the final step the components are singulated using the CNC tool and resulted in the components shown in figures 5-2 and 5-3. Although the components are readily functional in this form, it is also possible and recommended to further package these components in conventional epoxy based packages (as could be seen in the final integrated device in figure 5-1) in order to ensure the mechanical integrity of the components and also ensure a flat surface on top of the component, to meet the packaging requirements of the automated pick and place surface mounting process widely used in industry.

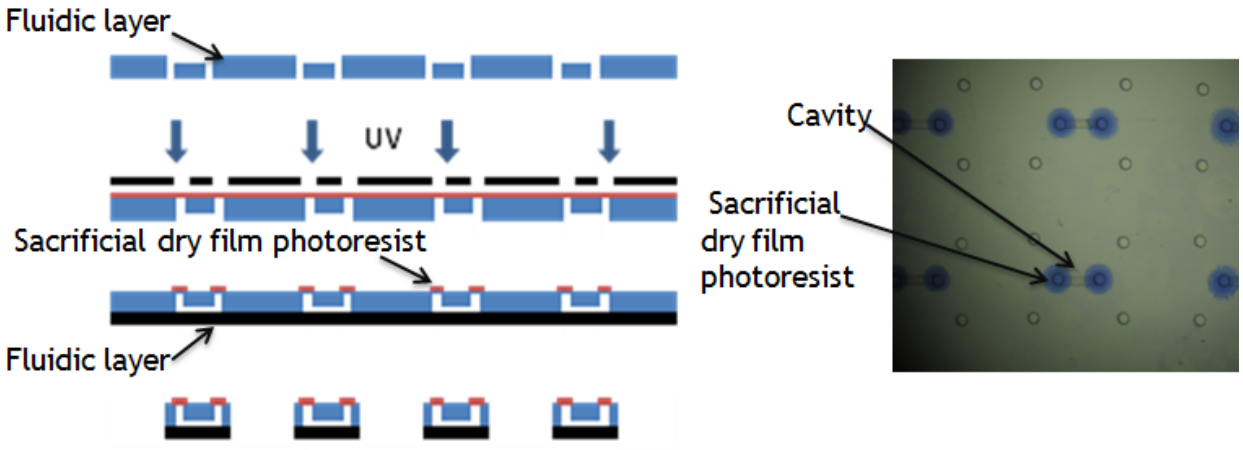

Figure 5-4 Fluidic component fabrication process and lamination of sacrificial caps

The microfluidic PCB device was fabricated following the standard process described in chapter 3 and using PDMS for the polymer layers on the PCB. The device was tested for generating water droplets in oil. Vegetable oil (the carrier fluid) was loaded in the main channel reservoir and dionized water stained with red dye (the dispersed fluid) was loaded in the secondary reservoir connected to the T junction of the droplet generator component. A vacuum pressure was applied to the waste reservoir, at the end of the main channel, to induce pressure driven flow in the channels. The oil and water where observed as they flowed into the droplet generator, and generated water droplets in the oil carrier was immediately observed at the outlet of the component as shown in figure 5-5. The generated droplets flowed through the main microchannel of the device and into the Coulter counter. As the droplets flowed through the coulter counter the electric current through the counter recorded sharp peaks indicating the detection of the droplets, as shown in figure 5-6.

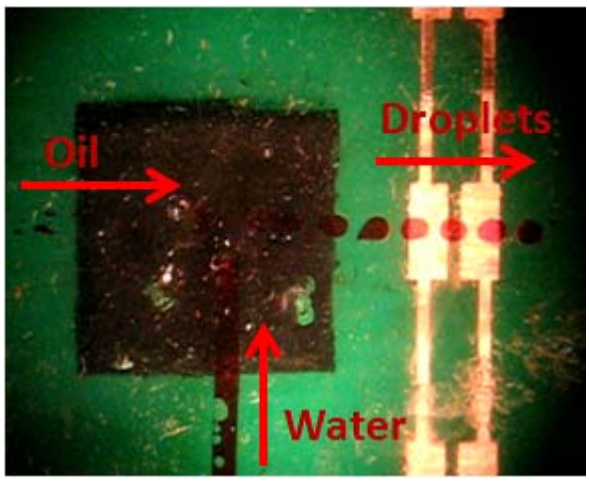

Figure 5-5 Generated droplets on the microfluidic PCB

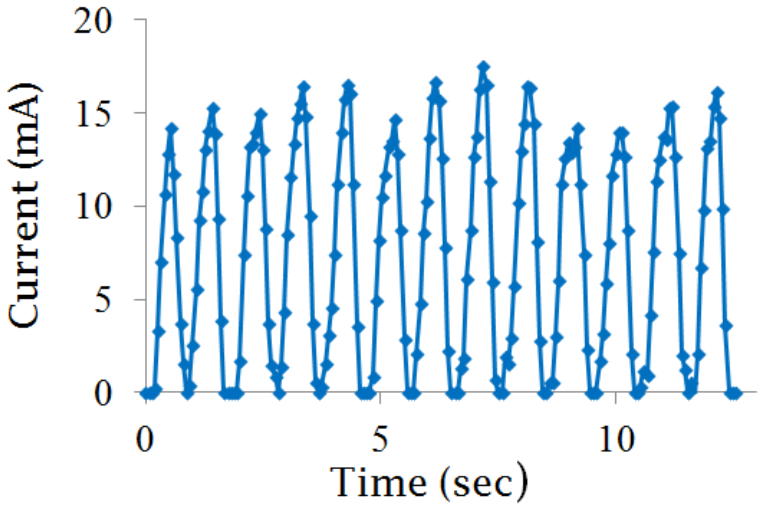

Figure 5-6 Coulter counter component output

Each peak corresponds to a droplet passing through the component

5.2. Point of care diagnostics:

Point of care diagnostics tests are designed to be performed at home or in the field with minimal process steps and dependency on laboratory equipment [4, 5]. Ideally, it is desired to perform the whole analysis on a single LOC device. Therefore a point of care LOC device has to satisfy a set of requirements from both the assay point of view and the user point of view. From the user point of view the requirements could be summarized as follows:

- Start analysis with raw, small volume samples (blood, saliva, urine, etc.)
- Provide high quality diagnostics in minutes
- Can be used by non-professionals

- Can be powered and controlled by a battery or via cell phone or a laptop
- Can be cheap and disposable

In order to satisfy the user requirements the LOC has to integrate a sample to answer assay on the chip, or a number of sequential assays which would allow starting the analysis with raw unprocessed samples, and yielding meaningful analysis results. The most common target analytes in diagnostic tests are the proteins and nucleic acids. The diagnosis is often based on determining whether a specific protein molecule or a specific nucleic acid sequence is present in the raw sample. Therefore such analysis is generally complex as it seeks to isolate and identify a specific target molecule with extremely low concentration in the complex matrix of the raw sample. There is a set of bio-chemical processes or steps to analyze raw, biological samples. These can be summarized in the following:

- Sample preparation
- Analyte extraction
- Analyte amplification
- Detection

These steps, which are also illustrated in figure 5-8, are essential for a sample to answer analysis on the chip. And therefore point of care LOC devices should integrate all of these steps on the chip (assay requirements).

This work demonstrates the integration of a number of functions on the chip to realize the aforementioned assay requirements. Primarily the focus is on the sample preparation of raw blood sample and the electrophoretic extraction of nucleic acids from the raw sample, and the

fluorescence detection of the extracted fluorescent species. Integration on the chip of other methods of extraction and methods of analyte amplification and detection should be the subject of future studies, in order to realize a complete point of care LOC device.

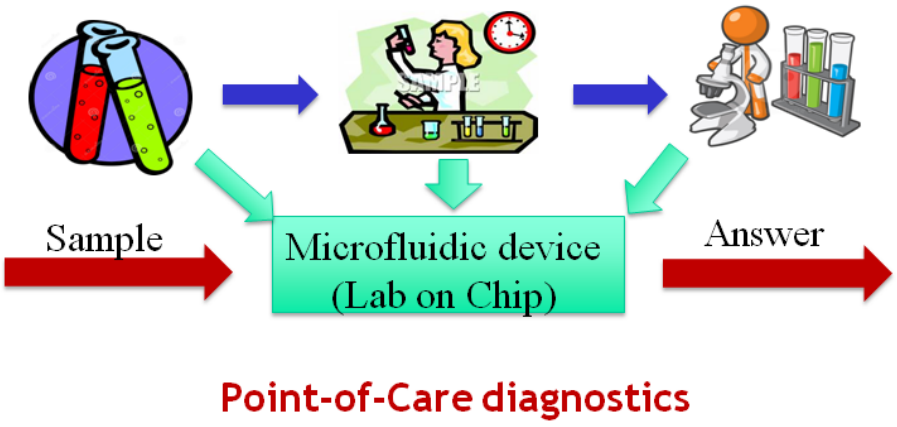

Figure 5-7 LOC device user requirments for Point-of-Care diagnostics

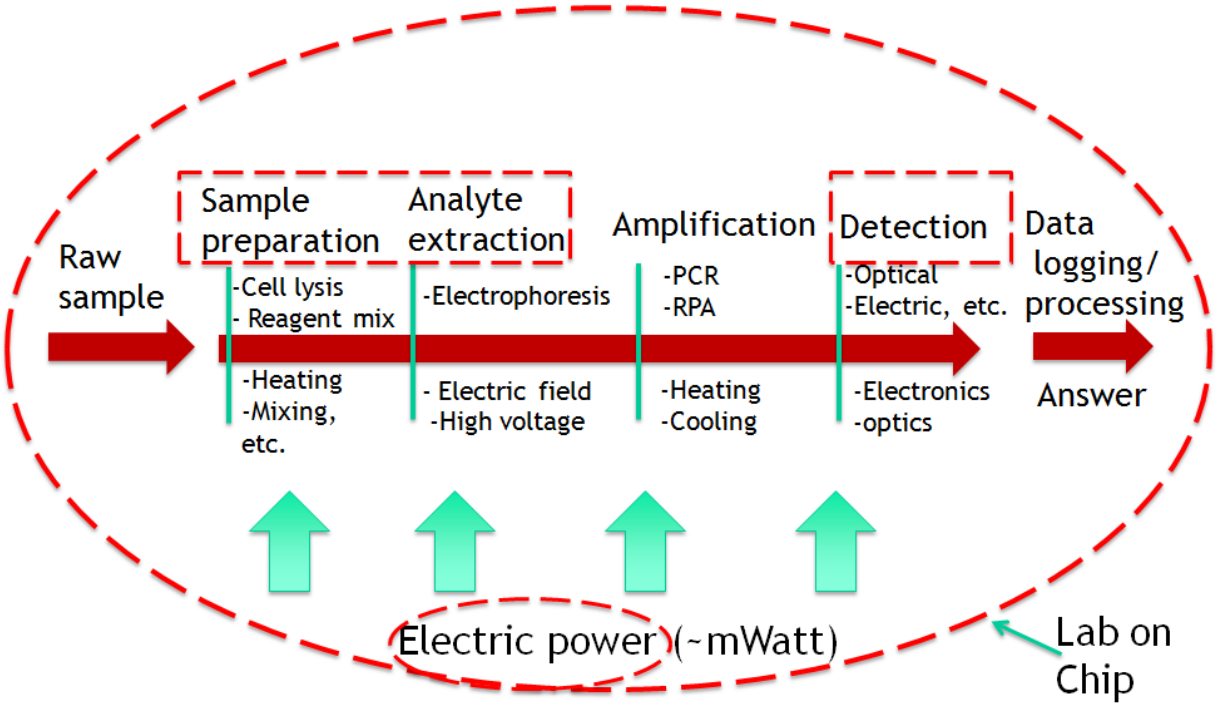

Figure 5-8 LOC device assay requirments for Point-of-Care diagnostics

5.2.1.Sample preparation device

A sample preparation and analyte extraction microfluidic PCB LOC device was designed and fabricated to analyze raw blood samples spiked with malaria pathogen [6]. The device is shown in figure 5.9. It features a single straight microchannel with dimensions of 4 cm x 300 µm x 70 µm, and two reservoirs (sample and collection) integrated with thermal components [7] underneath the reservoirs for on chip heating of the sample. The device has dimensions of 7 cm in length, 3 cm in width and 0.5 cm in height. The device integrates sample preparation and analyte extraction assays, as explained in Figure 5-10.

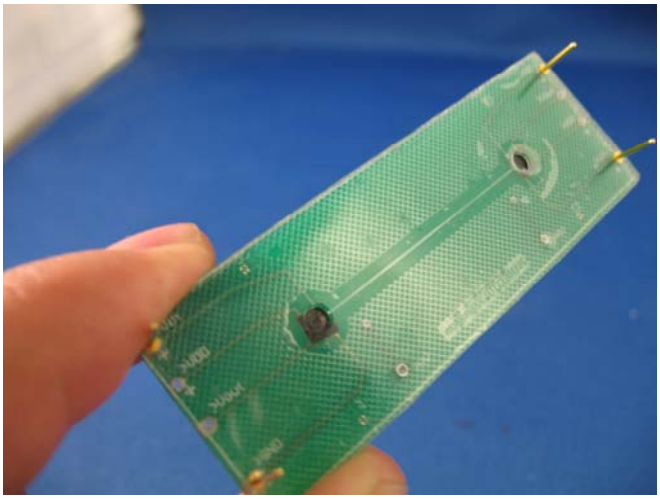

Figure 5-9 Sample preperation device

Malaria Pathogens reside inside the red blood cells and therefore analyzing the raw blood should start by the lysis of its cells, i.e. breaking down the cell walls to bring the constituents of the cells out. The lysis can be achieved in many ways, chemically, mechanically, by electric fields, or thermally. The microfluidic PCB device would thermally lyse the cells by

heating the raw blood sample on the chip. The heating process also performs a convective vigorous mixing of the sample with reagents of the extraction assay, which are preloaded on the chip. In the final step, the nucleic acids are separated by electrophoresis from the complex mixture and focused inside the microchannel.

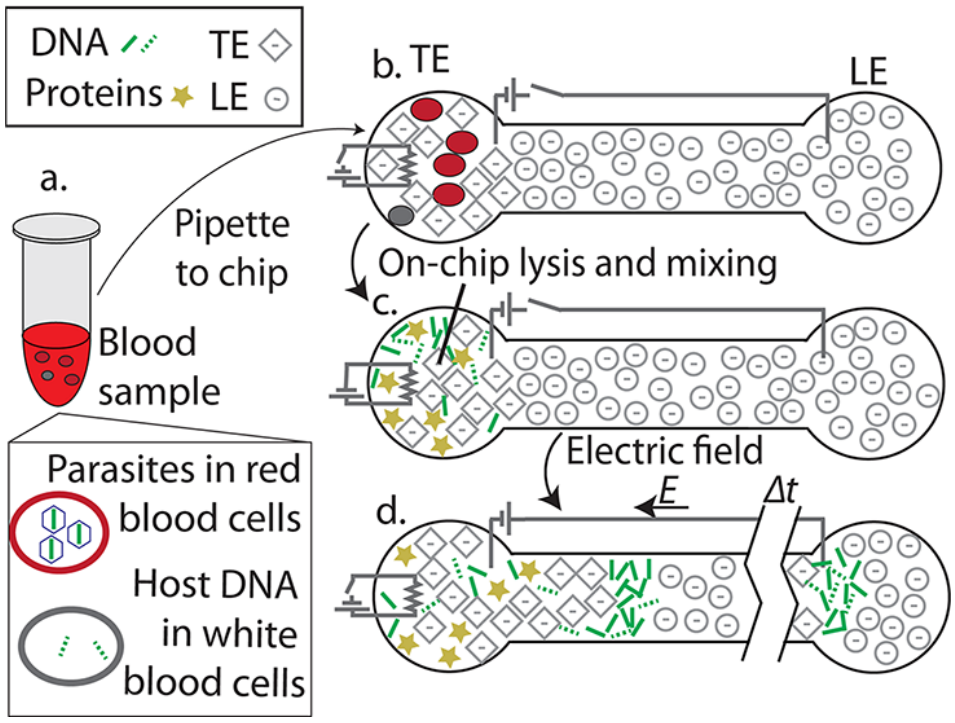

Figure 5-10 Sample preperation assayintegrated on chip

Isotachophoresis (ITP) is the separation technique used on this device. It is a modified version of capillary electrophoresis (CE) [8, 9]. The assay requires the use of two electrolyte solutions; a leading electrolyte (LE) designed to have ionic electrophoretic mobility higher than that of the target nucleic acids, and a trailing electrolyte (TE) designed to have ionic electrophoretic mobility lower than that of the target nucleic acids. The leading electrolyte is preloaded in the microchannel of the device while the

trailing electrolyte is preloaded in the sample reservoir. The application of an electric field along the microchannel would cause the molecules of the complex mixture in the sample reservoir to drift under the electrostatic force at different drift velocities. The drift velocity of each molecule is determined by the electric field strength and the electrophoretic mobility of the molecule, as described in figure 5-12. The electrophoretic mobility describes the charge to mass ratio of each molecule and thus molecules of different sizes, such as big protein molecules and small DNA molecules, would travel at different velocities and separate from each other as they drift inside the microchannel, as shown in figure 5.12. The target DNA molecules, however, would get “trapped” and focused at the interface between the leading and trailing electrolytes since their electrophoretic mobility is bounded by the mobilities of the two electrolytes. This ITP flow regime is called the peak ITP mode since the focused molecules concentration is peaked at the LE/TE interface and this peak travels along the microchannel as shown in figure 5.11.

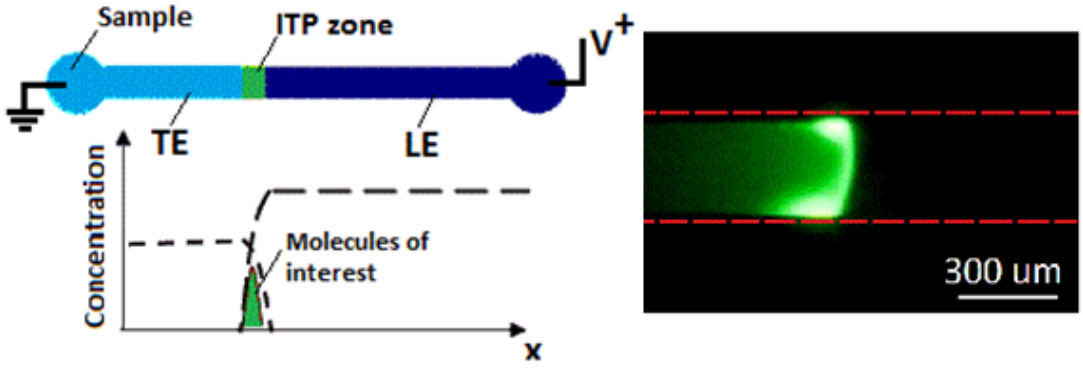

Figure 5-11 Isotachophoresis (ITP)

and ITP zone of Fluorescein fluorophore imaged with epifluorescence microscope

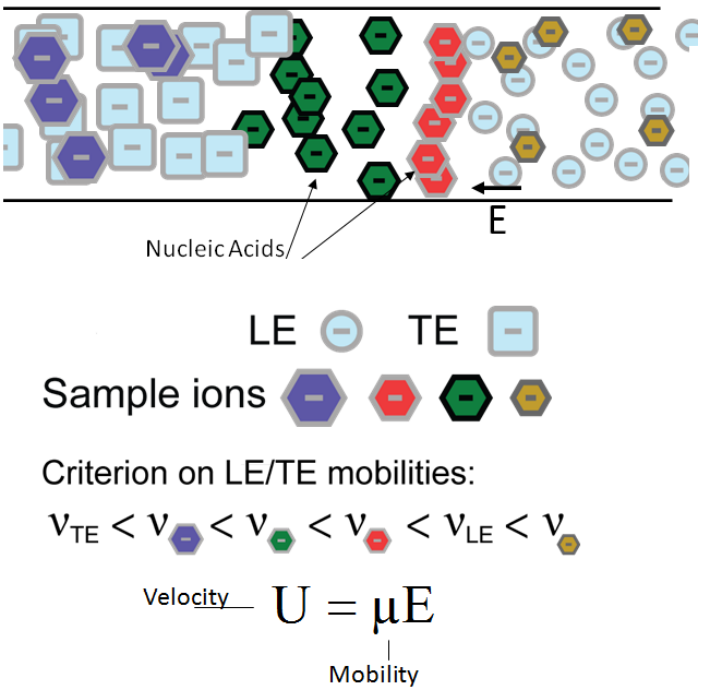

5-12 Molecules in ITP assay drift and seperate and focus

The sample preparation device was used to extract DNA from infected blood sample. LE electrolyte was loaded in the microchannel and the collection reservoir. TE electrolyte with Syto 60 fluorophore was loaded in the sample reservoir of the device. 15 uL of P. falciparum-infected human blood with 0.9% parasitimia cells was loaded in the sample reservoir of the device. The two thermal components under the two reservoirs of the device were turned on simultaneously to heat the sample and lyse the blood cells. The heater in the collection reservoir was turned on in order to maintain thermal equilibrium along the microchannel and prevent a convective flow in the channel. The cells were lysed within 3-5 minutes and the cell constituent was efficiently mixed with the trailing electrolyte by convective currents in the reservoir, as illustrated in 5-15. Following lysis and mixing, a

high voltage (1000 VDC) was applied along the microchannel to initiate ITP. The ITP zone of the blood DNA was observed ,by epifluorescence microscope, migrating in the microchannel and eventually reaching the collection reservoir. Figure 5.13 shows the successful ITP extraction of DNA from the infected blood sample. Imaging of DNA was realized using Syto 60 red fluorescent nucleic acid stain. Figure 5.14 shows the on chip cell lysis efficiency as a function to applied current in the thermal component.

In the following the design and characterization of the surface mount thermal component (the first FLEMS component) will be demonstrated.

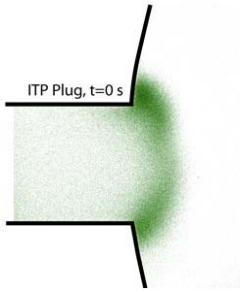

Figure 5-13 ITP extract of DNA eluting into the leading well

(Courtesy of L. Marshall) [6]

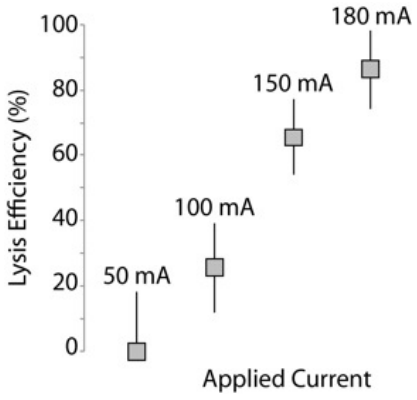

Figure 5-14 On chip cell lysis efficiency

(Courtesy of L. Marshall) [6]

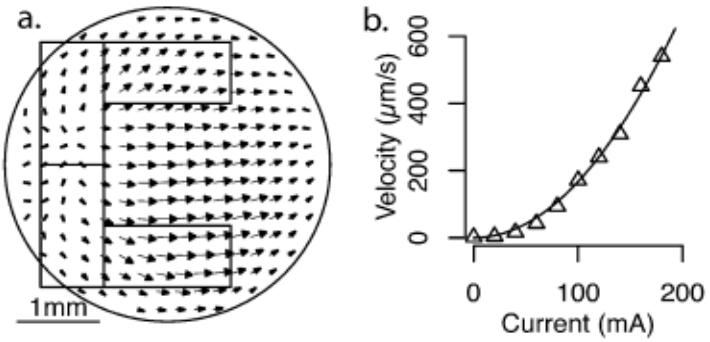

5-15 Convective currents in the reservoir provided vigorous mixing of reagents. (Courtesy of L. Marshall) [6]

5.2.2.Thermal component:

The thermal components are designed to enable temperature controlled heating on the chip [7]. The components were designed to operate at temperatures of up to 150 ˚C and provide 1 watt of continuous heat at 4 volts DC voltage and 250 mA current, making it suitable for use in a microfluidic accessory to portable electronic devices, such as laptop computers or mobile phones. Figure 5-16 illustrates the 3-D schematic design of the component. The component dimensions are 3.2 mm x 3.2 mm x 1 mm, and it features 6 electric contact pads on its backside. Each pad is 0.6 mm x 0.7 mm and the spacing between the pads is 0.7 mm. The component is built on a thin FR4 printed circuit board substrate (~200 µm thick) which can conveniently provide the electric connection between the component and the microfluidic chip, through the copper pads on the backside. The heat source consists of four standard surface mount resistors (Panasonic 32R9407 thick film SMD) connected in series. A surface mount integrated temperature sensor (LM94023 National Semiconductor IC

temperature sensor) was mounted at the center of the device to provide an analog voltage output that is inversely proportional to the sensed temperature. The components were bonded to the printed circuit board through a standard oven reflow process. Thermally conductive two parts epoxy system (50-3100 epoxy resin from Epoxies etc.) was used to encapsulate the component to provide electric isolation between the component and the fluid subjected to heating, and to allow seamless transfer of generated heat to the fluid. The parts were mixed in manufacturer recommended ratios to form a molding compound that had a viscosity of 45000 cps. The compound was degasified for 30 minutes under 76 cmHg vacuum pressure and then casted over the board and planarized by embossing. The resin was cured in the oven for 16 hours at 74 ºC to reach its maximum shore hardness of 90D. The thermal conductivity of the resin is 2.16 W/mK and it is capable of handling temperatures up to 200 °C. In the final step, the components were singulated using a CNC tool. Figure 5-16 also shows two thermal components on a penny.

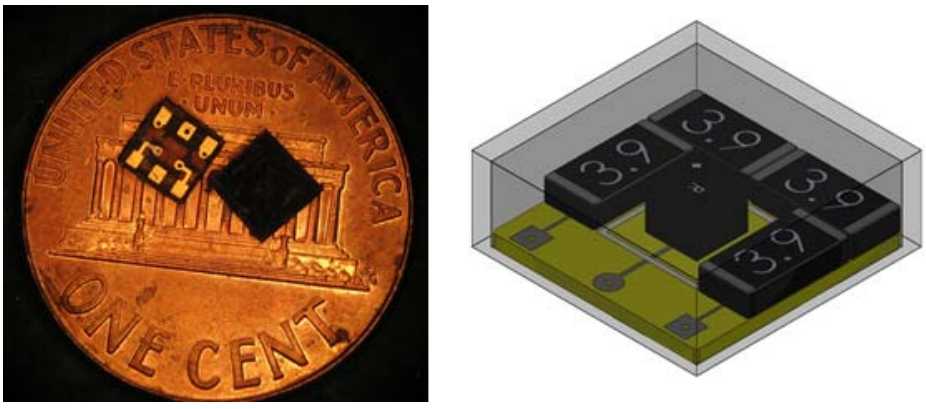

Figure 5-16 The Microfluidic Thermal Component in surface mount package

To evaluate the performance of the thermal component, a test device was built. The layout of the device and placement of the thermal component is shown in figure 5-17a. The component was placed underneath a reservoir which was used to hold water during the thermal heating tests.

For the sake of characterizing the component-PCB chip, 50 μL of deionized water was loaded into the reservoir. An external sensor was placed inside the reservoir at distance of 1 mm from the bottom to monitor the water temperature. Figure 5.17b shows the temperature response curves of the water and the component when the rated power of 1 watt (at 4 volts and 250 mA) was supplied to the heating resistors. The blue curve represents the actual temperature response of the water recorded from the external sensor; the green curve represents the temperature response of the component as recorded from the embedded temperature sensor. After about 3 minutes of continues heating, the system reached a steady state where the water temperature stabilized at 92 °C, whereas the embedded sensor reading stabilized at 115 °C. The difference in the readings is due to the temperature gradient in the chip. The embedded thermal sensor is closer to the heating resistors than it is to the water. It is not possible to measure the water temperature directly using the embedded temperature sensor unless the embedded heaters are turned off and the system allowed reaching thermal equilibrium. However, it would be ideal to use the embedded sensor exclusively for the precise control of reagent's temperature without the need to use a second external temperature sensor. In addition, a much

shorter transient time is desirable to avoid excessive evaporation of reagent and consequent change in its volume until reaching the designated temperature.

Table 5-1 Thermal paramiters of different layers in the microfluidic PCB

Material	Thermal Conductivity k [W/m·K]	Heat Capacity Cp [J/kg·K]	Density ρ [kg/m³]
FR4	0.3	1369	1900
Polyurethane	0.3	1400	1250
Epoxy	2.16	1500	1360
PMMA	0.19	1420	1190

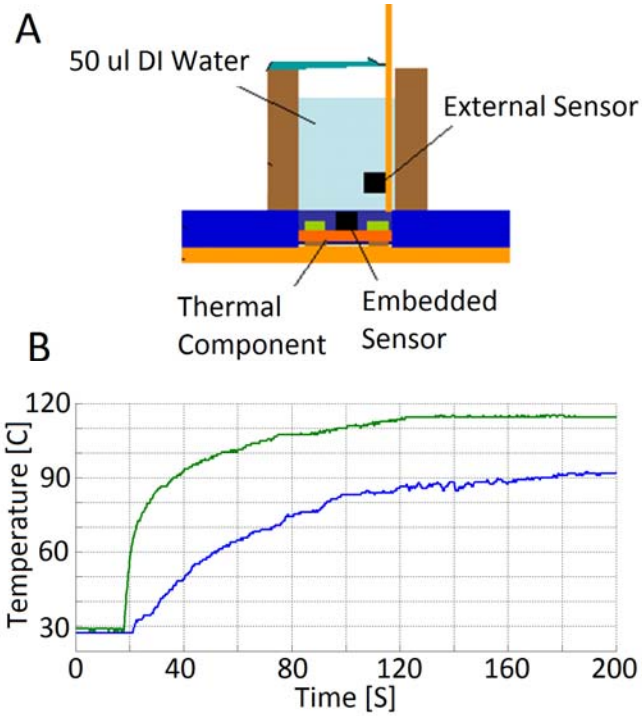

Figure 5-17 Temperature gradient between embedded thermal component and the fluid reservoir

Blue curve registering fluid temperature (lower temperature) and the green curve registering component temperature (higher temperature) when the rated power of 1 watt (at 4 volts and 250 mA) was supplied to the heating resistors.

5.2.2.1. Temperature Control scenarios

To control the water temperature in the reservoir, two possible scenarios were investigated. In the first scenario we monitored the water temperature directly using the embedded sensor by turning off the heaters and allowing the system to reach thermal equilibrium. After a certain amount of time (τ) thermal equilibrium in the system was reached and at which point the embedded sensor reading was equivalent to the water temperature. The equilibrium state (and transient time, τ) was identified by the first intersection point between the actual water temperature curve and the embedded sensor reading as shown in figure 5-18. After that time, the two sensors shared nearly the same reading. In this system, τ was observed to be in the order of several seconds (~6 sec) and is a function of the difference in temperature ΔT between the two measurement points at the time when the power is switched off, as well as the thermal properties of the overall system, such as the thermal mass of the PCB, volume of water, and thermal conductivity of the component package material.

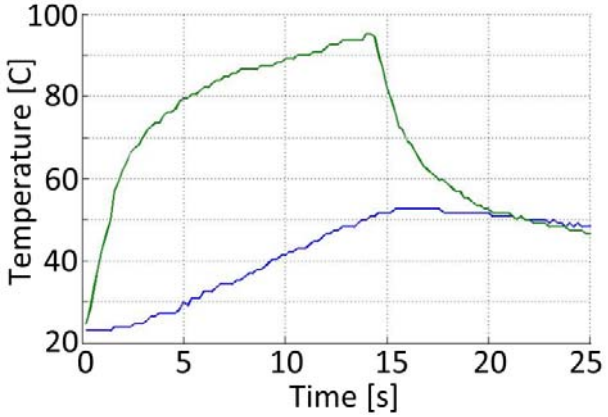

Figure 5-18 Thermal transient charactristics (τ = 6 sec)

In principle, it is possible to estimate the time to reach thermal equilibrium by carefully monitoring the shape of the temperature decay curve. When the change in temperature becomes nearly constant and negative, the first derivative of the temperature curve acquires a constant and negative value. The point at which the embedded sensor temperature is approximately the same as the water temperature and thermal equilibrium is reached. This is shown in figure 5-19 which is the first and second derivative of the embedded sensor's temperature over time.

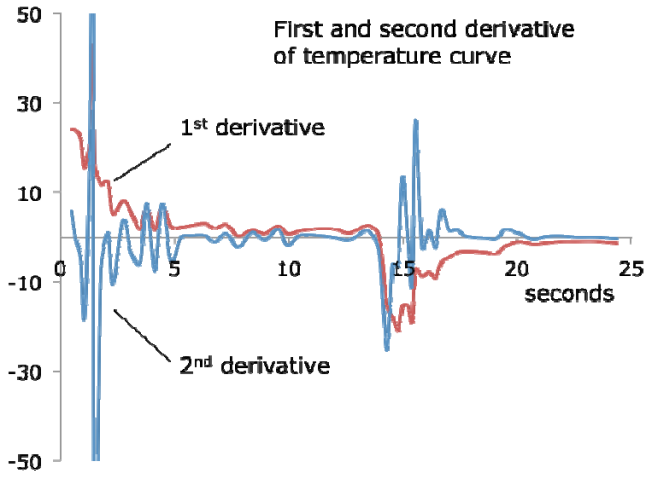

Figure 5-19 The second and third derivatives of the transient

The trailing edge of the temperature response can be seen in the flattening of the temperature change over time, indicating that the liquid-component system has reached thermal equilibrium and that the system is in a steady state of cooling. This is seen in the flat (and negative) value of the first derivative of temperature, and the zero value of second derivative that occurs at t = 20 seconds.

For the sake of continues temperature reading during a heating process the power could be switched off for an estimated period of (τ) at regular intervals. At the end of each off period the temperature of the water would be recorded. Figure 5-20 shows the temperature response of the water and the temperature reading from the embedded sensor when 8 V pulses were applied to the terminals of the component. This caused the heater to turn on for a period of 1.4 seconds, and turn off for 6 seconds between consecutive pulses (i.e. τ = 6 sec). At the end of each off period, the system reached thermal equilibrium state, which was determined by the intersection point between the two curves. Although following this method enabled the embedded sensor to directly measure the water temperature during the entire heating time, it had several downsides rendering it unfeasible for use in most applications. The major drawbacks were the large fluctuations in water temperature (~10 °C) and the long time needed to reach the targeted value (the time needed to reach 80 °C was three minutes).

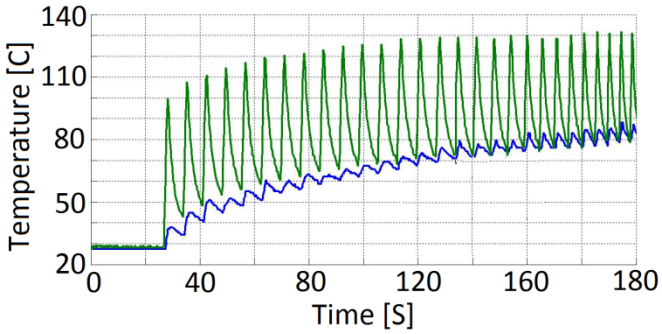

Figure 5-20 Pulsed heating with constant pulse width

Temperature response curves for heating 50 µL of DI water in sample reservoir when 8 V pulses were applied to the component. The off time between pulses (Δt =

6 sec) allowed the embedded sensor to estimate the temperature of the water.

In a second approach the extended off time is eliminated, and an offset in the feedback temperature is accepted and accounted for, assuming that it should be related to the water temperature in a known and well defined way. This would allow controlling the water temperature indirectly, by controlling the temperature of the embedded sensor. The temperature gradient in a fluidic reservoir with specific reagent type and specific targeted temperature can be determined during a calibration run and should not change every time the same assay is conducted. To precisely control the temperature of the component, and optimize its transient characteristics a pulse width modulation (PWM) algorithm was implemented. The heating resistors were supplied by a train of pulses that had a constant amplitude of 6.5 volts, frequency of 0.5 Hz and controllable pulse width. This caused the temperature inside the component to oscillate around an average value at the same pulsing frequency. A control algorithm was written in Matlab and implemented using a Labjack U12 ADC converter and a transistor load switch, to dynamically change the width of the pulses such that the average temperature of the component would be controlled to a set value. This caused the water temperature to rise to and stabilize at a less but a predictable and stable value throughout the entire heating period as shown in figure 5-21. Table 5-2 summarizes the experimentally obtained temperature readings when the average temperature of the component was controlled at constant values that were increased by 10 °C increments from

60 °C to 110 °C. For all cases the temperature of the water stabilized at a constant value with very small fluctuations. The standard deviation in the water temperature was less than 1% when the component set point was below 100 °C, i.e. when water boiling did not occur in the reservoir. At higher temperatures, the water had significant convection and some hot spots, which contributed to the variance in recorded temperature.

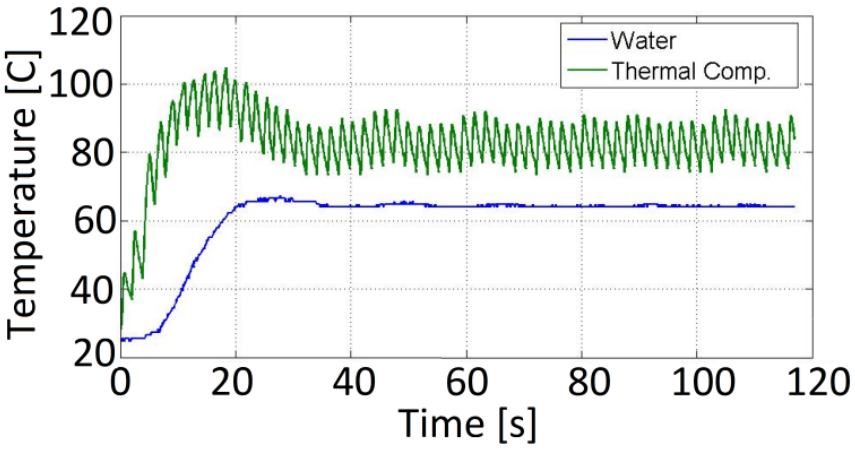

Figure 5-21 Pulsed heating with pulse width modulation (PWM)
Control of the temperature of 50 µl of DI water. The component temperature (in green) was oscillated at 0.5 Hz around a controlled average value of 80 °C. The water temperature stabilized at 65 °C in less than 40 sec.

The difference between the average temperature of the component and the average temperature of the water at the measurement location in the reservoir was recorded for repeated experiments and found to be approximately ~14 °C ± 1 ºC. For all of the values, the time needed to reach the steady state was less than 40 seconds. The excellent steadiness of the water temperature in spite of the oscillating nature of the component

temperature was due to the large thermal mass of the water comparing to the thermal mass of the component.

The stability of the temperature gradient for this system over a range of temperatures suggests that, once the temperature difference (between water and component) is known, the heating can be reliably repeated over a reasonable range of temperatures. One way to implement this would be to provide a calibration probe with a chip and perform a one-time calibration to relate fluid temperature to component temperature. This calibration could be done after manufacture of the system (similar to the way scientific instruments are calibrated at the factory prior to delivery), or a calibration could be performed by the user if needed.

Table 5-2 Thermal gradient and water temperature with PWM control

Heater Set Temp. ˚C	Water Ave. Temp. ˚C	St. Dev. in Water Temp. ˚C	Temperature Difference ˚C
60	47.0	0.343	13
70	55.9	0.527	14.1
80	64.6	0.526	15.4
90	75.6	0.541	14.4
100	89.2	1.005	10.8
110	95.5	1.433	14.5

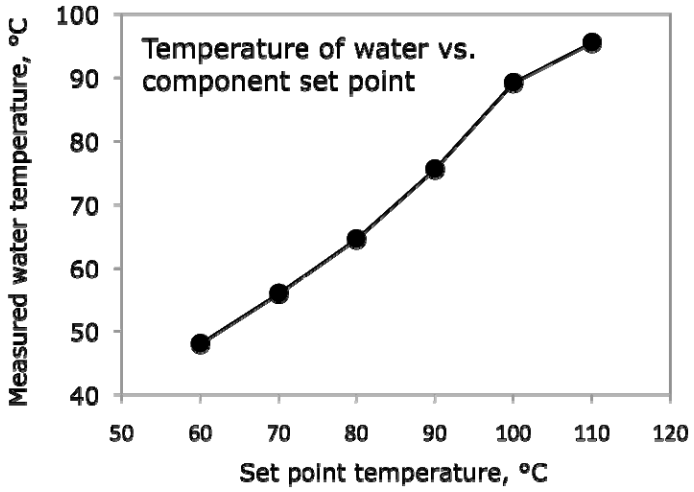

Figure 5-22 Water Temperature vs component temperature with PWM control

5.2.3.DC-DC converter circuit to drive ITP:

ITP and other electrophoretic separation methods require relatively high electric fields to drive the assays, i.e. drift and separate analytes under the influence of the electric field [8, 9, 29, 30]. Electrophoresis assays require constant electric fields in the order of 10~100 V/cm, which is obtained by applying DC voltages in the order of 100~1000 VDC between the end points of the microchannel. Thus, special power supply circuits need to be designed for LOC devices that incorporate electrophoretic assays. Such devices are often targeted for point-of-care diagnostics applications, and therefore should be powered entirely by batteries or portable computers or cell phones. However, such power sources can only provide a low level DC voltage, in the order of ~1-10 VDC. A DC-DC converter circuit would convert the low level voltage to the desired high level voltage required by the LOC device. On the other hand, the current requirements of

the electrophoretic assays are generally low, in the order of 100~1000 µA. Thus, a battery or a portable device can sufficiently power an LOC device incorporating these assays.

A DC-DC converter circuit was designed to drive the sample preparation device, which incorporated the ITP assay [28]. The circuit, shown in figure 5-23, generated high DC voltages (up to 1000 volts) when powered through a low voltage power source, such as a USB port (5 VDC). The feedback loop of the circuit provided a constant ITP current to the device, which is crucial for controlling the width and the drift velocity of the ITP zone in the microchannel. Figure 5-24 shows the electrical characteristics of the ITP assay which was performed on the sample preparation device. Figure 5-24a shows the characteristics when the ITP is powered in voltage source mode (i.e. constant voltage). The drop in the current over time is due to the flow and replacement of the electrolytes in the microchannel. At time t=0 the channel is filled with the leading electrolyte, which has a lower electrical resistivity (higher electrophoretic mobility). As the ITP zone proceeds in the channel, the leading electrolyte is gradually replaced by the trailing electrolyte, which has higher resistivity (lower electrophoretic mobility) causing the ITP current to drop. Figure 5-24B shows the electrical characteristics when ITP is powered in current source mode (i.e. constant current), which was realized by the feedback loop of the converter.

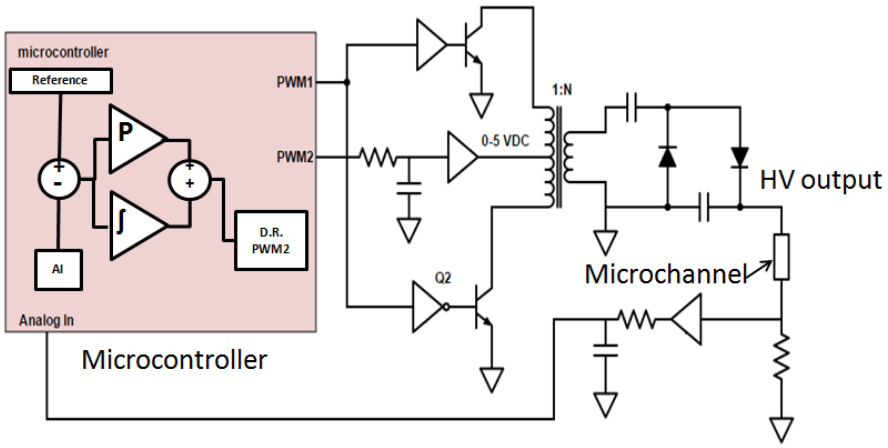

Figure 5-23 DC-DC converter circuit with feedback control designed to generate the required high voltage (~ 300 VDC) for the ITP from a low voltage source, namely a USB port (5 VDC)

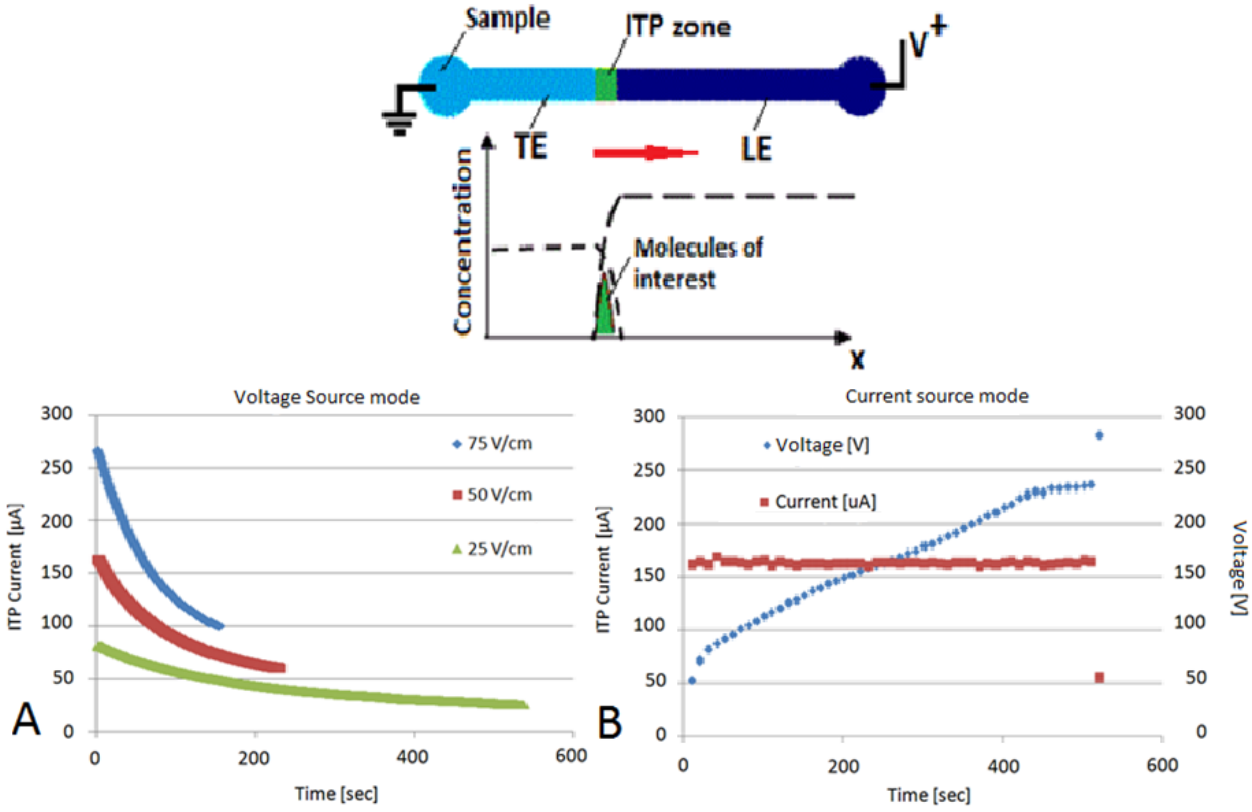

Figure 5-24 Electrical Charactristics of the ITP assay

A: Voltage source mode. B: Current source mode

5.3. On chip optical detection:

Enabling of the on-chip optical detection in the LOC device is one of the most important and most challenging integration problems facing LOC technology [5,10,11]. In general, an integration strategy to combine optical detection with other essential fluid handling and processing components of a LOC device is lacking. Most proposed optical detection methods for microfluidics in the literature are off the chip, which would yield miniaturized versions of conventional optical systems (e.g. epifluorescence) utilizing high end components such as lasers, lenses, filters, photomultipliers and detectors. Some high end work has been done to monolithically integrate on the chip all or some of the optical components of the detection system such as embossed waveguide structures, fiber optics, and thin film deposited filters and organic photodiodes [10-16]. Unfortunately, these monolithic methods to build on-chip optics are difficult to integrate with other functional components of a lab-on-chip device, such as fluid transport, pumping, mixing, heating, separation of analytes to name a few. On the other hand off chip systems use high quality optical components requiring precise optical alignments resulting in devices that are bulky and expensive, as well as making manufacturing complicated and expensive. Most microfluidic diagnostics devices on the market are designed to use bench top optical readers which accept passive microfluidic cartridges [5]. However, these do not provide a true low cost,

portable, point-of-care diagnostics solution, one in the form factor of a home glucose meter.

In this chapter we demonstrate methods for integrating the optical detection in microfluidic PCB LOC devices. We demonstrate two lab-on-chip devices with on-chip optical detection using low cost components, which are also readily integrated with other functional components on the PCB, and with suitable signal processing, can cleanly extract the signal from noisy output.

5.3.1.Lensless imaging using embedded pixel array sensor

To realize low profile, low cost optical detection in microfluidic PCBs, we propose a lensless imaging approach utilizing a large area pixel array detector, such as the complementary metal oxide semiconductor (CMOS) sensor device, as shown in figure 5-25. Several groups have reported the use of Lensless CMOS imagers to image beads or cells in the bright field [17-20], as well as fluorescence by integrating custom filters on the imager (interference or absorption) which are tailored to reject the specific excitation wavelength and pass the emission wavelength [21-23] or chemiluminescence [24] . In this work the use of a standard off-the-shelf CMOS imager embedded with a standard RGB Bayer color filter is explored. Small, low cost CMOS sensors would be ideal for microfluidic applications, due to being inexpensive, compact and compatible with the microfluidic PCB architecture. The pixel array, as opposed to single point detector, may

perform a large number of simultaneous optical measurements in 2D space and time. While the system (especially without lenses) is of much lower optical quality compared to conventional (bulky) optical systems, the large number of simultaneous measurements over a spatially diverse region, allows for one to exploit digital signal processing techniques in the detection methods, including dynamic subtraction, signal averaging, spatial correlation, and model fitting. This can make up for lower quality optical systems on the front end.

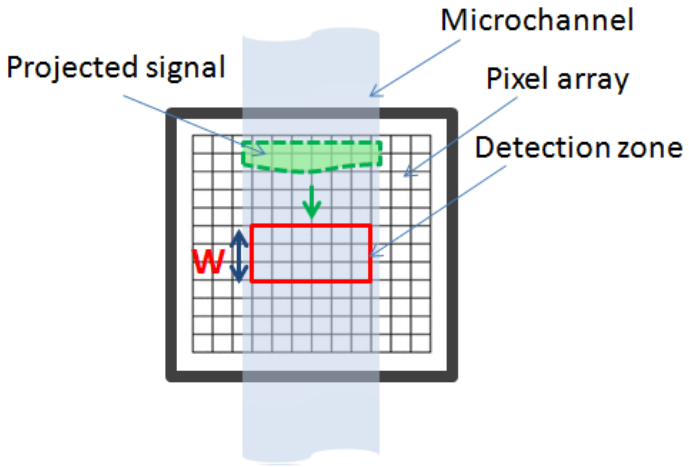

Figure 5-25 Lensless imaging with pixel array
The signal projected image convolves over the detection zone, as the analyte (the saurce of the signal) flows through the microchannel and over the pixel array

In a lensless imaging scenario, the signal "image" of an analyte in the microchannel is projected on the pixel array. It is possible to formulate a mathematical description of this imaging process with a convolution operation. The projected signal image of the flowing analyte effectively scans the detector surface at constant speed. This can be viewed as the matrix convolution of the projected signal over a defined detector area. This

defined area could be a sub area of the pixel array, labeled as the “detection zone” hereafter. The result of this physical convolution is given mathematically by equation 5.2.

$$S * C = \sum\big(s(i,j) \cdot c(i,j)\big) \qquad 5\text{-}2$$

S is a matrix representing the projected signal, whereas C is the matrix representing the detection zone, defined as the convolution matrix. The result of the convolution is the weighted average of the signal over the detection zone, where the convolution matrix determines the weight. Utilizing the large pixel array enables the possibility to dynamically change the size and the weight of the detection zone (the convolution matrix) and tailor it to optimize the detection parameters such as signal to noise ratio (SNR). It could be shown by simulation that the signal to noise ratio, and ultimately the sensitivity of the detection system, could be maximized when choosing a detection zone with a geometric shape and size matching that of the projected signal. Figure 5-26 shows the simulation results for the detection of two signals with different form factors. One has a circular (or dot) projection representing the particle class of analytes such as beads, droplets and cells. The other signal has an arbitrary shape (crescent) representing the class of analytes in electrophoretic assays such as protein and DNA, where these molecules focus and flow in the microchannel in tight bands (electrophoretic focusing) [8, 9]. The simulation shows how the SNR improves as the shape and size of the detection zone approaches to that of the projected signal. This optimization technique which is implemented in

image processing software is similar in nature to the pixel binning technique implemented on the circuit level to improve SNR in CCD and CMOS imagers [25, 26].

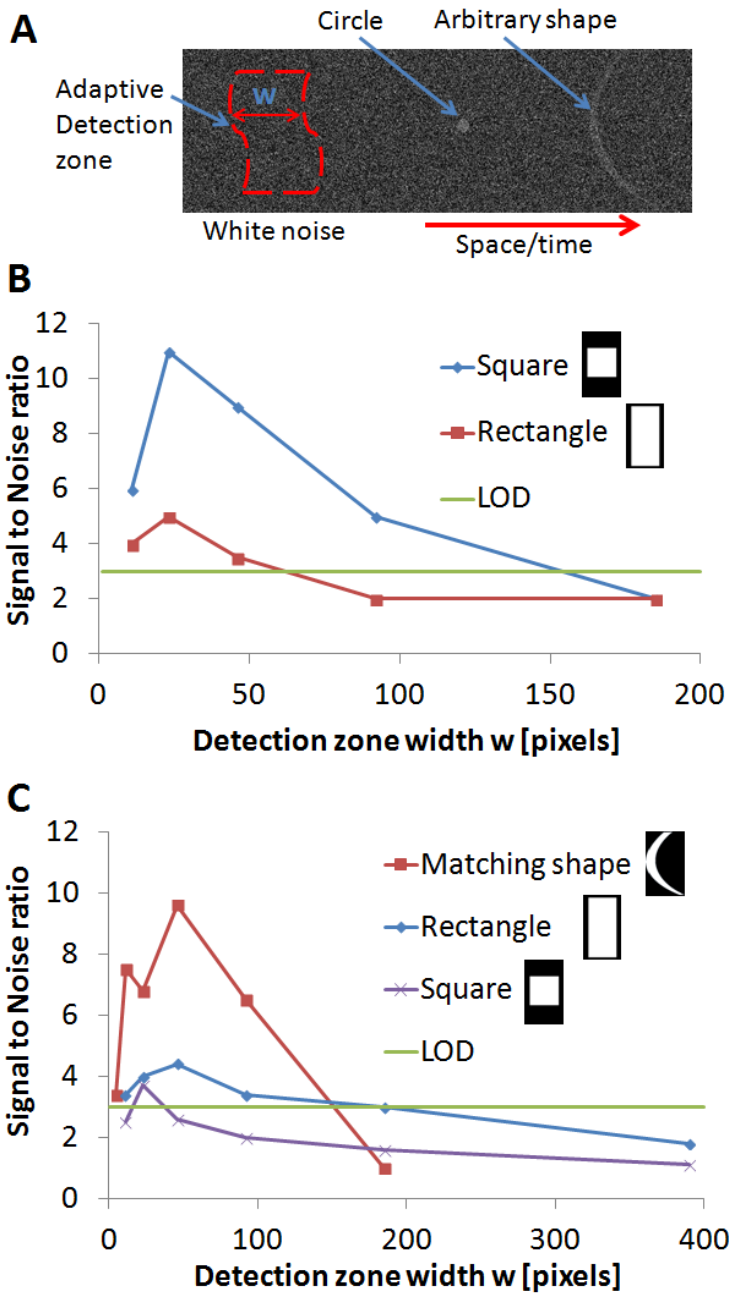

Figure 5-26 The signal to noise ratio as a function to the geometric shape and size of the detection zone

Simulation results, B for circular/dot signal and C for crescent shape signal

Thus, the lensless imaging array approach would utilize the unique characteristics of the signal (shape, size, motion) in addition to the amplitude and color information in the detection method. In the following we demonstrate the lensless imaging and DSP methods to realize an on-chip particle/cell counting device and on-chip fluorescence detection device for Isotachophoresis (ITP) applications.

5.3.2. The opto-fluidic cell counter

Following the processes described in this work, an opto-fluidic component for cell and particle counting applications is demonstrated [27]. The component is 4 mm x 4 mm x 2 mm in dimensions and embeds a 2 Megapixel CMOS imaging array with a fluidic cavity (a 2 mm x 250 µm x 100 µm microchannel) in surface mount fluidic package as shown in figure 5-27. The component can function as particle/cell counter when imbedded in a microfluidic PCB LOC device. As cells or beads or particles flow through the component, their shadows are imaged/detected by the CMOS sensor underneath the cavity. Figure 5-28 shows the fabricated components.

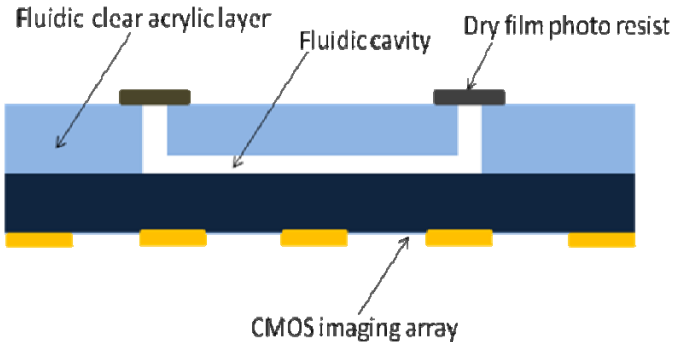

Figure 5-27 The bead/cell counter optofluidic compoent- section view

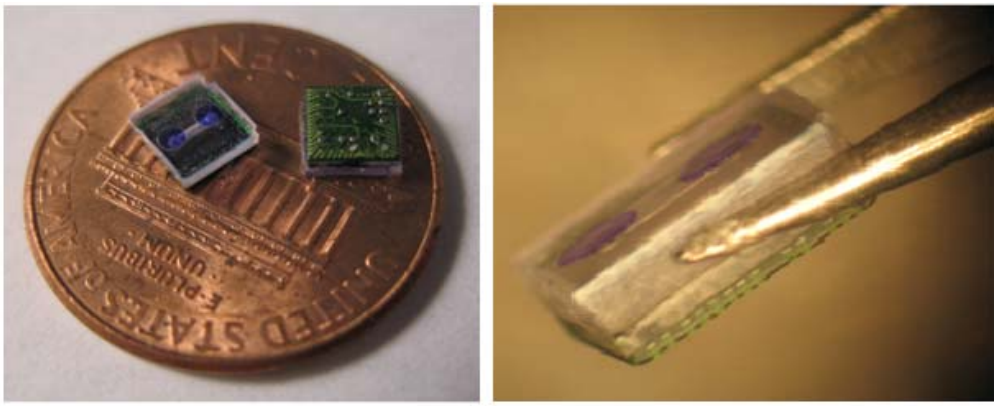

Figure 5-28 The bead/cell counter optofluidic component

5.3.2.1. Fabrication process:

The component was fabricated using a multilayer stacking and lamination technique as described in chapter 4. First the fluidic layer of the component was fabricated by machining the microchannel and the inlets on thin acrylic sheet using CNC milling tool. Then a dry film negative photoresist (manufactured by DuPont) was hot laminated and patterned by photolithography such that the photoresist would cover and seal the fluidic inlets. The dry film photoresist was laminated on the acrylic sheet by hot press at 90 °C. The negative mask was placed on the sheet and aligned with the holes, and the photoresist was exposed to UV light for 1 minute and placed in developing solution for 10 minutes. The fluidic layer was singulated into squares and bonded to a surface mount CMOS imaging chip. In a scaled manufacturing scenario it is possible to laminate the microfluidic panel to a panel of CMOS sensor arrays, and the stack would be singulated into individual components at the final step as shown in figure 5-

29. This fabrication process followed the architecture of lamination-based micro fabrication, where different layers (parts) of the device are fabricated separately and stacked/laminated on top of each other to form the final device.

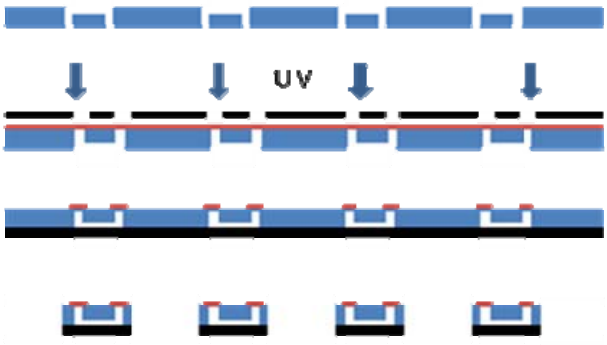

Figure 5-29 Fabrication and packaging process diagram

The components are fabricated in arrays with multilayer stacking, lamination and singulation- processes.

5.3.2.2. Integration process

The packaged opto-fluidic component was embedded on a microfluidic PCB following the aforementioned integration process as demonstrated in chapter 4. The PCB board was designed using Eagle CAD software and fabricated in a PCB fabrication house. All electronic components where mounted on the PCB alongside the opto-fluidic component. For rapid prototyping purposes polydimethylsiloxane (PDMS) was used to fabricate the planarizing and fluidic layers. After mounting the component on PCB, the board was placed in a mold to cast the planarizing layer. Parts A and B of PDMS were mixed at 10:1 ratio, casted on the board,

degassed in vacuum chamber for 30 minutes and cured on a hot plate for 1 hour at 70 °C forming the planarizing layer. Then the fluidic vias were machined and the sacrificial photoresist seal was dissolved by dilute solvent (acetone) to open up the inlets of the component. It is worthy to note that the use of acrylic to fabricate the fluidic part of the FLEMs device was not an optimal choice. When releasing the inlet/outlet openings, the acetone also attacked the acrylic, causing damage to the device. This was mitigated (but not eliminated) by using diluted solvent or milder solvent (such as methanol). Future versions of this device should use a material that is resistant to the release etchant, such as polyethylene terephthalate (PET) or polyester (PE). The microfluidic layer was molded separately in PDMS using a double molding process. A positive microfluidic channel mold was machined in acrylic sheet using a CNC milling machine. Positive microchannels were machined in the acrylic. Then PDMS was casted against the positive mold to produce a negative mold in PDMS. The negative PDMS mold surface was treated to be able to cast PDMS against PDMS. Silane was evaporated on the surface of the mold in a vacuum chamber. The mold was kept in the vacuum chamber for at least 4 hours. After surface treatment, a new PDMS layer was casted against the treated negative mold, degassed and cured on the hot plate for 1 hour at 70 °C. The microfluidic PDMS layer was released from the mold and the surface of the bonding side was plasma treated using a corona generating brush. Then the microfluidic PDMS layer was laminated on the planarizing PDMS layer on the PCB to form a

permanent bond between the two layers. The microfluidic PCB was further baked in the oven for 30 minutes at 70 ˚C to strengthen the plasma activated PDMS bond. Figure 5-30 shows the final microfluidic PCB device with the embedded opto-fluidic FLEM component. The channels were filled with water diluted red dye to highlight them and test the integrity of the layers and the fluidic vias between the component and the main microfluidic layer.

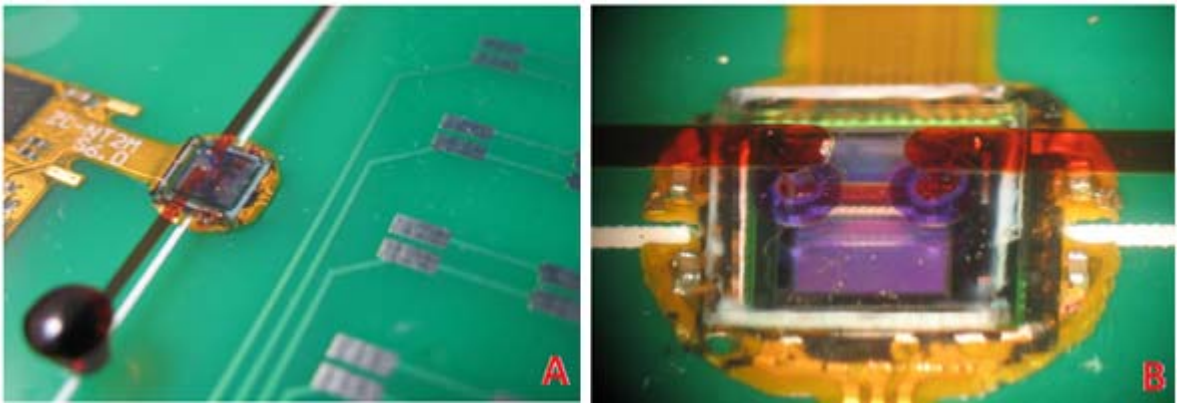

Figure 5-30 The opto-fluidic component embedded in the microfluidic PCB The channels are highlighted with red dye. B: a close up of the component showing the red dye flowing through the fluidic vias into and out of the component.

In a scaled fabrication scenario it is desirable to use thermal laminates such as the EVA or the 1002f to fabricate the planarizing and microfluidic layers, as explained in chapter 3.

5.3.2.3. Experimental:

After integration on the PCB the opto-fluidic FLEM component was tested for its intended function. In order to simulate the flow of cells, beads

with 25 μm diameter were suspended in deionized water and loaded in the device. The flow of the beads through the component was captured by the embedded CMOS sensor in real time. Figure 5-31 shows the experimental setup.

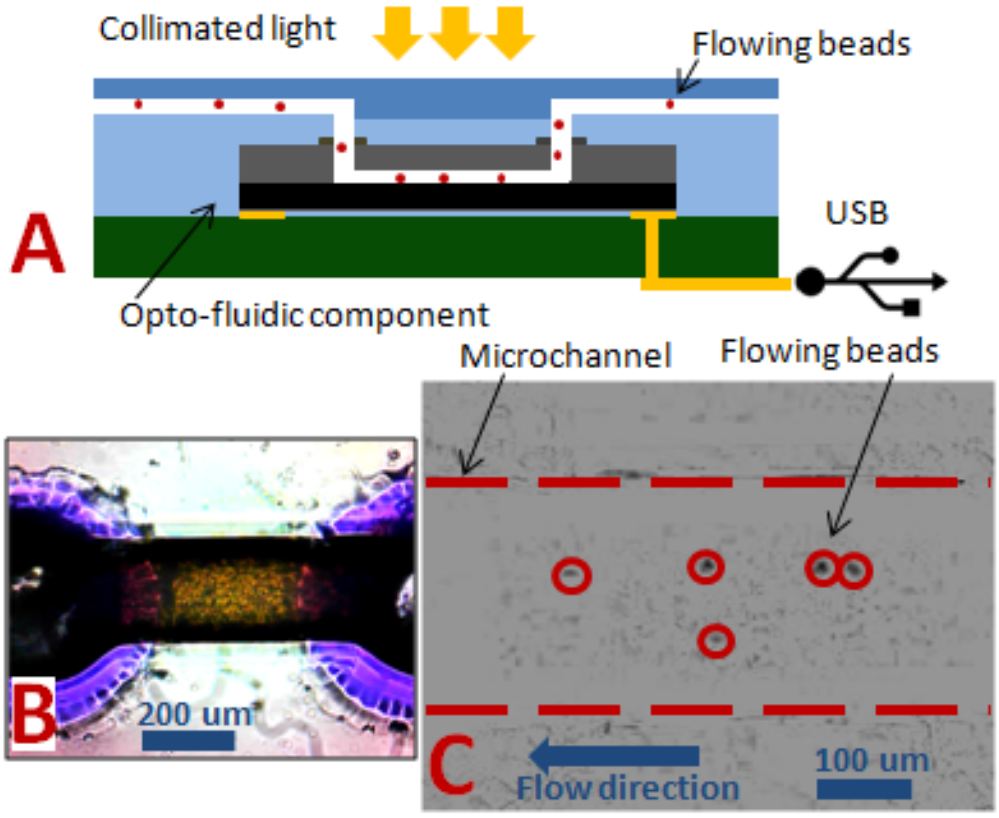

Figure 5-31 The experimental setup for imaging and counting beads in the opto-fluidic component.

B: the microchannel and fluid inlet/outlet of the component as imaged by the CMOS sensor. C: a frame from the sensor output video with beads flowing through the component microchannel.

The device is connected via USB to a computer to record the sensor output. An external collimated light source was used to illuminate the

sensor area in order to image the beads as they flew through the microchannel of the component. The beads were successfully imaged by the sensor which outputted a 640 x 480 pixels video to the computer. Figure 5-31c shows a single frame from the sensor output video with a few beads flowing in the microchannel. Further analysis of the video data using digital signal processing (DSP) and computer vision techniques can be performed to extract useful information such as bead count, bead size, flow rate, etc. A Code was written in Matlab to detect the beads based on the lensless imaging discussion in section 5.3.1. Color inversion, background subtraction and signal averaging was performed over optimized geometry detection zones which allowed the detection and counting of the beads with high accuracy as they flowed in the device. Figure 5-32 shows the results of the video analysis in Matlab. The beads flowing in the microchannel appear as sharp pulses in the output signal of the DSP algorithm.

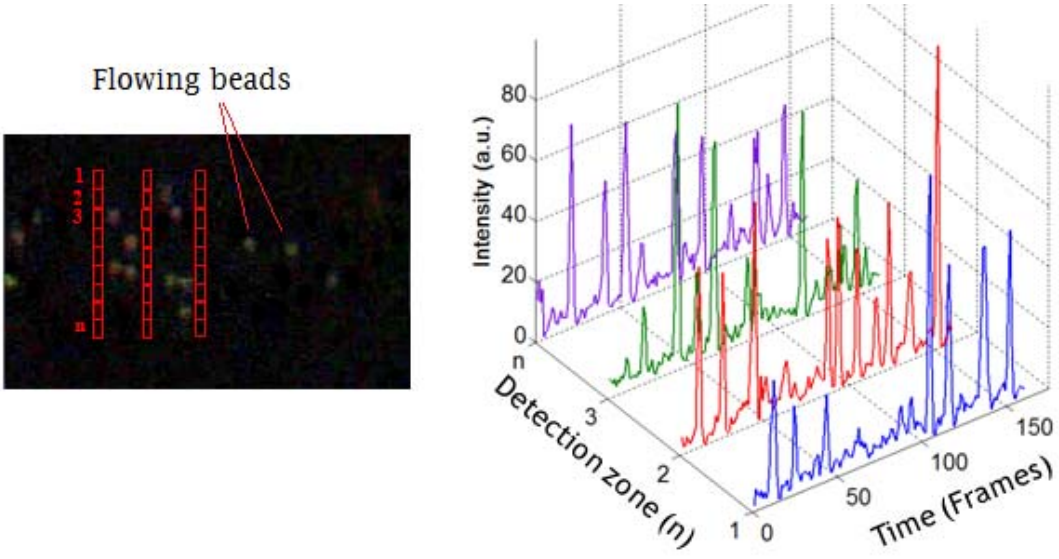

Figure 5-32 Beads flowing in the microchannel
can be detected and counted using DSP algorithms.

5.3.3.Embedded fluorescence detection system for ITP:

A microfluidic-opto-electronic PCB was designed and fabricated to integrate ITP and fluorescence detection in one device. An early version of this device was presented in [28]. Figure 5-33 shows the prototype device and the surface mount components that were integrated in this device. The device has a form factor of a credit card with dimensions of 7 cm x 5 cm x 4mm. The microchannel embedded in the device has dimensions of 5cm x 500 µm x 100 µm.

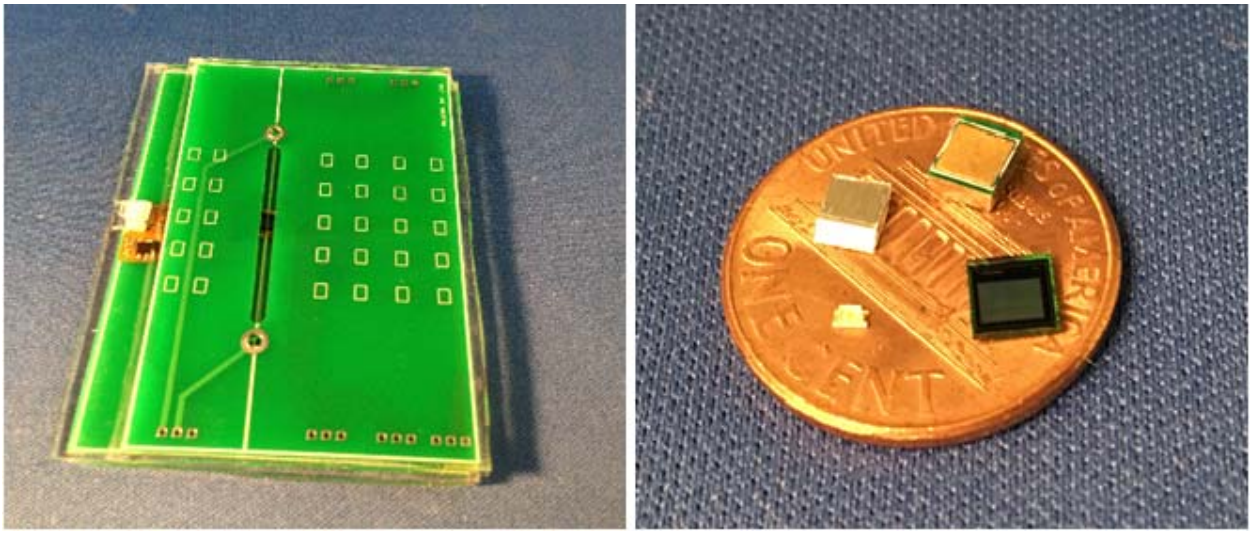

Figure 5-33 The micro-fluidic-opto-electronic PCB device and its surface mount components

As described in section 5.2.2 the analytes in the ITP assay are focused, under the influence of applied electric field, in a tight band, the so called "ITP zone" at the interface of a leading and a trailing electrolytes in a straight microchannel [29-31]. When target analytes are fluorescently

labeled, the ITP zone can be observed as a tight and bright band moving in the microchannel as shown in figure 5-34. Thus, in addition to its main function of separating and isolating target analytes from a complex sample matrix, ITP has also the useful effect of focusing and amplifying the fluorescence signal of labeled analytes. This signal amplification effect could be leveraged to improve the limit of the detection (LOD) of a device, as demonstrated by Kaigala et al. in their miniaturized ITP system with conventional optics [32]. The LOD is usually expressed in Molar units (M) and describes the sensitivity of an assay or a LOC device, i.e. it defines the minimum concentration of the target analyte in the analyzed sample that could be detected by the assay/device.

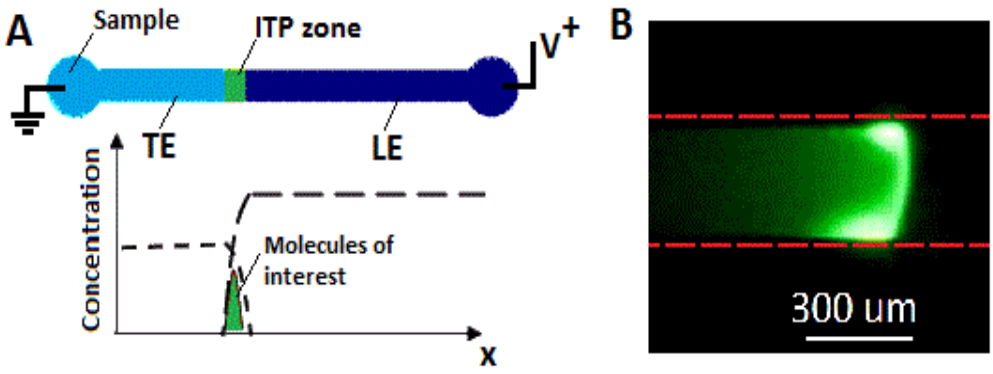

Figure 5-34 The schematics of the Isotachophoresis and a microscope image of the ITP zone

In this device ITP was used to focus Fluorescein fluorophore in the microchannel. The fluorescent ITP zone was then detected by the embedded lensless CMOS pixel array and with the help of a DSP algorithm.

5.3.3.1. Device Schematics and Fabrication

Figure 5-35 shows the schematics of the device. It consists of two PCB boards (parts). A non-disposable part called the reader and contains the active components of the device. And a disposable part called the microfluidic chip and contains the passive structures of the device: the microchannel, the high voltage electrodes and a micro machined light reflector.

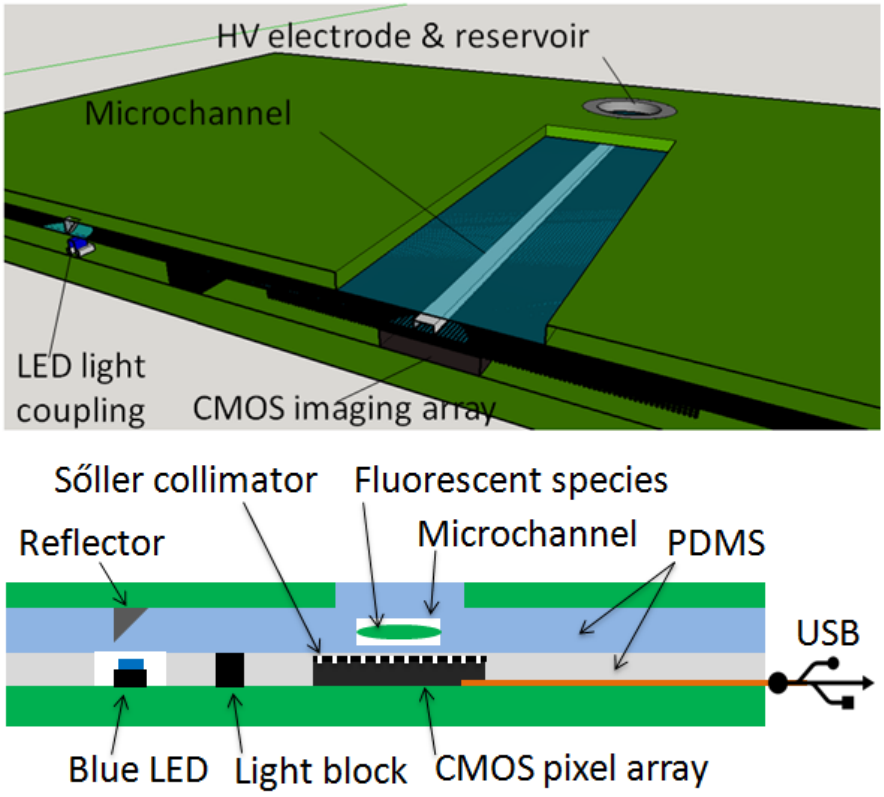

Figure 5-35 Cross sectional view of the micro-fluidic-opto-electronic PCB

The excitation light illuminates the channel from the side while the CMOS sensor images the microchannel from the bottom. The light block and the Sőller collimator film reduce the cross talk between the LED and the CMOS sensor.

The microfluidic PCB architecture allowed the use of low cost, off-the-shelf, consumer grade, optoelectronic components for the fluorescence detection in the device. A standard, surface mount blue LED (InGaN, dominant wavelength 470 nm, 140 mcd, manufactured by Dialight) is utilized to provide the excitation light for the fluorescein. Also, a standard, surface mount two mega pixels CMOS imaging array with RGB Bayer filters (HM2057-AWA manufactured by HIMAX Imaging Inc.) is utilized to detect the emitted fluorescence signal from the fluorophore. The micro-machined, surface mount light reflector is embedded in the microfluidic chip and aligned with the LED to couple the excitation light with the microfluidic channel, which is in turn aligned with the CMOS sensor as shown in figure 5-35. In this configuration the excitation plane is orthogonal to the detection plane in order to minimize the amount of excitation light reaching the detector. On the other hand, a slit cut was made in the PCB along the microchannel to avoid additional noise from the surface of the PCB due to scattering as well as auto fluorescence of the FR4 material of the PCB. Nonetheless some excitation light would reach the detector due to scattering off the microchannel walls and create a background noise in the sensor output. The background noise associated with the excitation light was further suppressed by a Söller collimator film laminated on top of the CMOS pixel array as shown in figure 5-35. The device was fabricated by the standard fabrication process of the microfluidic PCB. The two parts (the reader and the microfluidic chip) were fabricated separately, each on its

own PCB. Figure 5-36 describes the general fabrication process. The PCBs were designed using Eagle CAD software and fabricated in a PCB fabrication house. The surface mount LED and CMOS sensor were soldered on the reader PCB. Then the PCB was placed in a mold structure to cast the planarizing layer. PDMS parts A and B were mixed by 10:1 ratio and casted on the reader PCB. The mold was placed in vacuum chamber for 30 minutes to degas the PDMS and then transferred to a hot plate and cured at 70 ˚C for 2 hours forming a planarized and smooth surface on the reader. The microfluidic chip was fabricated in a similar fashion. The micro reflector was mounted on the PCB. A negative mold was prepared with negative microchannel features. PDMS was casted in the mold and the PCB was inserted/ immersed in the PDMS cast such that the PDMS would encapsulate the board with the reflector and form the microfluidic channel on the board. The PDMS in mold was degassed for 30 minutes and cured at 70 ˚C for 2 hours. Placing the microfluidic part on the reader part formed the final device as shown in figure 5-33. In this design the electric vias in the microfluidic board served as the high voltage electrodes whereas the holes of the vias as the fluidic reservoirs of the device. However, it is also possible to integrate surface mount gold electrodes (shown in figure 5-33) on the reader board to provide the electric field in the microchannel. In this prototype PDMS was used to fabricate the polymer layers of the device due to its rapid prototyping features and the optimal optical properties. In a scaled fabrication scenario, PDMS could be replaced by other optically clear

and PCB compatible thermal laminates, such as 1002f dry photoresist and Ethylene Vinyl Acetate films [33,34].

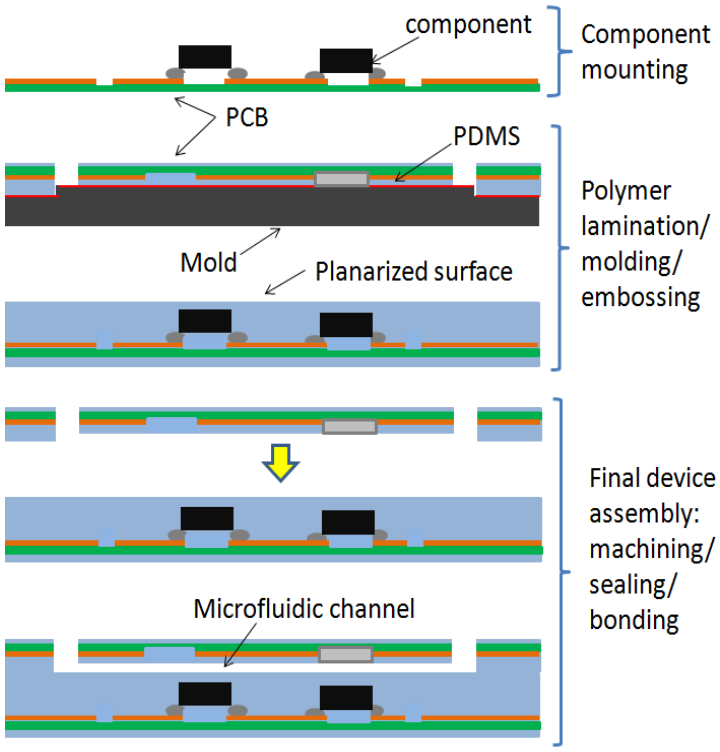

Figure 5-36 The fabrication process of the microfluidic-opto-electronic PCB

5.3.3.2. Experimental:

A series of ITP experiments were carried on the device. Fluorescein fluorophore was focused in the microchannel and detected at varying initial concentrations. The Leading and trailing electrolytes for the ITP were prepared such that the electrophoretic mobility of the Fluorescein molecules would be bounded by the mobilities of the leading and trailing ions, thus fluorescein is focused at the interface between the two electrolytes. The leading electrolyte consisted of 100 mM HCL, 200 mM Tris, 1% PVP and deionized water, whereas the trailing electrolyte consisted of

100 mM Hepes, 200 mM Tris and deionized water. For each experiment the microchannel was washed with deionized water before loading the electrolytes. 16 µL of the leading electrolyte was loaded in the leading reservoir and the microchannel. Another 15 µL of the trailing electrolyte was mixed with the Fluorescein and loaded in the sample reservoir of the device, such that the two reservoirs maintained the same head of fluid. An electric field was applied along the device by a constant current high voltage power supply circuit (demonstrated in section 5.2.3 and figure 5-23). The blue LED light excited the ITP zone as it flowed in the microchannel, and over the detection zone. The CMOS pixel array recorded the projected signal from the microchannel over the entire duration of the ITP, and outputted a real time video at a frame rate of 30 frames per second. The experiment was performed repeatedly starting with low concentration of Fluorescein and increasing the concentration every time to determine the limit of the detection of the device. A limit of detection of 10 nM initial (pre-focusing) concentration was observed in the device for Fluorescein.

5.3.3.3. Digital filtering and signal to noise ratio calculations

The sensor output was dominated by the background excitation noise, due to the absence of sharp cut filter tailored to reject the excitation light. The fluorescence signal image was extracted by digitally subtracting the background noise from each frame of the sensor output as described in the matrix equation 5-3, using Matlab. I(n) and S(n) are three dimensional

matrices representing the RGB values of the pixels in each frame n in the raw, and digitally filtered sensor outputs respectively. B is a three dimensional matrix containing the RGB values of the background noise.

$$S(n) = I(n) - B \qquad 5\text{-}3$$

Figures 5-37a and 5-37b show a single frame from the sensor output before and after digitally subtracting the background noise. The Fluorescence signal image from the ITP zone appears clearly as a green band in the microchannel's projected image.

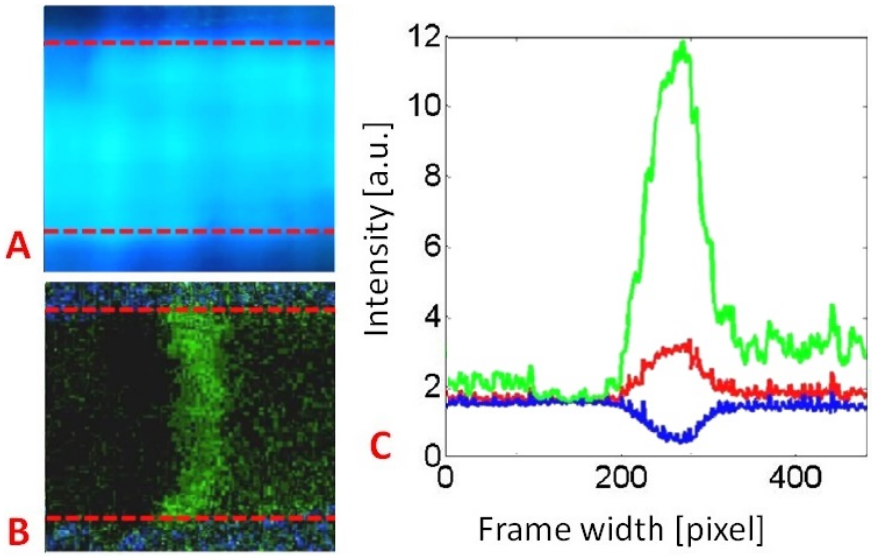

Figure 5-37 Digital filtering and ITP zone detection

A: one frame from the noisy cmos sensor output. B: the extracted ITP image after background subtraction in Matlab. The colors of the image is amplified to facilitate the visualization of the ITP signal (c) The ITP signal after integrating the signal image over the channel width in Matlab.

Figure 5-37c shows the red, green and blue components of the frame after integrating along the columns of the frame. The fluorescence signal

appears as a big peak on the green component, as expected for Fluorescein emission. However, a small peak on the red component is noticed too. A small portion of the Fluorescence signal is mapped on the red component also. The red component of the signal is expected for two reasons: the fluorescence spectrum of the Fluorescein extends up to 600 nm wavelength, and the RGB filters of the CMOS imager have overlapping transmission spectra, as shown also in figure 5-38. On the other hand a drop in the blue component of the ITP signal is observed, and this is attributed to the fact that the Fluorescein "absorbs" the blue wavelengths. These characteristics where observed consistently in all of the experiments performed on the device which would suggest a distinct pattern for the ITP zone.

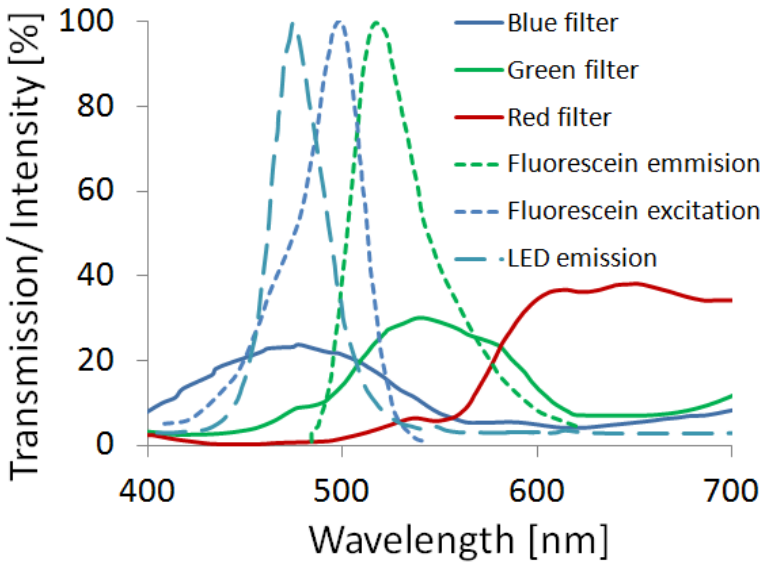

Figure 5-38 The spectral information of the device components

The excitation LED spectrum, the Fluorescein emission spectrum, and the transmission spectra of the RGB Bayer filters in the CMOS imaging array.

To calculate the signal to noise ratio (SNR), a rectangular detection zone was chosen on the pixel array and represented with a convolution matrix of ones (all values are 1). Convoluting the green component of the filtered sensor output according to equation 5-2, resulted in the mean value of the green component over the n frames as shown in figure 5-39. From this figure we can deduce the distribution of the mean value of the reminiscent background noise as well as the maximum mean value of the fluorescence signal after background subtraction. The signal to noise ratio was calculated according to equation 5-4, where μsig max is chosen as the maximum mean value (the amplitude of the peak in figure 5-39 and σ_{noise} is the standard deviation of the mean values of the reminiscent noise calculated from the frames prior to the passing of the ITP zone over the detector.

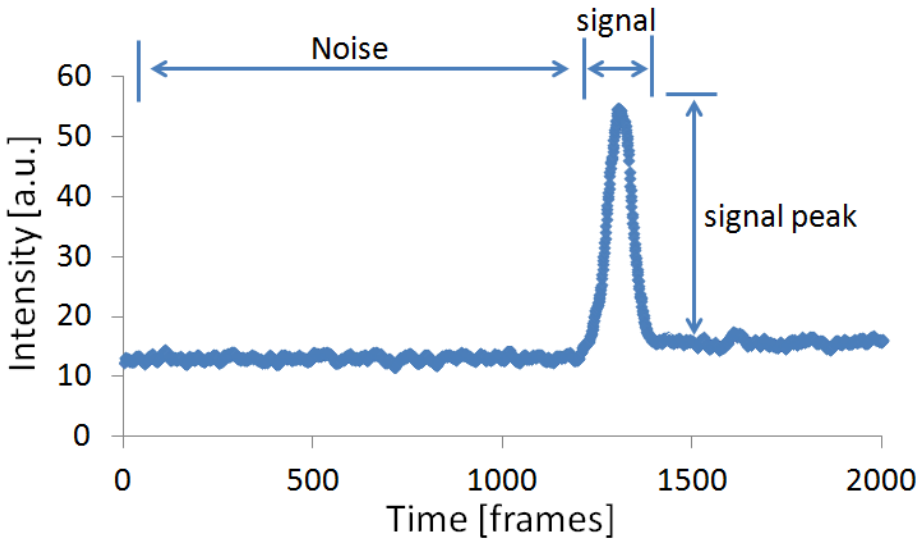

Figure 5-39 The mean values of noise and signal in the green component of the sensor output after background subtraction and convolution over a detection zone with a width of w=76 pixels

$$SNR = \frac{\mu_{sig\,max}}{\sigma_{noise}} \qquad 5\text{-}4$$

Figure 5-40 shows the signal to noise ratio as a function to the detection zone width w for different Fluorescein initial concentrations. The experimental results clearly show the pattern of the SNR varying with w. This pattern agrees with the theory and the simulation results discussed in the section 5.3.1 and figure 5-26.

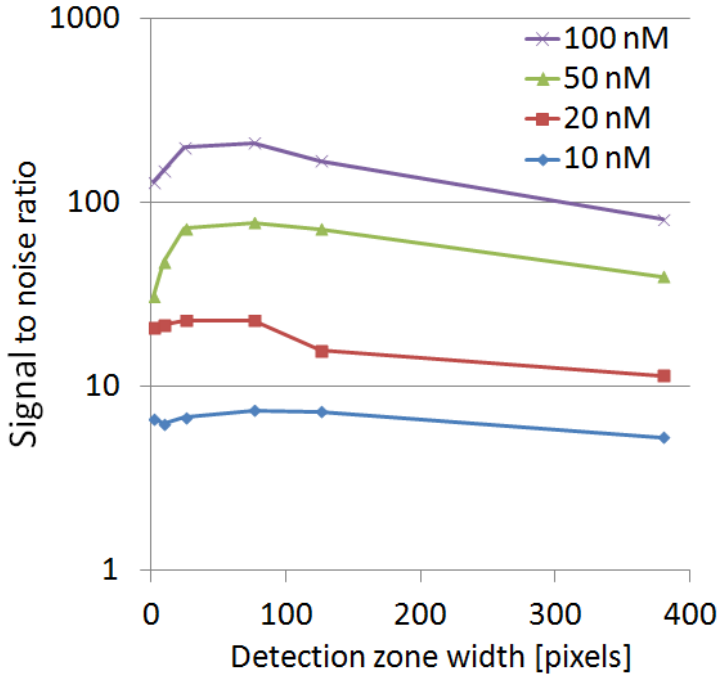

Figure 5-40 The signal to noise ratio as a function to the detection zone width w and at different Fluorescein initial concentrations

Figure 5-41 shows the SNR as a function of the Fluorescein concentration at a given width for the detection zone (w=76 pixels). The limit of the detection with high confidence was determined at LOD= 10 nM, which had an SNR=9, well above the usually accepted value of SNR_{LOD}=3.

Although the reported LOD is relevant to many applications [26], the sensitivity could be further improved with optimized assay and device designs. For example, utilizing focusing 2D optics in the excitation plane, or carefully choosing the fluorophore and the light source to better match the excitation/ emission spectra of each and also the transmission spectra of the pixel array filters, or by increasing the amount of focused analytes (increase sample size). It is also worthy to note that using the standard CMOS sensor with Bayer filter allows the use of any fluorophore in the device without the need to make any changes to the imaging array (no wavelength specific imaging filters).

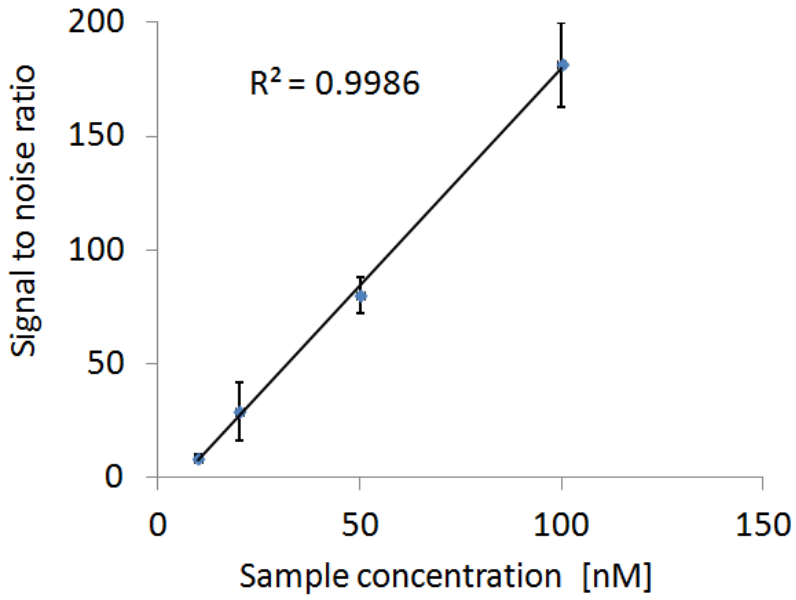

Figure 5-41 The signal to noise ratio as a function to the Fluorescein initial concentration

at a detection zone width of w=76 pixels.

5.4. Summery

In summary, this chapter presented the feasibility of the microfluidic PCB architecture and processes to produce integrated, highly functional micro-fluidic-opto-electronic PCB LOC devices. This was demonstrated by integrating four well established technologies (PCB, ITP, microelectronics, and DSP) to realize a sample preparation PCB device and two micro-fluidic-opto-electronic PCB devices. The microfluidic PCB architecture and processes provided seamless integration of components and microfluidics in these LOC devices. With an assistance of DSP techniques, a lensless imaging and fluorescence detection systems were implemented with consumer grade optical and electronic components in PCB platform, demonstrating a cell counting device and an ITP assay on chip with high signal to noise ratio and detection limit of 10 nM. The lensless optical detection systems were implemented by a CMOS pixel array with Bayer filter and DSP algorithm. A high signal to noise fluorescence detection was realized, attributed to ITP effectively amplifying the fluorescent signal in the microchannel, and to incorporating the shape and motion characteristics of the ITP zone in the DSP algorithms. It is believed that higher quality optical components and more sophisticated DSP methods could further improve the detection sensitivity with this approach. It is noticed that in general isotachophoresis is an ideal extraction method to integrate on portable platforms due to the speed (minutes), low power

requirements (milliwats) and simple mechanics of the assay (no mechanical actuation). Thus, a complete sample to answer (extraction, amplification and detection) assay could be realized in microfluidic PCBs.

5.5. References

1. S. The, R. Lin, L. Hung and A. P. Lee *"Droplet microfluidics"* Lab Chip, 2008, 8, 198–220
2. Hao Gu *, Michel H. G. Duits and Frieder Mugele *"Droplets Formation and Merging in Two-Phase Flow Microfluidics"* Int. J. Mol. Sci. 2011, 12, 2572-2597.
3. Rodriguez-Trujillo *et al. "Label-free protein detection using a microfluidic Coulter-counter device"* Sensors and Actuators B 190 (2014) 922– 927
4. M. Biehl, T. Velten "*Gaps and Challenges of Point-of-Care Technology"* IEEE Sensors Journal, Vol. 8, No. 5, May 2008
5. C. D. Chin, V. Linder, and S. K. Sia, *"Commercialization of microfluidic point-of-care diagnostic devices.,"* Lab Chip, vol. 12, no. 12, pp. 2118–34, Jun. 2012.
6. L. a Marshall, L. L. Wu, S. Babikian, M. Bachman, and J. G. Santiago, *"Integrated printed circuit board device for cell lysis and nucleic acid extraction.,"* Anal. Chem., vol. 84, no. 21, pp. 9640–5, Nov. 2012.
7. S. Babikian, L. Wu, G. P. Li, and M. Bachman, *"Microfluidic thermal component for integrated microfluidic systems,"* 2012 IEEE 62nd Electron. Components Technol. Conf., pp. 1582–1587, May 2012.
8. D. Kaniansky, M. Masár, R. Bodor, M. Zúborová, E. Olvecká, M. Jöhnck, and B. Stanislawski, *"Electrophoretic separations on chips with hydrodynamically closed separation systems.,"* Electrophoresis, vol. 24, no. 12–13, pp. 2208–27, 2003.
9. James W. Jorgenson, Krynn DeArman Lukacs *"High-resolution separations based on electrophoresis and electroosmosis"* Journal of Chromtography, 218 (1981) 209-216
10. F. B. Myers and L. P. Lee, *"Innovations in optical microfluidic technologies for point-of-care diagnostics."* Lab Chip, vol. 8, no. 12, pp. 2015–31, Dec. 2008.
11. B. Kuswandi, Nuriman, J. Huskens, and W. Verboom, *"Optical sensing systems for microfluidic devices: a review.,"* Anal. Chim. Acta, vol. 601, no. 2, pp. 141–55, Oct. 2007.

12. P. Novo, V. Chu, and J. P. Conde, "*Integrated fluorescence detection of labeled biomolecules using a prism-like PDMS microfluidic chip and lateral light excitation.,"* Lab Chip, vol. 14, no. 12, pp. 1991–5, Jun. 2014.
13. J. R. Webstert, M. A. Burns, C. Science, and A. Arbor, "*ELECTROPHORESIS SYSTEM WITH INTEGRATED ON-CHIP FLUORESCENCE DETECTION,"* in MEMSYS2000, 2000, pp. 306–310.
14. M. L. Chabinyc, D. T. Chiu, J. C. Mcdonald, A. D. Stroock, J. F. Christian, A. M. Karger, and G. M. Whitesides, *"An Integrated Fluorescence Detection System in Poly (dimethylsiloxane) for Microfluidic Applications,"* Anal. Chem., vol. 146, no. 18, pp. 4491–4498, 2001.
15. M. Dandin, P. Abshire, and E. Smela, *"Optical filtering technologies for integrated fluorescence sensors.,"* Lab Chip, vol. 7, no. 8, pp. 955–77, Aug. 2007.
16. M. Lab-on-a-chip, A. Banerjee, A. Pais, I. Papautsky, and D. Klotzkin, *"A Polarization Isolation Method for High-Sensitivity , Low-Cost On-Chip Fluorescence Detection for Microfluidic Lab-on-a-Chip,"* IEEE Sensors, vol. 8, no. 5, pp. 621–627, 2008.
17. U. A. Gurkan, S. Moon, H. Geckil, F. Xu, S. Wang, T. J. Lu, and U. Demirci, *"Miniaturized lensless imaging systems for cell and microorganism visualization in point-of-care testing.,"* Biotechnol. J., vol. 6, no. 2, pp. 138–49, Feb. 2011.
18. H. Zhu, S. O. Isikman, O. Mudanyali, A. Greenbaum, and A. Ozcan, *"Optical imaging techniques for point-of-care diagnostics.,"* Lab Chip, vol. 13, no. 1, pp. 51–67, Jan. 2013.
19. J. Guo, X. Huang, D. Shi, H. Yu, Y. Ai, C. M. Li, and Y. Kang, *"Portable resistive pulse-activated lens-free cell imaging system,"* RSC Adv., vol. 4, no. 99, pp. 56342–56345, Oct. 2014.
20. X. Huang, H. Yu, X. Liu, Y. Jiang, and M. Yan, *"A single-frame superresolution algorithm for lab-on-a-chip lensless microfluidic imaging,"* IEEE Des. Test, vol. 32, no. 6, pp. 32–40, 2015.
21. M. L. Adams, M. Enzelberger, S. Quake, and A. Scherer, *"Microfluidic integration on detector arrays for absorption and fluorescence micro-spectrometers,"* Sensors Actuators A Phys., vol. 104, no. 1, pp. 25–31, Mar. 2003.
22. C. Y. Minkyu Kim *et al. "Lab on a Chip,"* Lab Chip, vol. 15, no. 6, pp. 1417–1423, 2015.
23. K. S. Shin, Y. H. Kim, K. K. Paek, J. H. Park, E. G. Yang, T. S. Kim, J. Y. Kang, and B. K. Ju, *"Characterization of an integrated fluorescence-detection hybrid device with photodiode and organic light-emitting diode,"* IEEE Electron Device Lett., vol. 27, no. 9, pp. 746–748, 2006.
24. R. R. Singh, S. Member, L. Leng, A. Guenther, R. Genov, and S. Member, *"A CMOS-Micro fl uidic Chemiluminescence Contact Imaging Microsystem,"* IEEE J. Solid-State Circuits, vol. 47, no. 11, pp. 2822–2833, 2012.

25. P. Epperson and M. Denton, *"Binning spectral images in a charge - coupled device,"* Anal. Chem., vol. 61, p. 1513, 1989.
26. Z. Zhou, B. Pain, and E. R. Fossum, *"Frame-transfer CMOS active pixel sensor with pixel binning,"* IEEE Trans. Electron Devices, vol. 44, no. 10, pp. 1764–1768, 1997.
27. S. Babikian, G.P. Li and M. Bachman *"Packaging Architecture for Fluidic Components in Microfluidic PCBs"* IEEE 66th ECTC Conf. submitted for publication, 2016
28. S. Babikian, G. P. Li, and M. Bachman, *"Portable Micro-Fluidic-Opto-Electronic Printed Circuit Board for Isotachophoresis Applications,"* µTAS Conf. pp. 1293–1295, 2015.
29. P. Gebauer, Z. Malá, and P. Bo□ek, *"Recent progress in capillary ITP,"* Electrophoresis, vol. 28, no. 1–2, pp. 26–32, 2007.
30. B. Jung, Y. Zhu, and J. G. Santiago, *"Detection of 100 aM fluorophores using a high-sensitivity on-chip CE system and transient isotachophoresis,"* Anal. Chem., vol. 79, no. 1, pp. 345–349, 2007.
31. L. Chen, J. E. Prest, P. R. Fielden, N. J. Goddard, A. Manz, and P. J. R. Day, *"Miniaturised isotachophoresis analysis.,"* Lab Chip, vol. 6, no. 4, pp. 474–87, 2006.
32. G. V Kaigala, M. Bercovici, M. Behnam, D. Elliott, J. G. Santiago, and C. J. Backhouse, *"Miniaturized system for isotachophoresis assays.,"* Lab Chip, vol. 10, no. 17, pp. 2242–2250, 2010.
33. Liang Li Wu, Sarkis Babikian, Guann-Pyng Li, and Mark Bachman *"Microfluidic Printed Circuit Boards"* Electronic Components and Technology Conference (ECTC), 2011 IEEE 61st
34. S. Babikian, W. a. Cox-Muranami, E. Nelson, G. P. Li, and M. Bachman, *"Ethylene-Vinyl Acetate as a low cost encapsulant for hybrid electronic and fluidic circuits,"* IEEE 63rd Electron. Components Technol. Conf., pp. 1800–1805, May 2013.

6. CONCLUSIONS AND FUTURE DIRECTIONS:

As of today, Lab-on-Chip devices lack standard fabrication and integration processes. Most LOC devices are in the form factor of passive microfluidic chips (cassettes), which would require off-chip functionalities, equipment and bench top readers to perform the bioassays. This specially hinders the wide and successful implementation and commercialization of LOC devices for point of care diagnostics applications.

In this work heterogeneous integration architecture was proposed to fabricate highly functional LOC devices on PCBs. It was demonstrated that the PCB is a powerful integration platform for LOC devices. The proposed architecture enabled modular integration of standardized components and functions on the chip. Micro pumps, micro valves and other like fluidic, optical, mechanical, and electronic components (FLEMS) can be packaged in surface mount form factor and readily embedded in the layers of the microfluidic PCB. This allows the seamless integration of LOC functions on the chip. The microfluidic PCB technology was demonstrated by fabricating a number of LOC devices which incorporated a number of FLEMS components as well as off-the-shelf electronic components.

A holistic view was adopted in the integration strategies. In such approach the bioassay's unique characteristics are incorporated in the signal detection strategy on the LOC device, and as well as in assistive signal processing algorithms which optimize the device performance. This

allowed reducing the design complexity and constraints of the physical sensors and components of the device while maintaining an acceptable or a sufficient performance for the desired application. Thus, several technologies (such as the bioassays, electronics and digital signal processing) could be implemented in a complementary fashion in the PCB LOC device to achieve the desired combination of device performance, complexity and cost. This was demonstrated in chapter 5 through the sample preparation device and the on-chip optical detection examples, all of which were powered and controlled through a lap top computer via USB port.

Finally, this work demonstrates the feasibility and the value of leveraging the manufacturing tools of PCB and microelectronic packaging technologies, as well as the value of leveraging the signal processing power of mobile electronic devices in order to realize scalable heterogeneous and cost effective integration for LOC devices.

There is considerable room for future work towards integrating standard bioassays on microfluidic PCB devices for specific LOC applications. This would involve optimizing both the standard assays and the microfluidic PCB technology; including designing and fabricating novel surface mount fluidic electronic and optical components, in order to achieve a successful “marriage” between the assay and the device. Further considerable work is needed to find optimum ways to modify the existing PCB manufacturing and packaging infrastructure in order to service the emerging LOC device industry.